REOVIRUS CAPSID STABILITY AND DISEASE PATHOGENESIS

By

Joshua David Doyle

Dissertation

Submitted to the Faculty of the

Graduate School of Vanderbilt University

in partial fulfillment of the requirements

for the degree of

DOCTOR OF PHILOSOPHY

in

Microbiology and Immunology

December, 2012

Nashville, Tennessee

Approved:

Professor Terence Dermody

Professor Christopher Aiken

Professor Jennifer Pietenpol

Professor Earl Ruley

Professor John Williams

ACKNOWLEDGEMENTS

I am grateful for the support of the Cellular Biology and Molecular Sciences (CBMS) training grant (T32GM008554-11) and the Cell Entry of Reovirus Grant (Public Health Service Award R01 AI32539). Additional funding was provided by the Lamb Center for Pediatric Research and I wish to specifically thank the Lamb family for their generosity.

Thank you to my mentor, Terry Dermody. Terry is a tremendous scientist, a patient teacher, a gifted writer and editor, and a thoughtful leader. Terry's latent genius is his ability to say and do the precise thing needed to reassure and motivate the individuals under his charge, whatever their personality type, work patterns, or personal problems. Terry has helped me more in recent years than almost anyone I can think of. Tremendous thanks.

Thank you as well to the many wonderful scientists I've had the opportunity to work with and learn from in the Dermody Lab. Pranav Danthi, a brilliant virologist and my rotation mentor, taught me the whys and wherefores of the lab and got my project off to a great start. Elizabeth Johnson involved me in her work, providing the foundation for my own studies with cathepsins and was always available for ideas and questions. Thanks to Karl Boehme for teaching me about mousework, radiation, microscopy, and drywall with equal aplomb. Mine Ikizler has been a wonderful bench- and deskmate, sharing with me her wealth of research experience as well as the green and purple Skittles. Thanks to Bernardo Mainou for sporadic and enlightening conversations that always generated more ideas than I knew what to do with. Thank you as well to Greg Wilson for help and

ideas with reovirus disassembly mutants and for companionship at odd hours. Thank you to Laurie Silva for sharing her quirky sense of humor and scientific insights with me. Thanks to Andrea Pruijssers and Jennifer Konopka for ideas about mice, neurons, apoptosis, and so much more. Finally, tremendous thanks to Denise Wetzel, for all that she did for the Dermody lab in general and for my work in particular.

The Dermody lab has felt like home largely because of the other students with whom I've shared time and space. In particular, I'll remember Jason Iskarpatyoti for conversations about sports, food, and so much else, Caroline Lai for basketball in the morning and therapeutic discussions in the mouseroom in the afternoon, Alison Ashbrook's knack for instantly improving even the worst 'Bad Science Day', Magda Bokiej's perseverance and unique sense of humor, Johnna Frierson's unrelenting cheer and encouragement, and Jennifer Stencel for her invaluable help with immunology and general life in science. There are many, many other students, postdocs, and others who made my graduate training memorable; thank you to all.

I am indebted to collaborators who assisted me along the way. First, I am grateful for the assistance of Courtney Copeland and Jillian Rhoads, two eager, diligent rotation students who advanced my studies considerably. At Vanderbilt, I received tremendous assistance from the Division of Animal Care, with particular thanks to Chae Logan, Jessica Cantrell, and Atef Khalil. I am extremely grateful for the help of the Vanderbilt Translational Pathology Shared Resource core, particularly Kelli Boyd, in assisting with immunohistochemistry slides, and to Ty Abel for help in their interpretation. I have enjoyed several collaborations outside Vanderbilt, as well. In particular, I would like to

acknowledge BVV Prasad, Leslie Schiff, Kartik Chandran, Barbara Sherry, Rachel Nygaard, and Julie Pfeiffer.

My deepest thanks to my dissertation committee. Chris Aiken, Jennifer Pietenpol, Earl Ruley, and John Williams have been wildly supportive and helpful throughout my graduate career. I always looked forward to committee meetings for the discussion, ideas, and enthusiasm everyone contributed- thank you so much for your help. In addition to my committee, there are several Vanderbilt faculty and staff who have contributed much to my education, including Mark Denison, Michelle Becker, Jim Chappell, Tim Cover, Jim Patton, Larry Swift, Melissa Krasnove, and Michelle Grundy.

I owe a tremendous debt to my family. My parents, Randy and Sandy, have always encouraged me to work hard and chase my dreams. I am unbelievably fortunate to have Sarah as my sister; she has always been a ready companion for adventures and steady source of support. Since I was small, my family has emphasized education, and years later here I am taking those admonishments far too seriously. My family is sharp, funny, and unbelievably caring. I love you all.

Thanks finally to Cameron. I have no idea why you thought accompanying me on this journey was a good idea- all the meals delayed, weekends spent in lab, missed dates, late (sometimes laaate) nights only to discover I'd used the wrong secondary antibody hours before…thanks so much for everything. All my love.

TABLE OF CONTENTS

LIST OF TABLES

LIST OF FIGURES

CHAPTER I

INTRODUCTION

Thesis Overview

The successful propagation of any virus depends on the capacity to deliver its genome into the interior of an uninfected target cell. To do so, viruses must transit across a limiting membrane, either at the cell surface or within a vesicular compartment. Disparate virus families have evolved a variety of specialized proteins to facilitate trans-membrane passage. Activation of these cell-entry systems often requires structural rearrangement of capsid components in response to receptor binding or environmental cues. However, the viral cell entry machinery is tightly regulated to ensure that it is triggered only at the proper time and place for productive infection. Thus, viral capsid components are frequently poised at the fulcrum between stability and instability, and perturbation of that balance may have ramifications for viral fitness and disease pathogenesis.

Mammalian orthoreoviruses (reoviruses) are nonenveloped viruses that feature a segmented, double-stranded (ds) RNA genome. Reovirus was first isolated from the respiratory and intestinal tracts of human patients in the 1950s (120), yet is rarely associated with human disease. The name "reovirus", derived from the phrase ***r***espiratory ***e***nteric ***o***rphan, is a reference to this lack of clinical disease. However, newborn mice are quite susceptible to reovirus infection, providing an excellent experimental system for studies of viral pathogenesis.

To initiate infection, reovirus particles undergo a stepwise uncoating process catalyzed by host endosomal proteases. The reovirus disassembly cascade exposes hydrophobic domains of specialized capsid proteins that disrupt endosomal membranes, an essential requirement for productive cell entry. This well-characterized disassembly process makes reovirus an excellent system for studies of nonenveloped virus cell entry. My dissertation research focuses on molecular determinants of reovirus capsid protease sensitivity and the influence of capsid stability on reovirus-mediated disease and host-to-host transmission.

Introduction to Reovirus

Mammalian orthoreoviruses display a very broad natural host range, having been isolated from monkeys, chimpanzees, rabbits, mice, swine, cattle, dogs, and cats (34, 41, 117, 121). The majority of humans are seropositive for reovirus by the time they reach adulthood (84, 122, 134). Most people likely contract reovirus as an unremarkable childhood infection (134). However, reovirus infection is occasionally associated with mild upper respiratory or gastrointestinal symptoms (69, 72). Reovirus infection is also associated with neonatal biliary atresia (112, 138), but further study is required to establish what role, if any, reovirus plays in precipitating this condition.

The natural route of reovirus transmission is presumed to be fecal-oral. Like other nonenveloped viruses, such as the picornaviruses (enteroviruses and rhinoviruses) and caliciviruses, reovirus is relatively stable in the environment and retains infectivity for several days when dried on nonporous surfaces (59). Reovirus-specific sequences have been detected by PCR in water samples from coastal estuaries, but it is unclear whether

waterborne transmission plays a role in reovirus transmission. Despite the near ubiquity of reovirus infection, sequence data is relatively sparse for primary isolates, complicating an understanding of the diversity of circulating reovirus populations and dynamics of virus spread.

There are three major serotypes of reovirus as defined by antibody neutralization (120). The prototype strains of each serotype are named for the patient from which they were originally isolated, e.g., type 1 Lang (T1L), type 2 Jones (T2J), and type 3 Dearing (T3D). These reovirus strains differ in their receptor utilization, disassembly kinetics, capacity for apoptosis induction, and transcriptional efficiency, among other biological properties. Moreover, there are significant strain-specific differences in patterns of disease induced by strains T1L and T3D, discussed in greater detail below.

The reovirus genome is comprised of 10 segments of dsRNA, encoding 11 protein products. The segmented nature of the reovirus genome allows genetically distinct reovirus strains to co-infect a single cell and give rise to viable reassortant progeny that contain gene segments derived from both parents. Genomic RNA segments from different reovirus serotypes migrate to different positions when resolved by polyacrylamide gel electrophoresis, allowing straightforward genotyping of reassortant viruses. Genetic reassortment thus allows a given phenotype to be easily linked to a particular gene segment.

Reovirus reverse genetics facilitates the introduction of specific mutations, insertions, and deletions in otherwise isogenic viral genetic backgrounds (77). The reovirus reverse genetics system utilizes plasmids containing all 10 reovirus genes, along

with their 3' and 5' untranslated regions (UTRs), in the context of a T7 polymerase promoter and hepatitis delta ribozyme. These constructs are transfected into BSR cells that stably express T7 polymerase. Following a 72-hour incubation period, viable reovirus can be recovered by freeze/thaw and plaque selection. Strains recovered by reverse genetics are denoted "rs" for "recombinant strain" (i.e., ***rs***T3D) and may be amplified to high titers with limited passage, reducing the accumulation of nonspecific mutations. Site-directed mutagenesis of parent rescue plasmids allows the construction of reovirus strains with desired mutations, providing a versatile tool for studying all aspects of reovirus biology.

Reovirus Structure

Reovirus virions lack an envelope and consist of concentric protein shells surrounding the dsRNA genome (55, 101) (Figure I-1). The innermost of these shells is referred to as the core and features a complex of λ1 and σ2 proteins (113), the viral RNA-dependent RNA polymerase, λ3, and the polymerase co-factor, μ2 (33, 150). Core particles also contain hollow, turret-like pentamers of λ2 protein at each fivefold axis of symmetry (113). Core particles are transcriptionally active and can direct mRNA transcript synthesis *in vitro* (89, 135). However, it is thought that reovirus gene segments remain inside the core throughout the viral life cycle. Thus, λ2 turrets serve as channels through which mRNA transcripts are extruded during transcription (53). In addition, λ2 functions as an mRNA capping enzyme, adding 5' guanyl and methyl groups to nascent transcripts (29, 88, 135).

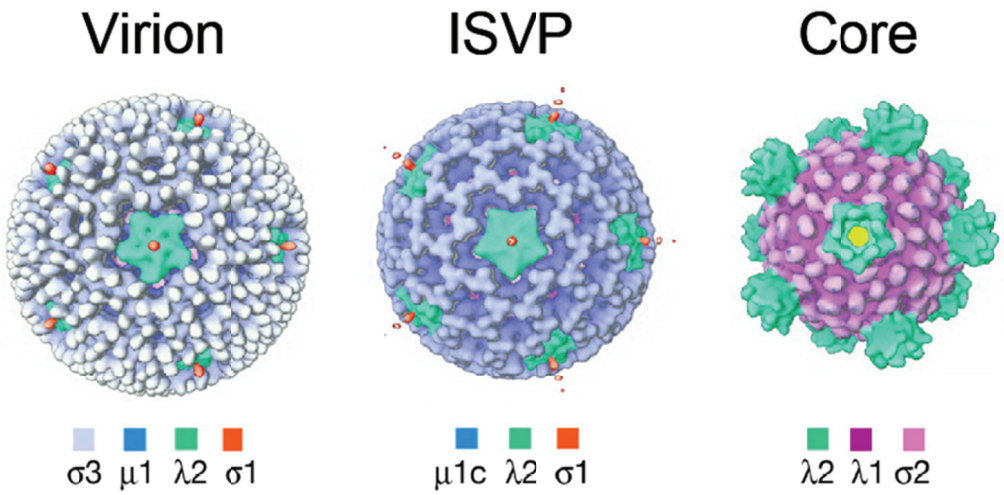

Figure I-1. Reovirus Structure. Cryo-EM image reconstructions of reovirus virions, ISVPs, and cores. Note density corresponding to σ1, depicted in red, extending from λ2 turrets (adapted from Dryden 1993) (46).

Reovirus virions have an outer capsid comprised of 600 molecules each of μ1 and σ3 proteins arranged in a heterohexameric lattice that completely overlies the viral core, the protruding λ2 turrets excepted (85) (Figure I-1). Interestingly, μ1/σ3 heterohexamers form spontaneously when the proteins are co-expressed *in vitro* and can be condensed onto viral cores to generate "recoated" virions (23, 85). Finally, virions contain 36 copies of the filamentous attachment protein, σ1. Trimers of σ1 are bound to the pentameric λ2 turrets via hydrophobic residues in the σ1 N-terminus (46, 51, 81, 82).

During uncoating, reovirus particles proceed through a well-defined series of disassembly intermediates. Reovirus uncoating begins with proteolysis of σ3, resulting in its removal from the viral particle. Sigma 3 proteolysis exposes proteolytic cleavage sites in the other major outer-capsid component, μ1, which is cleaved to generate the species μ1N, μ1-δ, and μ1-φ (21, 104, 108). Reovirus particles in which σ3 and μ1 have both

been cleaved are referred to as *i*nfectious *s*ub*v*irion *p*articles (ISVPs) (Figure I-1). ISVPs also can be generated by treating virions with purified proteases, including cathepsins (47) and digestive enzymes such as trypsin and chymotrypsin (15, 47). Formation of ISVPs during cell entry requires the activity of host endosomal proteases (5, 133). Further proteolytic cleavage in cells results in removal of σ1 to generate a transcriptionally active species referred to as an ISVP* (20). The μ1N, μ1-φ, and μ1-δ species have hydrophobic domains that disrupt lipid bilayers, allowing ISVP*s to penetrate endosomal membranes and access the cytoplasm of infected cells (65, 87). Having already undergone disassembly, infection by *in vitro-generated* ISVPs are not blocked by inhibitors of endosome acidification and protease activity, such as ammonium chloride and E64 (5, 133). Accordingly, ISVPs are also approximately two-fold more infectious than virions (103).

Reovirus Attachment and Internalization

The initial step in reovirus cell entry is the binding of the virus to cell-surface receptors via the σ1 attachment protein. Early studies showed that reovirus agglutinates erythrocytes, suggesting that the virus binds cell-surface carbohydrates (83). Subsequent studies revealed that type 3 reovirus strains bind sialic acid moieties on glycosylated proteins via a carbohydrate-binding domain in the body portion of σ1 (42, 52). A high-resolution crystal structure of the T3D σ1 protein in complex with siallylactose was published in 2011 (114). There is evidence that type 1 reovirus strains also engage terminal sialic acid moieties (62), but the exact nature of the glycans bound by T1L and the carbohydrate-binding domain of T1L σ1 are still unclear. In addition to

carbohydrates, all reovirus serotypes utilize junctional adhesional molecule A (JAM-A) as a receptor (8). JAM-A is a member of the immunoglobulin protein superfamily that localizes to tight junctions linking polarized cells (86, 94, 146). Structural studies reveal that the head domain of σ1 binds JAM-A with nanomolar affinity (Figure I-2) (26, 58, 76). Interestingly, a soluble sialic acid analogue inhibits reovirus infection at early but not late timepoints post-adsorption, whereas an antibody that blocks JAM-A binding inhibits infection at both early and late timepoints (7). These findings suggest a multi-step adhesion strengthening model in which initial, low-affinity binding to carbohydrates potentiates subsequent high-affinity interactions with JAM-A. Animals that lack JAM-A are susceptible to reovirus administered intracranially, suggesting the possibility of a CNS-specific reovirus receptor, but this molecule has yet to be identified.

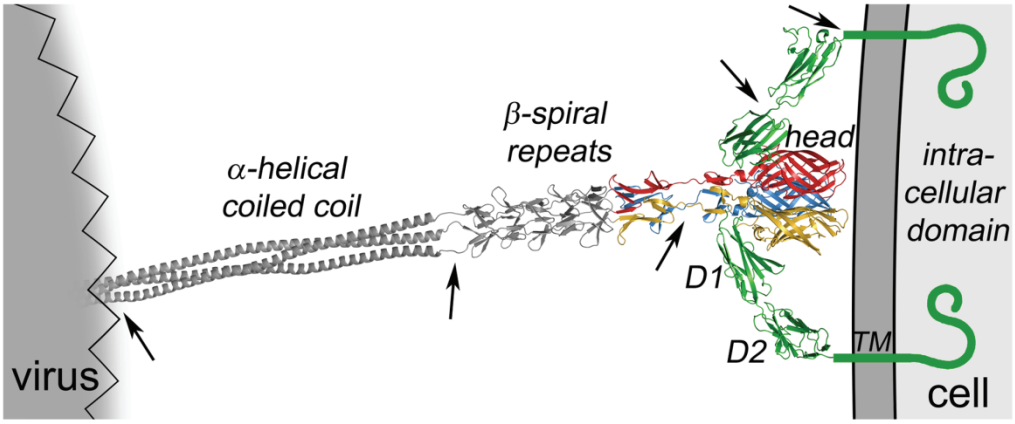

Figure I-2. Reovirus σ1-JAM-A binding. A model of full-length σ1 binding is shown with predicted portions of σ1depicted in grey and the known structure of the C-terminus shown in color. The reovirus receptor JAM-A is shown in green. Adapted from Kirchner, 2008 (76).

Following σ1 binding to JAM-A, reovirus particles are internalized via endocytosis. Electron microscopy reveals internalized viral particles localized to structures resembling clathrin-coated pits (119, 133). Fluorescent microscopy also provides evidence of co-localization between reovirus and clathrin (50). Chlorpromazine, which selectively inhibits clathrin-mediated endocytosis, limits reovirus infectivity in cell culture (91), providing functional evidence for clathrin-dependent uptake of reovirus. However, it is still unclear how reovirus receptor binding initiates internalization. JAM-A constructs lacking a cytoplasmic tail, which is required for JAM-A intracellular signaling, are still capable of conferring reovirus infection, suggesting a role for other cell-surface molecules in reovirus internalization (90). There is evidence that β1 integrins are involved in reovirus internalization. There are RGD and KGE integrin-binding motifs in the reovirus λ2 protein, and treatment of permissive cells with antibodies against β1 integrin diminishes reovirus infectivity (90). However, direct interactions between reovirus particles and integrins have not been demonstrated, and the signal transduction events required to trigger reovirus internalization are as yet undefined.

Internalized reovirus particles must access late endosomes containing the requisite proteases and acidic pH for proper disassembly. To do so, reovirus takes advantage of a series of vesicular sorting events mediated by Src-family tyrosine kinases. The role of Src in reovirus cell entry emerged following a screen in which genistein and PP2, a tyrosine-kinase inhibitor and Src-family kinase inhibitor, respectively, were found to diminish reovirus infectivity (92). Cells pretreated with PP2 target reovirus virions to lysosomes instead of late endosomes where they are degraded, indicating that Src plays a key role in directing internalized particles to the proper compartment for disassembly. Rab GTPases

also function in vesicular sorting of reovirus and influence the fate of internalized reovirus virions (Figure I-3)(93). Fluorescently-labeled reovirus virions and JAM-A co-localize in early endosomes marked by Rab5A and Rab5C. From there, virions proceed to either Rab7-marked late endosomes where productive disassembly occurs or Rab4- and Rab11-marked recycling endosomes that presumably return viruses to the cell surface. Transfecting cells with dominant-negative Rab5A, Rab5C, or Rab7 diminishes reovirus infectivity, but transfection with dominant-negative Rab4 and Rab11 does not, suggesting a functional requirement for Rab GTPases in sorting reoviruses to the proper compartments for productive infection (Figure I-3). Although some of the signaling events responsible for proper reovirus trafficking have been elucidated, the mechanisms by which reovirus induces or modulates this process are unclear.

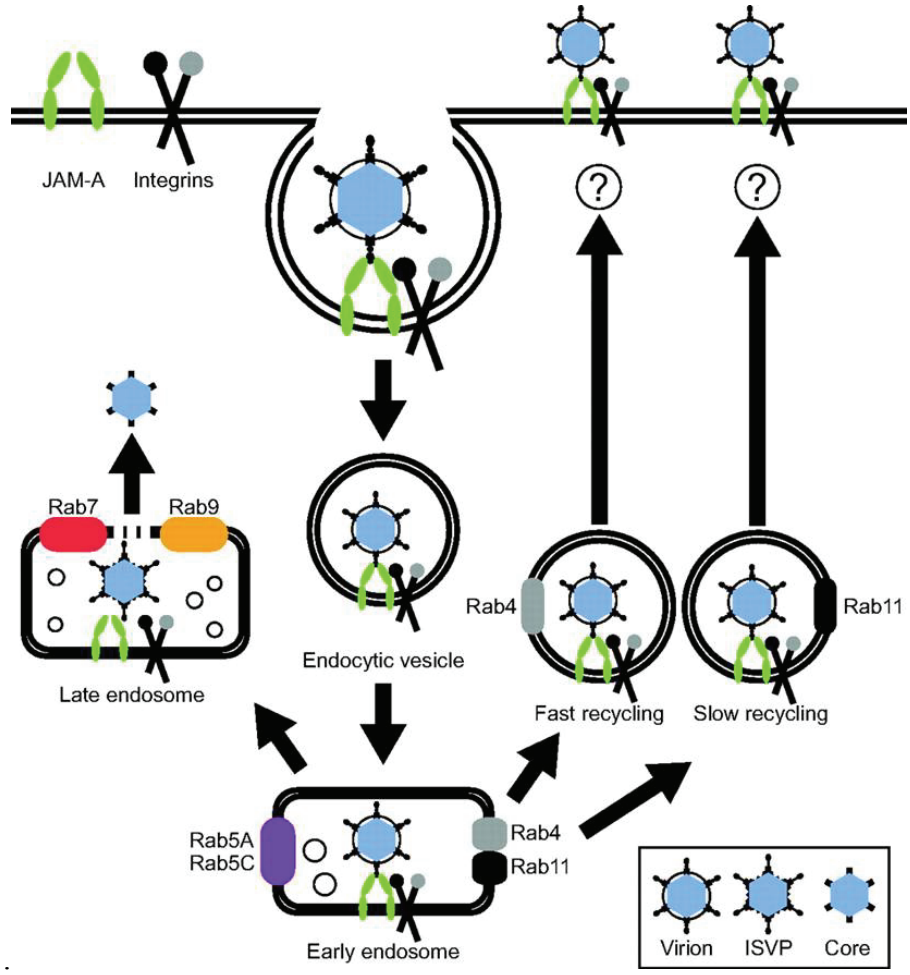

Figure I-3. Reovirus cell entry. After attachment to cell surface glycans and JAM-A, reovirus is internalized via receptor-mediated endocytosis using a mechanism dependent on β1 integrin. Reovirus traffics to early endosomes marked by Rab5A or Rab5C, where viral particles are sorted into productive or nonproductive entry pathways. Virions in the nonproductive pathway enter recycling endosomes marked by Rab4 or Rab11 and may return to the cell surface. Virions in the productive pathway enter endosomes marked by Rab7 or Rab9, where viral disassembly takes place. The disassembly intermediate penetrates endosomal membranes, releasing the transcriptionally active viral core into the cytoplasm. From Mainou and Dermody 2012 (93).

The Reovirus Disassembly Cascade

Stepwise disassembly of reovirus virions within target cells is catalyzed by acid-dependent cathepsin family members (47). Cathepsins are a family of approximately twelve proteases primarily localized to endocytic compartments (98). Several cathepsins, including cathepsin B and cathepsin L, are constitutively expressed in most cell types and play roles in protein turnover and MHC class II antigen processing (98). However, some cathepsins serve tissue-specific functions, including cathepsin K, which is primarily expressed by osteoclasts and is involved in bone remodeling, and cathepsin S, which is primarily secreted by immune cells (98, 149). Cathepsin L also has a specialized function in the thymus, where it is involved in removal of the invariant chain from MHC II molecules in cortical thymic epithelial cells, a process essential for the proper development of CD4+ and NK T cells (64, 102). Most cysteine-protease cathepsins are endopeptidases, but cathepsin B also has significant exopeptidase activity (98).

The role of cathepsins in reovirus disassembly was foreshadowed by the observation that reovirus uncoating is acid-dependent (43, 133). Later studies identified σ3 proteolysis as the rate-limiting step in reovirus disassembly and noted that pan-cysteine protease inhibitors block uncoating in cell culture (5). The role of cathepsins, particularly cathepsin B and cathepsin L, was definitively established by a previous graduate student in the Dermody laboratory, Dan Ebert. Ebert showed that inhibitors specific for cathepsin B and cathepsin L limit reovirus disassembly in fibroblasts and that the reciprocal addition of specific cathepsin inhibitors to cathepsin B- and cathepsin L-deficient fibroblasts completely abrogated reovirus disassembly (47).

Another series of experiments by a different graduate student in the Dermody lab,

Elizabeth Johnson, probed the role of cathepsins in disease pathogenesis using mice deficient for cathepsins B, L, or S (*Ctsb-/-*, *Ctsl-/-*, and *Ctss-/-*, respectively) (71). Given the essential requirement for proteolysis in reovirus cell entry, Johnson hypothesized that cathepsin-deficient animals would be protected from reovirus challenge. Indeed, *Ctsb-/-* animals have higher survival rates than wildtype animals following reovirus infection, and peak viral titers in all three cathepsin-deficient strains are lower than those in wildtype mice. However, reovirus clearance is delayed in *Ctsl-/-* and *Ctss -/-* animals, likely due to the involvement of those proteases in T cell maturation and macrophage function, respectively. The immunodeficiencies imposed by cathepsin ablation thus complicate analysis of viral substrate-protease interactions in reovirus pathogenesis. This study also showed that mice pre-treated with cathepsin L-specific inhibitor CLIK-148 have higher survival rates than control animals, suggesting that transient protease inhibition may be a viable therapeutic strategy for viruses reliant on cathepsins for cell entry (71).

Sigma 3 is a Key Protease Substrate

The initial step in reovirus disassembly is the proteolysis of outer-capsid protein σ3. Following σ3 cleavage, the reovirus disassembly cascade proceeds, eventually culminating in endosomal membrane penetration. Sigma 3 is a globular protein, 365 residues in length, encoded by the S4 gene segment. A crystal structure of T3D σ3 was obtained in 2001 (109). The molecule is generally organized into a virion-proximal domain that binds μ1 and tethers the protein to the virion surface and a solvent-exposed virion-distal domain (109) (Figure I-4). There is substantial sequence identity between T1L and T3D σ3 proteins, with only 12 amino acids differing between the two (73). *In*

vitro biochemical studies suggest that σ3 proteolysis proceeds in a tightly regulated, stepwise fashion. Treatment of T1L σ3 with purified cathepsin L *in vitro* leads to an initial cleavage of σ3 at its extreme C-terminus, generating a species that migrates slightly faster when resolved by polyacrylamide gel electrophoresis (47). Further cathepsin L cleavage generates two fragments of approximately 29 kDa and 13 kDa, corresponding to the N- and C-termini, respectively. Protein sequencing of the cleavage products identified internal cathepsin L cleavage sites that reside between residues 243-244 and 250-251 (47) (Figure I-4). It is still unclear whether both or neither of these cleavage sites are utilized *in vivo*. However, these sequences fall within a so-called "protease-hypersensitive domain" of the protein that contains cleavage sites for several other proteases including chymotrypsin, proteinase K, and thermolysin (70, 96). Cleavage at these internal sites globally disrupts σ3 structure and results in the removal of σ3 from the virion. Together, these data suggest a model in which an initial, rate-limiting protease cleavage event occurs at the σ3 C-terminus, removing it from the molecule and exposing internal sites for subsequent cleavage events.

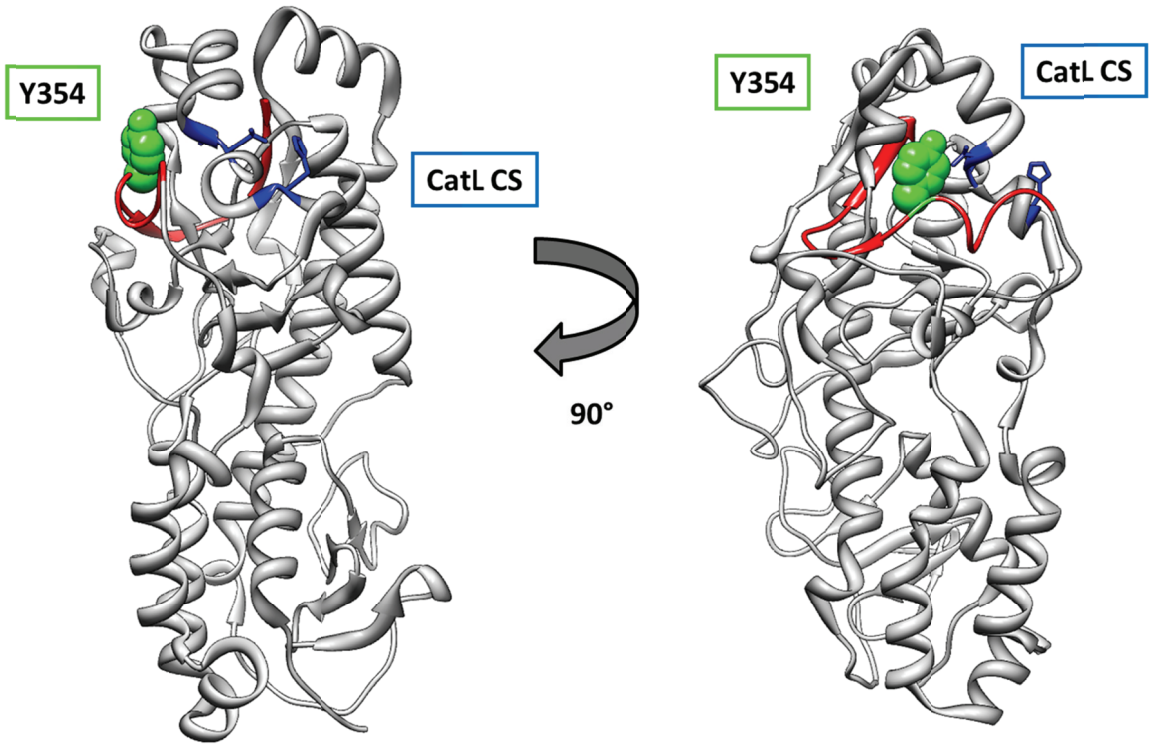

Figure I-4. Sigma 3 structure. A ribbon diagram of the σ3 protein is depicted in grey, shown in rotation. The C-terminal twenty amino acids are depicted in red. The side chains of two known cathepsin L cleavage sites (47) are depicted as stick models and shown in blue. The Y354 residue, a critical regulator of σ3 protease susceptibility(147), is shown as a green space-filling model. Modified from Olland 2001 (109).

A Tyr-to-His Mutation in Sigma 3 Diminishes Capsid Stability

Several previous have identified a single tyrosine-to-histidine mutation at σ3 position 354 as a key determinant of the kinetics of reovirus disassembly (5, 27, 49, 145) (Figure I-4). Viral isolates from cells persistently infected with reovirus undergo proteolysis more rapidly than parental viruses, a property that segregates with the σ3-encoding S4 gene (145). Sequences of S4 genes from these isolates revealed the Y354H mutation among others. Interestingly, persistently infected cells have altered expression

of cathepsins B and L, providing a mechanism of selection for viruses with accelerated disassembly kinetics (48). In subsequent studies, reovirus variants adapted to replication in the presence of the weak base, ammonium chloride, and the pan-cysteine protease inhibitor, E64, were found to contain the same σ3-Y354H mutation and undergo proteolysis more rapidly than wildtype virus (5, 27, 49). Together, these studies indicate that σ3-Y354H arises readily in response to protease-limiting selection pressure and induces a highly penetrant rapid disassembly phenotype by promoting σ3 proteolysis. However, σ3-Y354H is absent from primary reovirus isolates, with a single documented exception, type 3 Abney (T3A) σ3 (73), suggesting σ3-Y354H faces limiting selection in circulating strains. It is plausible that enhanced sensitivity to protease correlates with diminished biochemical capsid stability, thus reducing viral fitness by diminishing environmental persistence or infectivity from fomite surfaces.

Tyr354 is located in the σ3 C-terminal domain in close proximity to the putative C-terminal cathepsin cleavage site (109). The σ3 C-terminus opposes a hydrophobic pocket in the virion-distal domain of σ3. It is hypothesized that substitution of the mildly hydrophobic tyrosine at position 354 with the polar histidine destabilizes intramolecular interactions of the σ3 C-terminus. In support of this hypothesis, cryo-EM analysis of a reovirus isolate containing σ3-Y354H, PI 3-1, revealed that the PI 3-1 σ3 structure differs markedly from that of its parent virus, T3D (147). A cleft normally formed between the virion-proximal and virion-distal domains of σ3 is occluded in PI 3-1 σ3, the excess density there perhaps representing the dislocated σ3 C-terminal domain. Rearrangement of the C-terminal domain by Y354H may obviate the need for an initial C-terminal

cleavage event, affording protease molecules direct access to the internal cleavage sites, leading to rapid σ3 proteolysis.

With the advent of reverse genetics it became possible to introduce σ3-Y354H into an otherwise isogenic background, creating rsT3D-σ3Y354H (77). This virus replicates efficiently in the presence of E64 and displays accelerated disassembly kinetics when treated with exogenous protease, supporting the conclusion that residue 354 is capable of independently regulating σ3 proteolysis.

Reovirus Pathogenesis

Newborn mice are susceptible to reovirus infection and commonly used for studies of reovirus pathogenesis. Following peroral inoculation, reovirus replicates efficiently in the intestinal epithelium (3, 9, 118). Reovirus virions in the intestine undergo extracellular disassembly to ISVPs, a process catalyzed by digestive enzymes (2) and inhibited by peroral administration of protease inhibitors (2, 10). However, T3D does not efficiently infect mice per orum, likely because the T3D σ1 protein is hypersensitive to cleavage by digestive proteases (25, 103).

Reovirus disseminates throughout an infected host via both hematogenous and neural routes. Hematogenous spread from the intestine involves the lymphoid tissue of intestinal Peyer patches, which reovirus accesses via transcytosis through overlying microfold (M) cells (148). Type 1 reoviruses disseminate primarily via the hematogenous route, but it is unclear whether bloodstream-borne virus is cell-associated, and if so, what cells are involved in dissemination. In addition to hematogenous dissemination, type 3 reoviruses are neurotropic and access the CNS via peripheral nerves (100). Sectioning of

the sciatic nerve in animals inoculated in the hindlimb with type 3 reovirus prevents virus access to the spinal cord (137) but not the brain(13), suggesting type 3 viruses also access the brain via the bloodstream.

Apoptosis is an important means of tissue injury in reovirus-infected animals. Reovirus induces apoptosis in cell culture and *in vivo* (40, 115, 116, 139) using a process that requires virion-to-ISVP disassembly (31). Furthermore, membrane penetration by μ1 cleavage products μ1-φ and μ1-δ is required for apoptosis induction (35, 36). The finding of an isoleucine-to-lysine mutation in the μ1-φ domain that abrogates apoptosis induction but not membrane penetration suggests that μ1-φ induces apoptosis directly (35). Indeed, transient expression of isolated μ1-φ is sufficient to induce apoptosis in cell culture (30). T3D induces apoptosis more efficiently than does T1L, a difference that segregates with the S1 and M2 genes encoding σ1 and μ1, respectively (116, 140). Reovirus-mediated apoptosis requires NF-κB activation in most cell types (32), although there are important exceptions to this requirement, particularly in cardiac myocytes (28, 106).

The brain is an important end organ for reovirus infection. Type 3 reovirus strains are neurotropic (143, 144)**,** disseminate to the brain via both hematogenous and neural routes (3, 14), and induce a characteristic pattern encephalitis in infected animals (67). Type 3 strains infect neurons, in particular, in the pyramidal layers of the hippocampus and the Purkinje neurons of the cerebellum (3), resulting in a lethal encephalitis. Type 3 reovirus infection also damages neurons in the spinal cord, resulting in flaccid paralysis of the limbs of infected animals (57). Neurotropic reoviruses induce apoptosis in neurons both in cell culture and *in vivo* (36, 37, 56, 66, 107, 115), accounting for most of the reovirus-mediated damage in the CNS. Reovirus neuronal infection is independent of

both sialic acid (9) and JAM-A (3), suggesting that type 3 reovirus strains utilize an as-yet unidentified neural receptor. Type 1 reovirus strains also replicate in the brain of infected animals, but they primarily infect ependymal cells lining the ventricles of the brain, resulting in hydrocephalus (142) (14).

Reovirus reaches high titers in the hearts of infected animals and replicates efficiently in cultured cardiac myocytes (11, 124). Some reovirus strains induce significant cardiac injury with characteristic dystrophic calcification (127), a capacity that correlates with replication in cardiac myocyte cultures (11, 95), suggesting that cardiac injury in infected animals is directly attributable to virus-induced cellular damage. Reovirus is capable of myocardial injury in both immunocompetent mice and mice lacking either T cells (127) or T and B cells (126), indicating that adaptive immunity is not involved in reovirus myocarditis. However, there is ample evidence implicating interferon (IFN) as a modulator of reovirus-mediated myocarditis. Mice deficient in NF-κB subunit p50 (106), PKR (131), IRF1 (4), and IRF3(63) sustain enhanced cardiac injury following reovirus infection. Studies using reassortant reovirus strains indicate that the capacity to produce heart injury and replicate in cultured cardiac myocytes segregates with the viral S1, M1, L1, and L2 genes, encoding σ1, μ2, λ3, and λ2, respectively (95, 125, 127). Furthermore, μ2 suppresses IFN function by interfering with IRF9-stimulated interferon-stimulated gene (ISG) expression (151). Apoptosis induction also may play a role in reovirus-mediated myocarditis, as strain-specific differences in myocarditic capacity correlate with induction of apoptosis in cultured cardiac myocytes(97). Finally, cardiac damage in infected animals is greatly diminished by treatment with calpain- and

caspase-specific inhibitors, underscoring a role for apoptosis in reovirus myocarditis (38, 40).

Significance of the Research

Reovirus cell entry depends on enzyme-substrate interactions between host proteases and the viral outer capsid. The capsid protein σ3 is structurally and biochemically constrained by its required proteolysis at the appropriate time and place in an infected host. My dissertation research focused on the mechanisms that determine σ3 protease sensitivity, and in turn, how those mechanisms work to balance reovirus outer capsid stability at an optimal level for viral fitness. Furthermore, I am interested in the influence of protease utilization in reovirus disease pathogenesis.

Reovirus is not commonly associated with human disease. However, discoveries made using reovirus have applications to the study of other virus families, often in unanticipated fashion. For instance, the finding that cathepsins B and L are involved in reovirus disassembly was the first documentation of endosomal cathepsins mediating viral cell entry events. Since that discovery, cathepsins have been described in the entry pathways of several other viruses, including significant human pathogens such as the paramyxoviruses Hendra virus (111) and Nipah virus (44), the flavivirus Japanese encephalitis virus (99), and Ebolavirus (22). Cathepsins and other proteolytic enzymes are amenable to transient blockade and may thus represent attractive therapeutic targets, particularly for virulent pathogens for which treatment options are limited. Indeed, work conducted in our lab has shown that mice treated with a cathepsin-L-specific inhibitor tolerate the drug well and are protected from lethal reovirus challenge. Thus, enhancing

an understanding of protease-substrate interactions in the reovirus system may provide tangible benefits to studies of viruses more commonly associated with human disease.

Reovirus preferentially infects transformed cells in culture, suggesting its potential development as a cancer therapeutic. Treatment with reovirus impairs tumor growth in animal models and is well tolerated by human patients. In fact, type 3 Dearing (Reolysin™) is currently in Phase 3 clinical trials as an adjunct therapy for a variety of solid tumors (54, 74, 80). Although the precise mechanisms responsible for reovirus-mediated cytotoxicity in transformed cells are unclear (132), there are several pieces of evidence suggesting that proteolytic disassembly is key (1). Cathepsins and other cellular proteases are frequently upregulated and secreted in neoplastic tissues, leading to the hypothesis that the highly proteolytic milieu in the tumor microenvironment leads to rapid disassembly and enhanced reovirus-mediated cytotoxicity (1). Greater understanding of the interplay between cellular proteases and the reovirus outer capsid may facilitate refinements in oncolytic reovirus vector design.

Capsid protein rearrangement is an essential part of the replication cycle of most nonenveloped viruses. Accordingly, the ease with which capsid disassembly occurs is a quantifiable biophysical property of the virus particle and is likely to affect environmental persistence and transmission. It is also possible that ease of disassembly influences viral tissue tropism, kinetics of systemic dissemination, or any of a variety of factors that determine patterns of viral-mediated disease. However, very little is known about how altering viral capsid stability affects patterns of viral disease. With well-defined disassembly intermediates, a robust animal model, and facile reverse genetics,

reovirus is an excellent system for investigating capsid stability in nonenveloped viral pathogenesis.

To identify determinants of reovirus capsid stability, I focused on the outer-capsid protein σ3. We had previously identified a single tyrosine-to-histidine residue in the σ3 C-terminus, Y354H, as a critical regulator of σ3 protease sensitivity. This mutation is absent from circulating strains, with a single exception, strain T3A. However, T3A displays wildtype disassembly kinetics, supporting the conclusion that capsid stability is tightly regulated and suggesting the presence of a second-site Y354H suppressor. Using reverse genetics, I generated a panel of reovirus mutants incorporating T3A σ3 polymorphisms in the context of Y354H and identified a second determinant of σ3 protease sensitivity, the residue at position 198. Altering the glycine at residue 198 to a glutamate or a bulky hydrophobic residue ablated the Y354H disassembly phenotype, indicating that the two residues act in concert to control σ3 protease sensitivity.

Given the apparent fitness disadvantage imposed by σ3-Y354H, I tested whether viruses containing that mutation display altered disease in inoculated mice. I hypothesized that Y354H might limit reovirus-induced disease, impairing shedding and reducing host-to-host spread. Surprisingly, I found that viruses containing Y354H disseminated more rapidly than wildtype reovirus and induced greater lethality. Moreover, I observed that mice inoculated with Y354H mutant strains produced significantly greater cardiac injury than those infected with wildtype reovirus when administered perorally. Finally, I found that littermates of mice inoculated with σ3-Y354H-containing virus had greatly enhanced disease compared with littermates of mice

inoculated with wildtype virus, suggesting that diminished capsid stability imposed by σ3-Y354H actually enhances host-to-host spread.

Together, these studies provide new insights into the mechanisms by which reovirus modulates the stability of its outer capsid and established σ3 proteolysis as a key determinant of reovirus-mediated disease. Ultimately, this work may offer novel insights into our understanding of the disease pathogenesis of nonenveloped viruses and lead to improved reovirus therapeutics.

CHAPTER II

TWO POLYMORPHIC RESIDUES IN SIGMA 3 CONTROL PROTEASE SUSCEPTIBILITY AND CAPSID STABILITY

Introduction

The rate-limiting step in reovirus disassembly is the proteolysis of σ3, a component of the viral outer capsid. A single mutation in the σ3 C-terminus, σ3-Y354H, arises readily in response to protease-limiting selection and enhances the kinetics of proteolysis by altering σ3 structure (147). However, circulating strains of reovirus lack σ3-Y354H with the exception of T3A. Preliminary experiments showed that T3A is equally sensitive to the protease inhibitor E64 as T3D, suggesting that the σ3-Y354H phenotype is dampened in some way. Several σ3 residues are polymorphic between T3A and T3D, and I hypothesized that one of these polymorphisms in the T3A σ3 protein might oppose σ3-Y354H and negate its effect on disassembly. To test this hypothesis, I generated a panel of reovirus variants incorporating each σ3 polymorphism in the context of σ3-Y354H and tested their protease sensitivity, specific infectivity, particle stability, and kinetics of endosomal escape. I discovered that σ3 position 198, a glycine in T3D, suppresses Y354H when mutated to a glutamate, as in T3A σ3. I also observed the emergence of *de novo* tryptophan and valine mutations at position 198 that also suppressed Y354H, supporting the conclusion that Y354H imposes a fitness penalty on reovirus replication that is rescued by mutations at position 198. Finally, I demonstrated that purified virions containing unsuppressed His354 lost titer more rapidly when

exposed to heat than those with Tyr354, establishing a link between accelerated σ3 protease sensitivity and diminished reovirus biophysical stability.

Results

T3A and T3D are sensitive to protease inhibitor E64. The deduced amino acid sequences of T3A and T3D σ3 proteins contain eight polymorphic residues (Table II-1). Several of the T3A-T3D polymorphic residues including 354 are found in the virion-distal region of σ3, which is predicted to be accessible to protease (Figure II-1). To determine whether the Y354H polymorphism in T3A σ3 confers resistance to protease inhibitors, I tested the capacity of T3A, T3D, and T3D-σ3Y354H to grow in the presence of protease inhibitor E64. L929 cells were incubated in medium supplemented to contain 100 μM or 200 μM E64, adsorbed with T3A, T3D, and T3D-σ3Y354H, and incubated in the presence or absence of E64 for 24 h. Cells were lysed and viral titers in cell lysates were determined by plaque assay (Figure II-2). Despite the presence of histidine at position 354 in T3A σ3, yields of T3A were reduced 259-fold, approximating the reduction observed for T3D,195-fold, in the presence of 100 μM E64, whereas yields of T3D-σ3Y354H were diminished less than 10-fold at this E64 concentration. Replication of T3A and T3D was completely ablated in the presence of 200 μM E64, but yields of T3D-σ3Y354H were not further diminished. These findings suggest that one or more of the additional polymorphisms displayed by T3A σ3 suppresses the Y354H phenotype and restores optimal σ3 stability.

TABLE II-1. Polymorphic residues between T3A and T3D σ3. T3A and T3D differ at the eight indicated positions in the σ3 open reading frame.

Amino Acid Position	**28**	**108**	**180**	**198**	**215**	**233**	**347**	**354**
T3A	Thr	Ala	Val	Glu	Asn	Leu	Thr	His
T3D	Ala	Glu	Ile	Gly	Ser	Ser	Ile	Tyr

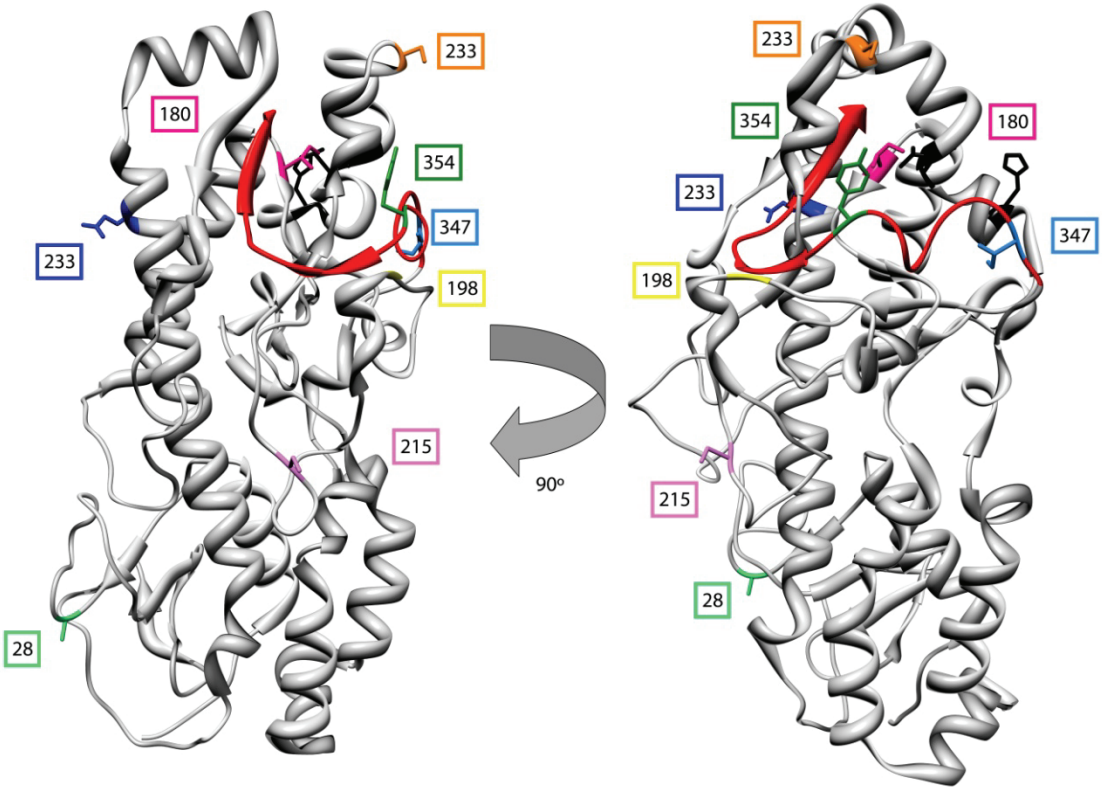

FIGURE II-1. Location of polymorphic residues in strains T3A and T3D σ3 proteins. A crystal structure of T3D σ3 (109) is shown highlighting polymorphic residues in T3A and T3D σ3 proteins, including Tyr354 (dark green), which is altered in reovirus variants selected for enhanced disassembly kinetics (27, 49, 145). The virion-distal domain of σ3 including the C-terminus (depicted in red) is at the top of the figure. The virion-proximal region including the N-terminus is at the bottom. Putative cathepsin L cleavage sites (determined for strain T1L) between amino acids 243 and 244 and between 250 and 251 are depicted in black (47).

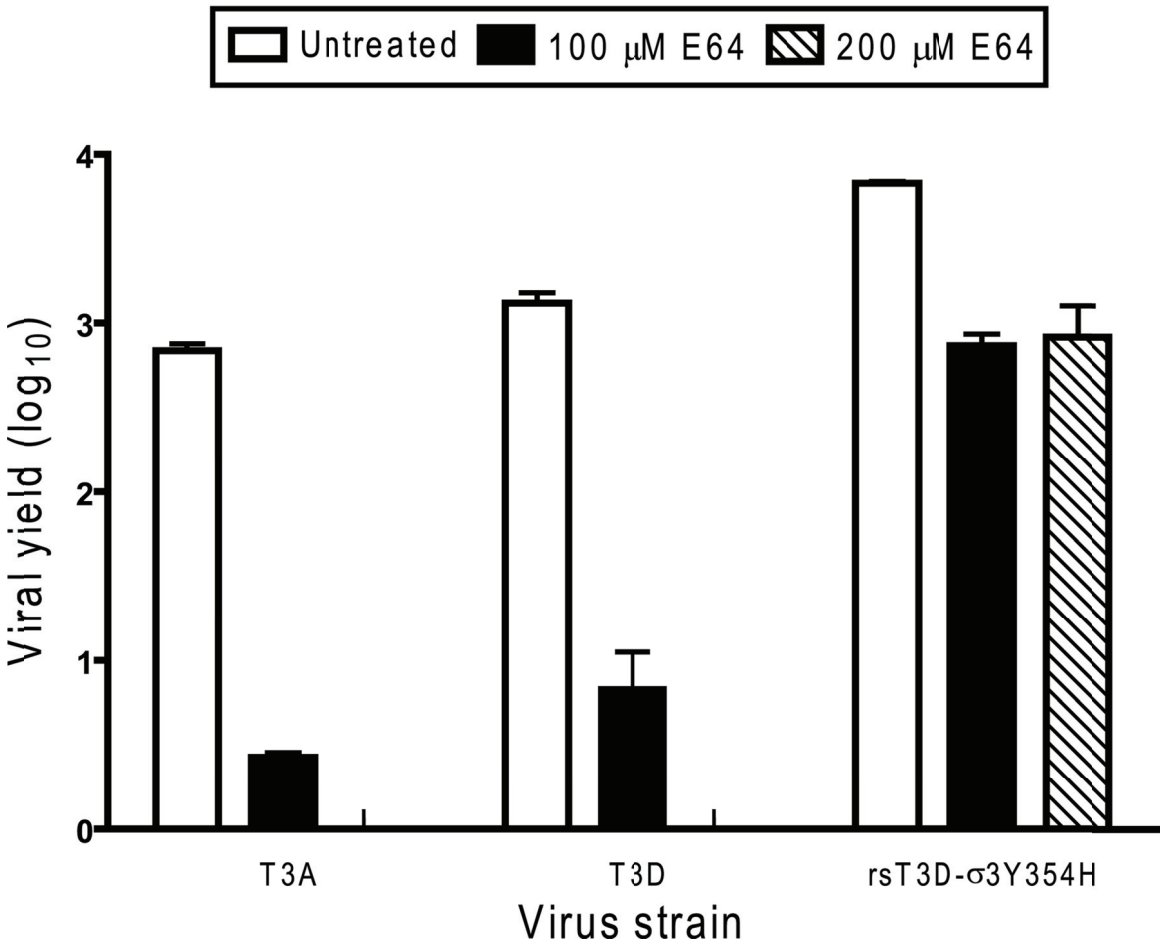

FIGURE II-2. Replication of T3A, T3D, and rsT3D-σ3Y354H in L929 cells treated with E64. Monolayers of L929 cells were preincubated for 4 h in medium supplemented with or without E64 at the concentrations shown. The medium was removed, and cells were adsorbed with virus at an MOI of 2 PFU per cell. After adsorption for 1 h, the inoculum was removed and fresh medium with or without E64 was added. After incubation at 37°C for 24 h, cells were frozen and thawed twice, and viral titers were determined by plaque assay. The results are presented as the mean viral yields, calculated by dividing titer at 24 h by titer at 0 h for each concentration of E64, for triplicate experiments. Yields of less than zero are not shown. Error bars indicate SD.

G198E confers susceptibility to E64 in the context of Y354H. To identify residues in T3A σ3 that suppress the capacity of the Y354H polymorphism to confer viral growth in the presence of protease inhibitors, I engineered a panel of reovirus variants that incorporate single T3A-T3D polymorphisms in the context of T3D-σ3Y354H but are otherwise isogenic with T3D (Table II-2). Despite several attempts, I could not recover T3D-σ3A28T,Y354H. In addition, T3D-σ3 S233L,Y354H was recovered only with a concomitant glycine-to-tryptophan mutation at position 198 of σ3. Each of the other variants was rescued and propagated to high-titer working stocks.

I tested each of the variant viruses for replication in the presence of E64 (Figure II-3). As before, yields of T3A and T3D were diminished substantially by this inhibitor, whereas yields of T3D-σ3Y354H were only modestly impaired. Similarly, yields of T3D-σ3E108A, T3D-σ3I180V, T3D-σ3S215N, and T3D-σ3I347T were only slightly diminished by E64. In sharp contrast, yields of T3D-σ3G198E,Y354H were markedly decreased in the presence of E64, approximating those of T3A and T3D. These findings suggest that a glycine-to-glutamic acid mutation at position 198 independently suppresses the Y354H phenotype in T3A and limits its sensitivity to the protease inhibitor E64.

TABLE II-2. Reovirus variants in which polymorphic residues in T3D σ3 are exchanged with those in T3A σ3. Reovirus variants were engineered using plasmid-based reverse genetics. Each reovirus variant is isogenic with T3D with the exception of His354 and a single additional T3A residue as shown. Italics indicate viruses that were not successfully recovered.

Amino Acid Position	**28**	**108**	**180**	**198**	**215**	**233**	**347**	**354**
T3D	A	E	I	G	S	S	I	Y
T3A	T	A	V	E	N	L	T	H
T3D-σ3Y354H	A	E	I	G	S	S	I	H
T3D-σ3A28T,Y354H	*T*	*E*	*I*	*G*	*S*	*S*	*I*	*H*
T3D-σ3E108A,Y354H	A	A	I	G	S	S	I	H
T3D-σ3I180V,Y354H	A	E	V	G	S	S	I	H
T3D-σ3G198E,Y354H	A	E	I	E	S	S	I	H
T3D-σ3S215N,Y354H	A	E	I	G	N	S	I	H
T3D-σ3S233L,Y354H	*A*	*E*	*I*	*G*	*S*	*L*	*I*	*H*
T3D-σ3I347T,Y354H	A	E	I	G	S	S	T	H

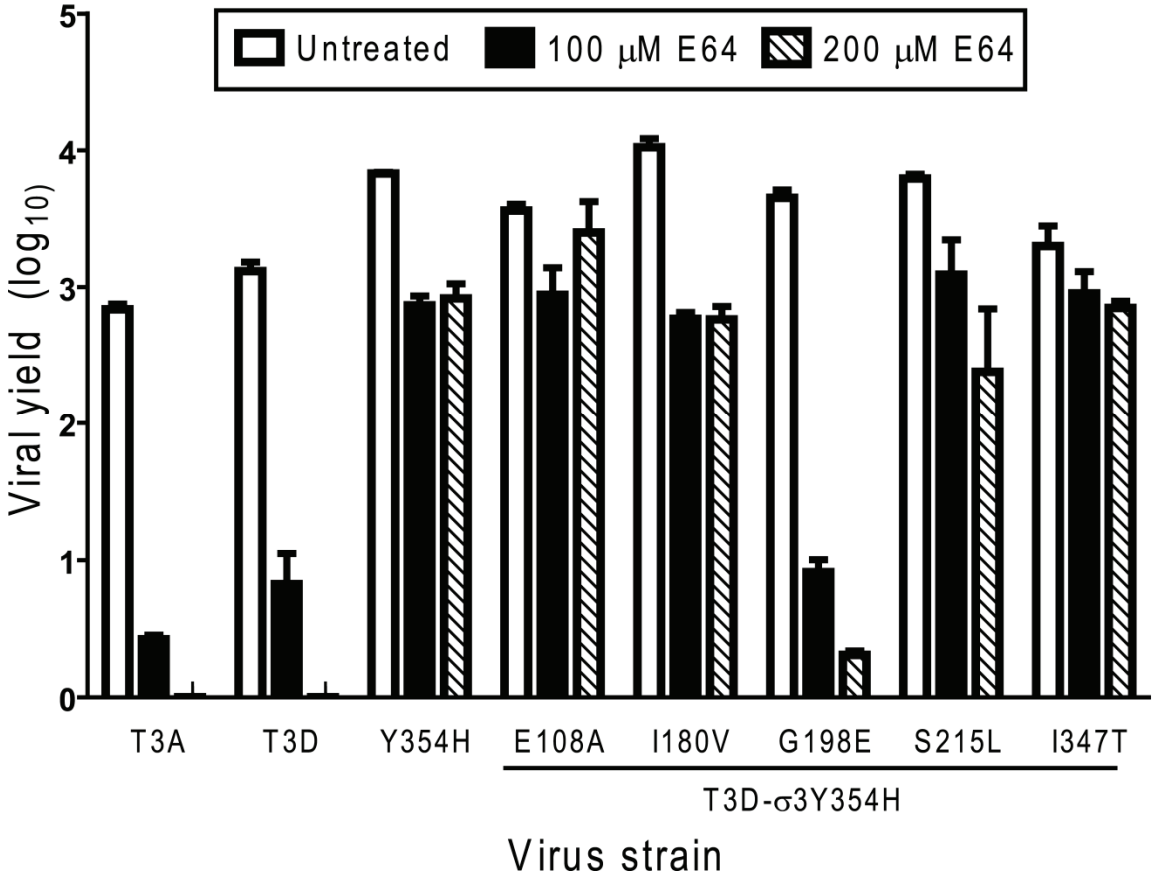

FIGURE II-3. E64 susceptibility of T3A-T3D variant viruses. Monolayers of L929 cells were preincubated for 4 h in medium supplemented with or without E64 at the concentrations shown. The medium was removed, and cells were adsorbed with virus at an MOI of 2 PFU per cell. After adsorption for 1 h, the inoculum was removed, and fresh medium with or without E64 was added. After incubation at 37°C for 24 h, cells were frozen and thawed twice, and viral titers were determined by plaque assay. The results are presented as the mean viral yields, calculated by dividing titer at 24 h by titer at 0 h for each concentration of E64, for triplicate experiments. Yields of less than zero are not shown. Error bars indicate SD.

Cathepsin L sensitivity of T3A-T3D variant viruses. Cathepsin proteases catalyze reovirus disassembly within cellular endosomes (47, 71). To determine whether T3A-T3D polymorphisms alter capsid disassembly when treated with endosomal proteases, I digested virions of T3A, T3D, T3D-σ3Y354H, and the T3A-T3D variants *in vitro* with purified human cathepsin L (18). At 30-min intervals, aliquots were removed from the digestion mixtures, and viral proteins were resolved by SDS-PAGE and visualized using colloidal blue staining (Figure II-4A). Intensity of the band corresponding to σ3 remained relatively constant for T3A and T3D over the 240-min time course, as did the band corresponding to μ1C. However, in these experiments, T3D-σ3Y354H displayed almost complete loss of σ3 protein within 60 min. In addition, the band corresponding to μ1C in T3D-σ3Y354H diminished in intensity over the course of protease treatment, and the appearance of a band corresponding to the δ fragment of μ1C was noted for this virus. Each of the variant viruses was observed to undergo disassembly with kinetics similar to those of T3D-σ3Y354H (Figure II-4A) with the exception of T3D-σ3G198E,Y354H, which displayed a digestion profile similar to that of T3A and T3D.

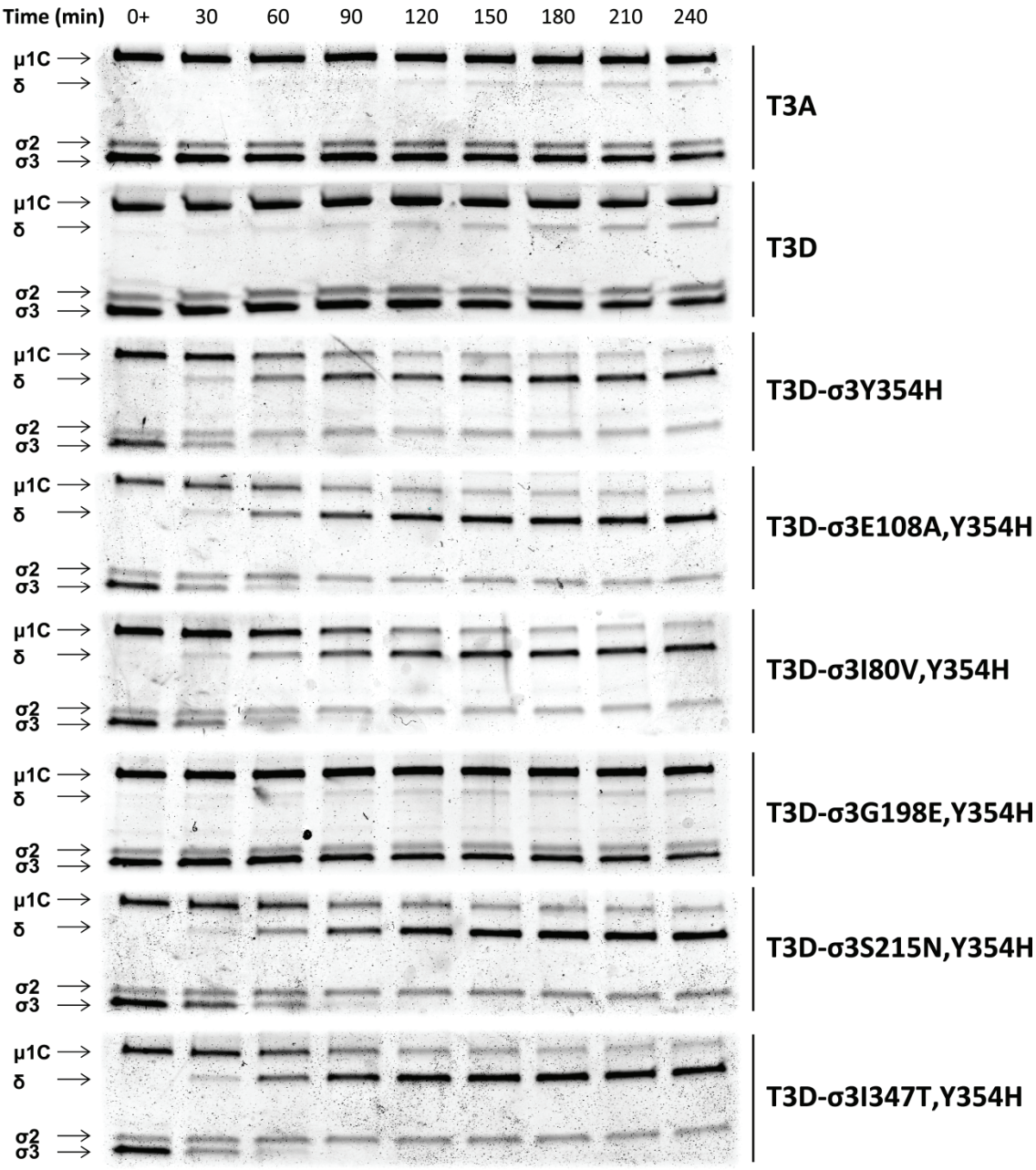

FIGURE II-4A. Digestion of reovirus strains with cathepsin L. A. Purified virions were treated with human cathepsin L (18) for the intervals shown and loaded into wells of 4-20% gradient polyacrylamide gels. After electrophoresis, the gels were stained with colloidal blue (Invitrogen). Viral proteins μ1C, δ, σ2, and σ3 are labeled at the left. The experiments shown are representative of two performed for each virus.

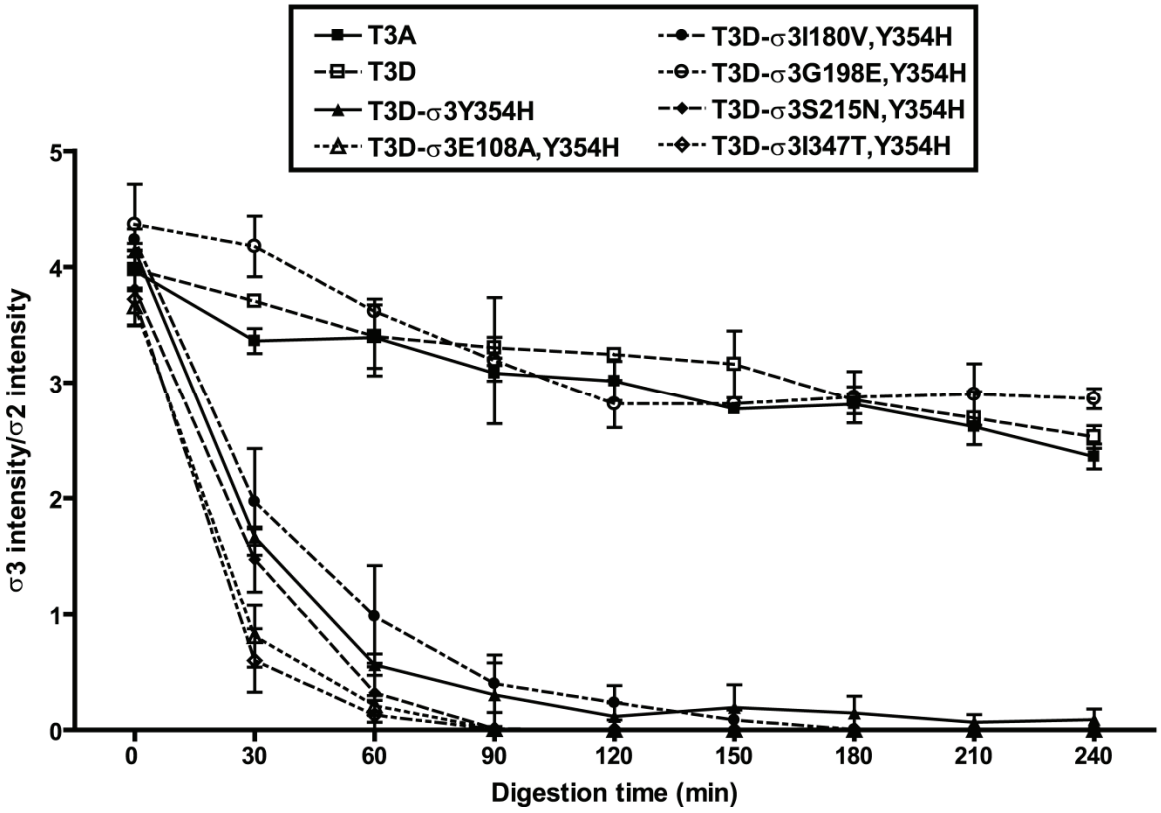

FIGURE II-4B. Digestion of reovirus strains with cathepsin L. B. Intensities of bands corresponding to reovirus proteins were quantified using the Odyssey software package (Li-Cor). Results are expressed as the ratio of σ3 band intensity to σ2 band intensity to control for differences in loading for two independent experiments. Error bars indicate SD.

Specific infectivity of reovirus variants. I next considered the possibility that one or more of the σ3 polymorphisms in our panel of variant reovirus strains might affect assembly of σ3 onto nascent virions and thus compromise infectivity. To test this hypothesis, I examined the specific infectivity of our variant panel by calculating particle/PFU ratios for several independent preparations of each virus (Figure II-5). I observed that most of the virion stocks tested displayed particle/PFU ratios between 100 and 500, consistent with reported values for type 3 reovirus strains (60) and our previous

observations (Dermody, unpublished observations). Although we observed some prep-to-prep variation, there were no significant differences between the variant and parental viruses (ANOVA, $P > .05$). I concluded that the σ3 mutations introduced in our variant panel do not substantially affect reovirus replicative efficiency and thus likely do not alter capsid assembly.

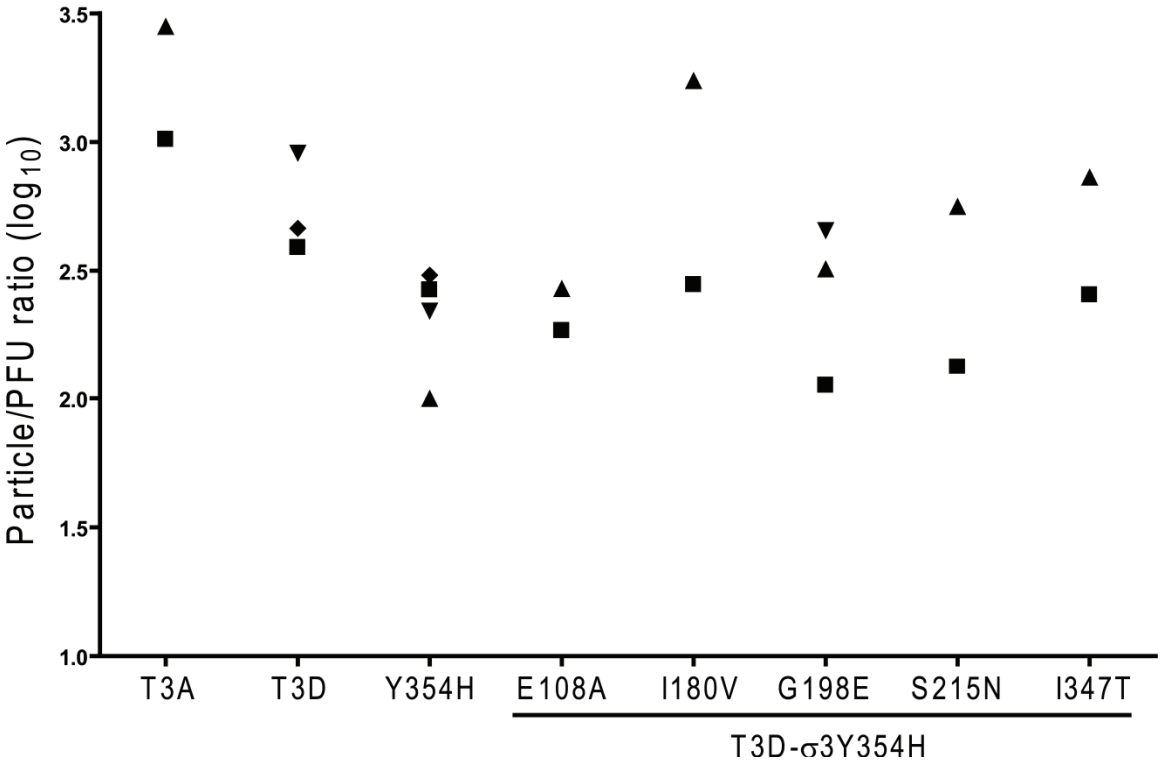

FIGURE II-5. Infectivity of reovirus variants. Purified virions of variant viruses were generated from independent cultures of L929 cells (approximately 4×10^8 cells) using CsCl-gradient centrifugation. Particle number was quantified using the equivalence 1 $O.D._{260} = 2.1 \times 10^{12}$ particles/mL. The titer of each preparation was determined by plaque assay. The results are presented as particle/PFU ratio. Data points indicate independent viral purifications.

Outer capsid mutations affect reovirus heat sensitivity. To assess whether the differences in protease sensitivity of our variant viruses correlate with biochemical measures of capsid stability, I determined the relative loss of titer of our variant panel following heat treatment. Samples of each virus were diluted to a titer of 2×10^8 and placed at 55°C for 1 h. Aliquots were removed at 15-min intervals, and titers were determined by plaque assay (Figure II-6). I observed that T3D-σ3Y354H lost titer more rapidly at elevated temperature than did either T3A or T3D. Additionally, each of the variant viruses tested lost titer at rates similar to T3D-σ3Y354H, again with the exception of T3D-σ3G198E,Y354H. The titer of that virus diminished at a rate commensurate with that observed for T3A and T3D. The fact that enhanced protease sensitivity and altered sensitivity to heat are correlated in the context of Y354H suggests that this residue controls both properties through a common structural mechanism.

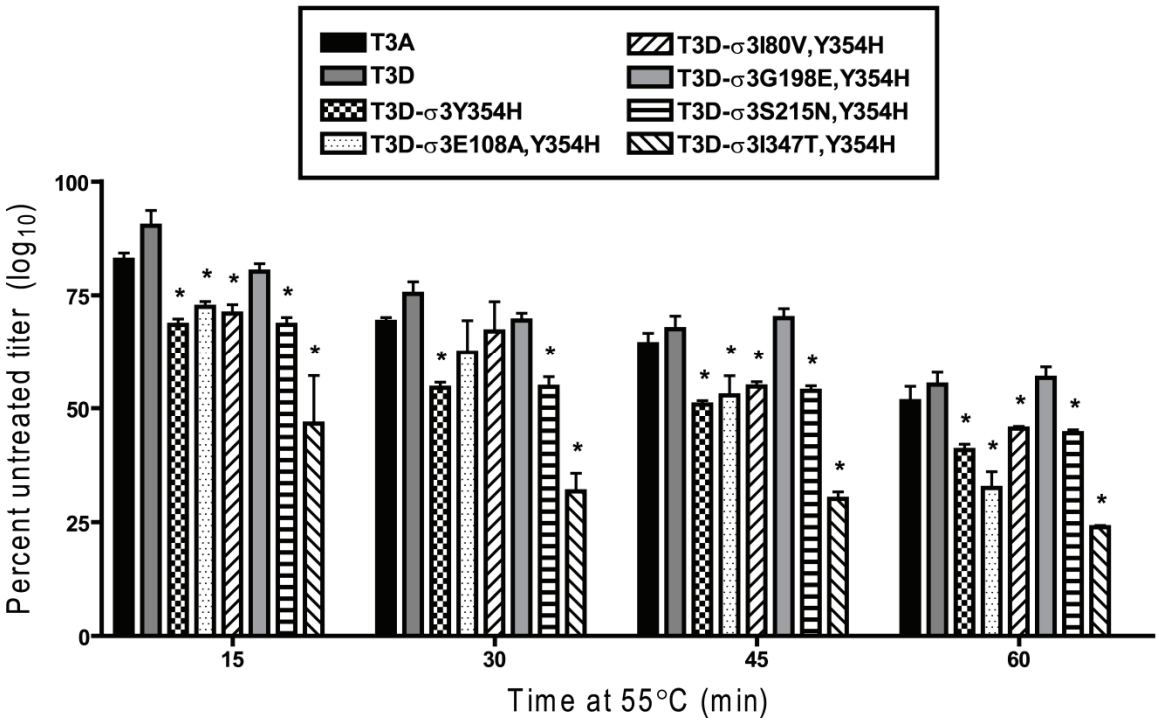

FIGURE II-6. Resistance of reovirus variants to inactivation by heat. Purified virions of reovirus variants were diluted to a concentration of 2×10^8 particles per ml in virion storage buffer and incubated at 55°C for 60 min. At 15-min intervals, samples were removed and placed on ice for 15 min. Titers were determined by plaque assay. Results are presented as percent of mean viral titer of untreated samples per interval of incubation, for triplicate experiments. Error bars indicate SD; *, $P \leq .05$ in comparison with T3D.

Enhanced outer-capsid protease sensitivity facilitates endosomal escape.

Following binding to cell-surface receptors, reovirus particles are thought to be internalized via clathrin-dependent endocytosis (16, 17, 50, 91). Cleavage of σ3 by endosomal cathepsins is required for particle disassembly and subsequent escape from the endosome into the cytoplasm (5, 6, 20, 24, 47, 68, 129) . To determine whether the enhanced susceptibility to proteolytic cleavage mediated by σ3-Y354H alters the kinetics with which reovirus particles escape host cell endosomes, I took advantage of the fact that reovirus disassembly is abrogated by preventing the pH drop required for efficient

cathepsin cleavage while intact particles are still resident in endosomes (43, 133). I adsorbed monolayers of L929 cells with variant reovirus strains at 4°C for 1 h to synchronize viral attachment, warmed the cells to 37°C, and added ammonium chloride at various intervals following warming to prevent endosome acidification. Cells were incubated overnight and scored for viral infectivity by indirect immunofluorescence (Figure II-7). Variant viruses containing the σ3-Y354H mutation, with the exception of T3D-σ3G198E,Y354H, escaped ammonium chloride blockade approximately 45 min earlier than either T3A or T3D. These findings indicate that enhanced outer-capsid protease sensitivity accelerates access of reovirus to the cytoplasm for subsequent steps in its replication cycle.

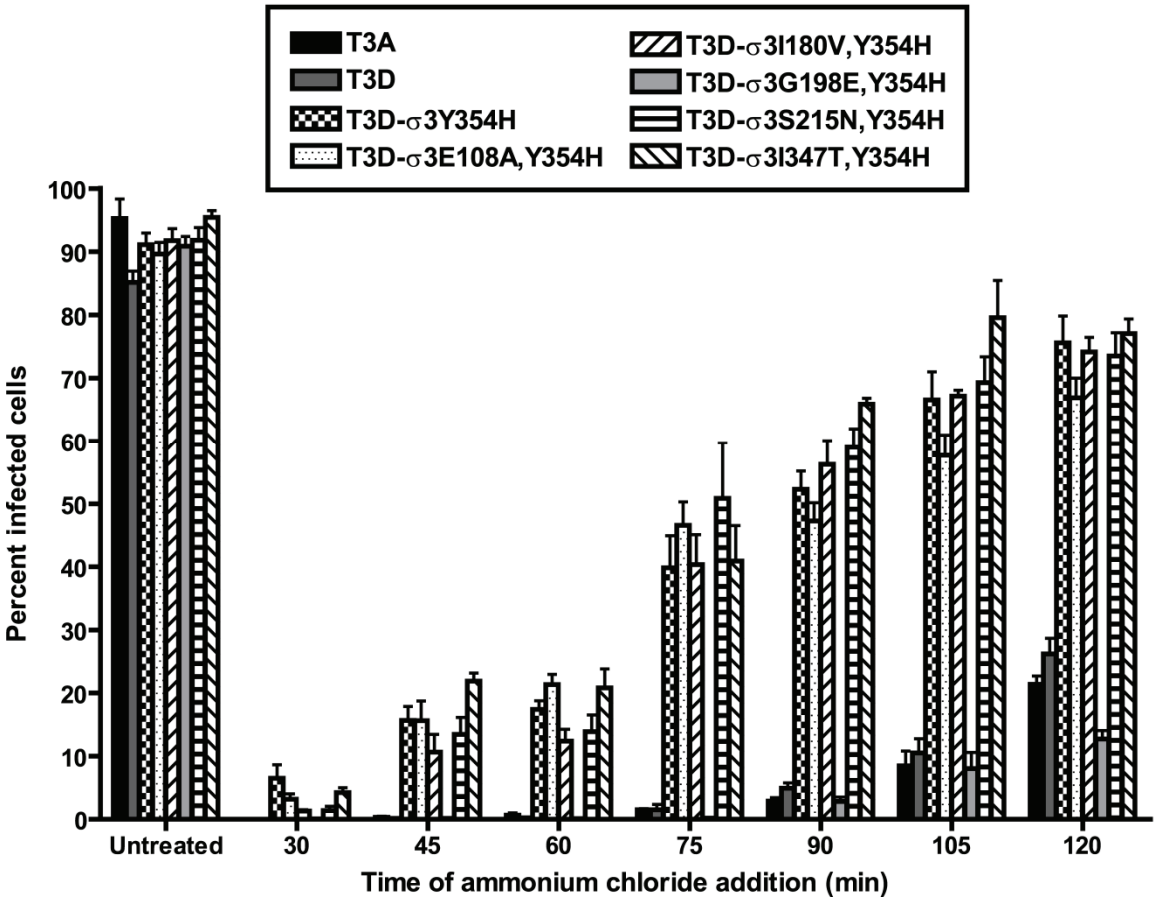

FIGURE II-7. Kinetics of ammonium chloride bypass by reovirus variants. Monolayers of L929 cells were adsorbed with reovirus variants at an MOI of 25 PFU per cell at 4°C. After adsorption for 1 h, the inoculum was removed, fresh pre-warmed medium was added, and cells were warmed to 37°C. At the times shown post-adsorption, ammonium chloride was added to a final concentration of 25 mM. After incubation at 37°C for 20 h, cells were fixed with methanol at -20°C, and infectivity was assessed by indirect immunofluorescence. The results are presented as percent of cells infected, normalized to untreated wells, for triplicate experiments. Error bars indicate SD.

Residue 198 second-site changes. One of the variant viruses, T3D-σ3S233L,Y354H, could be recovered only in combination with a glycine-to-tryptophan substitution at position 198. In addition, multiple isolates of T3D-σ3I347T,Y354H contained *de novo* glycine-to-valine mutations at position 198. To determine whether

these second-site mutations affect reovirus disassembly, I tested the effect of E64 treatment on the replication of variants containing these alterations (Figure II-8). Viruses containing either Val198 or Trp198 in the context of Y354H had modestly enhanced E64 sensitivity in comparison to that of T3D-σ3Y354H. In particular, introduction of Val198 restored the E64 sensitivity of T3D-σ3G198V,I347T,Y354H to that of T3D. The E64 sensitivity of T3D-σ3G198W,S233L,Y354H was intermediate between that of T3D and T3D-σ3Y354H, althoughT3D-σ3G198W,S233L,Y354H produced lower peak titers in the absence of protease inhibitor than did T3D. These findings underscore the importance of residue 198 in determining σ3 stability and suggest that the molecular basis of Y354H suppression may differ depending on the biochemical nature of the amino acid at that position.

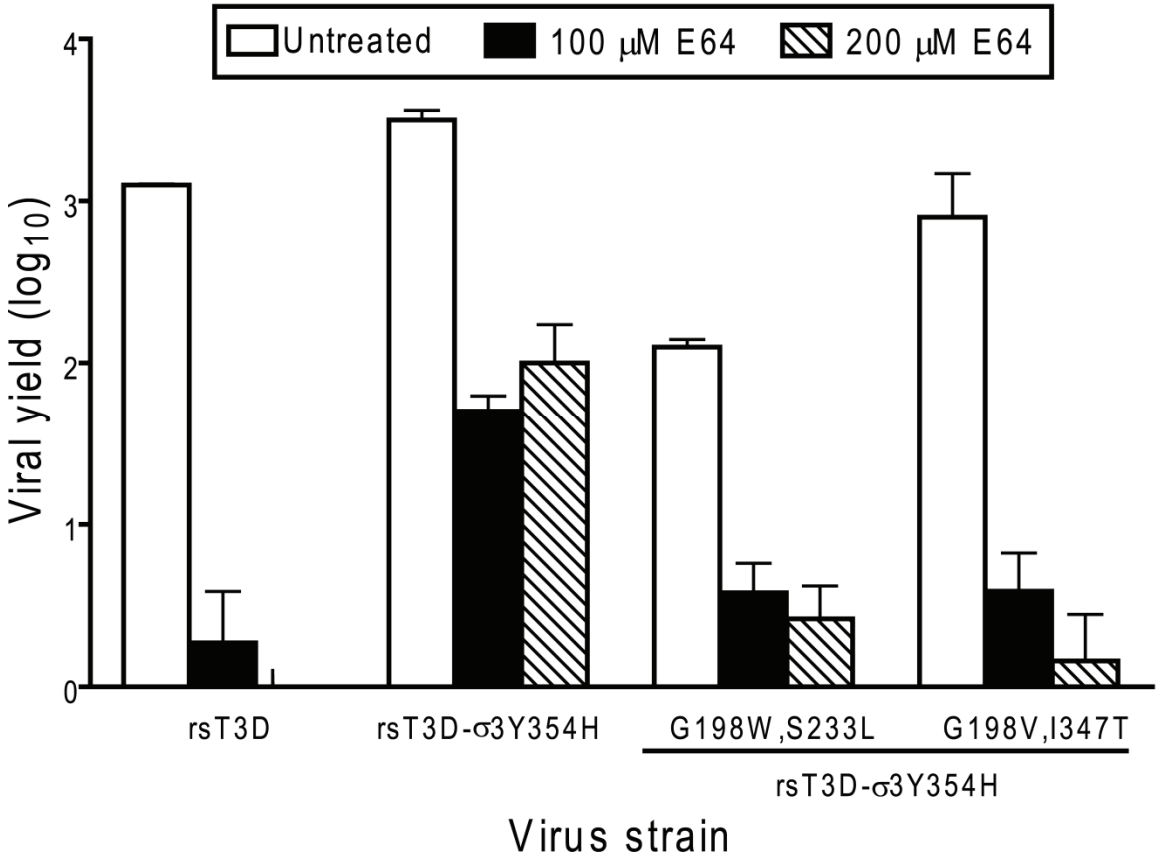

FIGURE II-8. E64 sensitivity of reovirus strains with second-site mutations. Monolayers of L929 cells were preincubated for 4 h in medium supplemented with or without E64 at the concentrations shown. The medium was removed, and cells were adsorbed with reovirus strains at an MOI of 2 PFU per cell. After adsorption for 1 h, the inoculum was removed, and fresh medium with or without E64 was added. After incubation at 37°C for 24 h, cells were frozen and thawed twice, and viral titers were determined by plaque assay. The results are presented as the mean viral yields, calculated by dividing titer at 24 h by titer at 0 h for each concentration of E64, for triplicate experiments. Yields of less than zero are not shown. Error bars indicate SD.

Discussion

Nonenveloped viruses must undergo particle disassembly to initiate an infectious cycle. The rate-limiting step in reovirus disassembly is the enzyme-mediated cleavage of σ3 protein in endosomes of infected cells (5, 17, 24, 129, 133). Surface features of σ3 that influence its capacity to serve as an enzyme substrate are not well understood. A single mutation in reovirus T3D σ3 protein, Y354H, enhances susceptibility of the reovirus virion to protease and confers viral resistance to protease inhibitors (5, 27, 49, 147). Structural evidence suggests that enhanced susceptibility to protease conferred by Y354H is due to an intra-molecular rearrangement of domains in σ3 that enhances access to internal protease-cleavage sites (147). However, this model has not been explicitly tested. Selection of reovirus mutants under conditions that diminish endosomal protease activity yields viruses containing the σ3-Y354H mutation (5, 27, 49), suggesting that capsid-destabilizing mutations are advantageous in certain settings. The importance of capsid stability in other phases of the reovirus life cycle is unclear.

In this study, I identified a new surface determinant of reovirus capsid stability located at position 198 in σ3. To our knowledge, reovirus strain T3A is the only field-isolate reovirus strain reported to date that contains a histidine at position 354 (73). Based on previous understanding of the phenotype of virus strains containing σ3-Y354H, I anticipated that T3A would be resistant to protease inhibitors and display enhanced susceptibility to proteases in comparison to T3D. Surprisingly, I found that T3A has E64 sensitivity similar to that of T3D despite the presence of His354 in σ3. I also observed that T3A and T3D have similar *in vitro* disassembly kinetics when treated with the

endosomal protease cathepsin L. Based on these observations, I hypothesized that other residues in T3A σ3 that differ from T3D σ3 suppress the Y354H phenotype.

I used plasmid-based reverse genetics to generate a panel of reovirus variants to test the contributions made by each T3A-T3D polymorphic residue to capsid stability in an otherwise isogenic background that includes Y354H. Despite numerous attempts, a virus containing an aspartate-to-threonine change at position 28, T3D-σ3D28T,Y354H, could not be recovered. Amino acid 28 is located in a virion-proximal domain of σ3 (Figure II-1) that is important for interactions of σ3 with μ1 during virion assembly (85). It is possible that mutations at position 28 impair interactions between σ3 and μ1 (85), hindering recovery of T3D-σ3D28T,Y354H. The recovered variant viruses had no overt defects in replication or specific infectivity (Figure II-5). All of the T3A-T3D variant viruses are resistant to cysteine-protease inhibitor E64 and thus phenocopy T3D-σ3Y354H, except the virus containing a glycine-to-glutamate change at position 198, T3D-σ3G198E,Y354H. Yields of T3D-σ3G198E,Y354H are markedly diminished in cells treated with E64. Concordantly, all members of the T3A-T3D variant panel except T3D-σ3G198E,Y354H display kinetics of digestion by cathepsin L similar to T3D-σ3Y354H. Moreover, I also observed that all of the variant viruses escape an endosomal infectivity block more rapidly than T3A or T3D, again excepting T3D-σ3G198E,Y354H. Together, these results provide strong evidence that suppression of the Y354H phenotype in T3A is solely attributable to the glycine-to-glutamate polymorphism at position 198.

Another virus, T3D-σ3S233L,Y354H, could be recovered only with an accompanying glycine-to-tryptophan mutation at position 198. In addition, four of the seven T3D-σ3I347T,Y354H clones sequenced contained a second-site mutation at

position 198, specifically, a glycine-to-valine substitution. I found that T3D-σ3G198W,S233L,Y354H and T3D-σ3G198V,I347T,Y354H had increased E64 susceptibility in comparison to that of T3D-σ3Y354H, although neither virus was as sensitive to this protease inhibitor as was T3A or T3D. The observation of two different, independently arising mutations at position 198 in σ3 supports the conclusion that residue 198 is a key determinant of σ3 protease susceptibility. It is plausible that mutations at positions 233 and 347 enhance selection of Y354-suppressive mutations, perhaps by further destabilizing σ3.

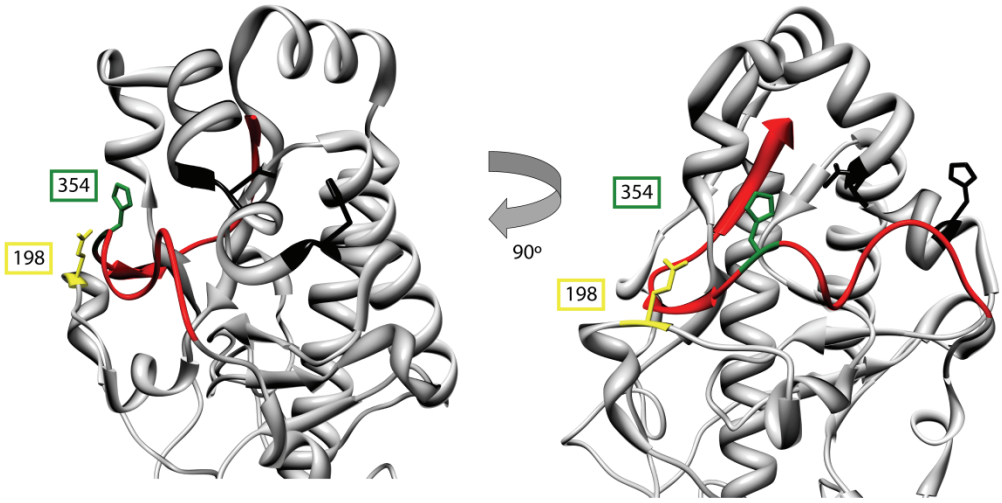

FIGURE II-9. Residues 198 and 354 define an amino acid network regulating σ3 proteolysis. The virion-distal domain of T3D σ3 is shown. The C-terminus is depicted in red. Glu198 and His354 are modeled in yellow and green, respectively, and are drawn in stick representation. The amino acids corresponding to the two putative cathepsin L cleavage sites, residues Val243-Thr244 and Gly250-His251 (47), are shown in stick representation.

The σ3 C-terminus is thought to control the rate of σ3 cleavage by restricting protease access to cleavage sites located internally within the protein (47, 85, 147). The C-terminal domain of σ3 localizes to a solvent-exposed surface of the σ3/μ1 heterohexamer and is not predicted to directly interact with other viral proteins (85). There is some structural evidence suggesting that the Y354H mutation accelerates σ3 cleavage by dislocating the σ3 C-terminus, affording easier access to internal cleavage sites (147). The observation that residue 198 suppresses Y354H indirectly supports this model (Figure II-9). The σ3 C-terminus (red) covers the cleavage sites (black) located between residues 243-244 and 250-251. Substitution of Tyr354 in the C-terminus (green) with histidine, a basic amino acid, may disrupt hydrophobic interactions required for proper folding of the σ3 C-terminus. Low-resolution cryo-EM reconstructions of σ3-Y354H reveal added density in a hinge region between the virion proximal and virion distal σ3 lobes that is absent in T3D σ3 (147). This increase in density may represent the dislocated C-terminus of the molecule. Residue 198 in σ3 is located on a loop directly opposed to residue 354. It is possible that the glycine-to-glutamate polymorphism observed in T3A stabilizes the C-terminus through charge-charge interactions with His354. Substitution of residue 198 with hydrophobic amino acids, such as tryptophan and valine as observed in this study, also may stabilize the σ3 C-terminus, perhaps by steric interactions that limit its mobility. The finding that alterations at positions 233 and 347 elicit compensatory hydrophobic mutations at position 198 suggests that more complex intra-molecular rearrangements of σ3 may occur in those viruses. Interestingly, a virus selected for growth in the presence of E64, D-EA3, contains two mutations in σ3, the expected Y354H and a glycine-to-arginine change at position 198 (49). In that study,

Arg198 failed to suppress Y354H, perhaps because it fails to neutralize the basic charge of His354. Although my results suggest that σ3 residue 198 is a key surface determinant of reovirus outer-capsid stability, the ready selection of mutations at position 198 that incorporate amino acids with a range of biochemical properties may point to subtle roles for residue 198 either in maintaining capsid stability or in other aspects of reovirus replication.

The observation that σ3-Y354H is rare in circulating reovirus strains and exists coincident with suppressor mutations in T3A σ3 suggests that reovirus strains suffer a fitness penalty for mutations that destabilize the outer capsid. The reovirus life cycle involves fecal-oral transmission between infected hosts, a process that requires some degree of resistance to degradation. Viruses with diminished outer-capsid stability may have decreased viability outside a mammalian host, which would reduce their likelihood of encountering a new host. We note that viruses containing uncompensated σ3-Y354H lose titer more rapidly at elevated temperature than T3A or T3D (Figure II-6), suggesting that such viruses incur diminished environmental persistence or decreased infectivity from fomite surfaces. However, it is also possible that destabilization of the outer capsid adversely affects other aspects of viral replication or virus-host interactions. More work is necessary to identify the specific steps of the viral life cycle that are so affected. The findings reported in this study identify a network of residues that determine the stability of reovirus σ3 and provide insight into mechanisms used by nonenveloped viruses to maintain optimum capsid stability. In the next chapter I present data demonstrating a role for σ3 protease sensitivity in determining patterns of reovirus-mediated disease.

CHAPTER III

DIMINISHED OUTER CAPSID STABILITY ENHANCES REOVIRUS VIRULENCE AND HOST-TO-HOST SPREAD

Introduction

Reovirus depends upon host proteases to catalyze disassembly. Key residues in reovirus outer-capsid protein σ3, particularly σ3-Y354H, control the rate of σ3 proteolysis, which in turn determines the kinetics of reovirus uncoating. In studies described in chapter II, I showed that the mechanism by which σ3-Y354H accelerates σ3 proteolysis also correlates with diminished biophysical capsid stability. Furthermore, utilization of host proteases during cell entry is a strategy shared by several families of viruses, and capsid stability is a universal physical property of nonenveloped virions. However, virtually nothing is known about the effect of altering protease utilization or overall capsid stability on disease pathogenesis. I therefore sought to investigate the differences in disease induced by reovirus strains with σ3-Y354H, particularly T3D-σ3Y354H. I chose this virus because its parent strain, T3D, is neurotropic and has a relatively low lethal dose when delivered into newborn mice intramuscularly or intracranially. Given the rarity of σ3-Y354H in primary reovirus isolates, I hypothesized that the mutation would attenuate reovirus virulence. Surprisingly, this series of experiments instead identified Y354H as a potent enhancer of reovirus virulence and identified a novel role for σ3 in reovirus disease pathogenesis.

Results

Diminished reovirus outer-capsid stability correlates with enhanced lethality. To investigate whether differences in outer-capsid stability influence reovirus disease pathogenesis, I inoculated newborn mice in the hindlimb with 10^5 PFU of either wild-type rsT3D or the protease-hypersensitive mutant rsT3D-σ3Y354H and monitored infected animals for survival (Figure III-1). Surprisingly, I found that a significantly higher percentage of mice inoculated with rsT3D-σ3Y354H succumbed to infection than those infected with rsT3D. The median survival interval for mice infected with rsT3D was approximately 4 days longer than that observed for animals infected with rsT3D-σ3Y354H, suggesting that the latter virus replicated to lethal titers more rapidly than rsT3D. Type 3 reovirus strains are neurotropic, inducing lethal encephalitis in infected animals (57, 142, 143). Accordingly, animals infected with both rsT3D and rsT3D-σ3Y354H displayed neurological signs, including bilateral flaccid paralysis, dyskinesias, myoclonic jerks, and occasional seizures.

To confirm that the enhanced virulence of rsT3D-σ3Y354H is attributable to the capsid-destabilizing effects of the Y354H mutation in σ3, I inoculated newborn mice with 10^5 PFU of rsT3D-σ3G198E,Y354H, which is isogenic with rsT3D-σ3Y354H with the exception of a glycine-to-glutamate mutation at position 198 in σ3. The G198E mutation suppresses the destabilizing effects of Y354H on the reovirus outer capsid and restores wild-type protease sensitivity and disassembly kinetics (45). Interestingly, rsT3D-σ3G198E,Y354H had reduced lethality in comparison with wild-type rsT3D and rsT3D-σ3Y354H. Thus, diminution of outer-capsid stability associated with σ3-Y354H results in a marked increase in reovirus virulence.

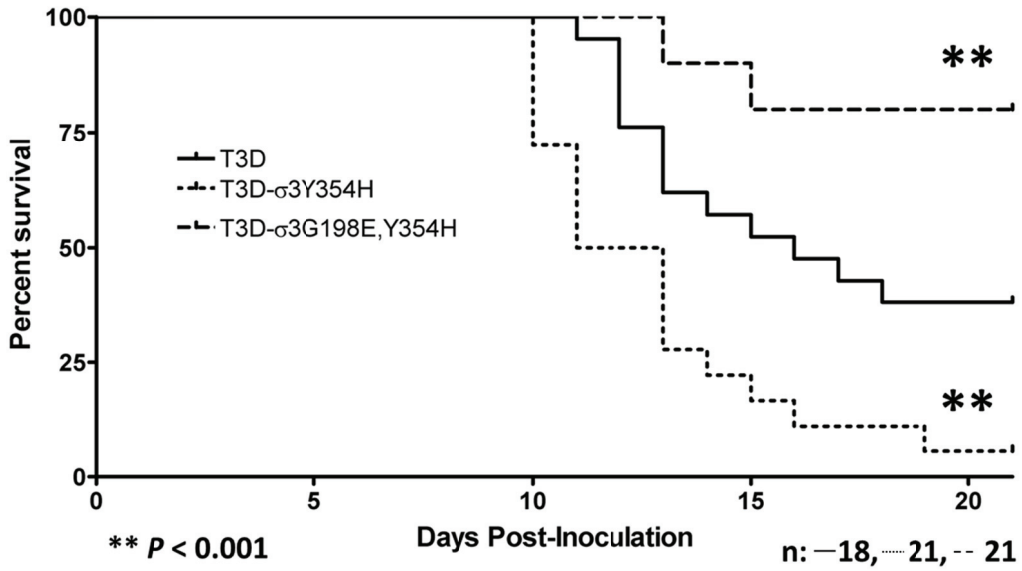

Figure III-1. The σ3-Y354H mutation enhances reovirus virulence following intramuscular inoculation. Newborn C57/BL6 mice were inoculated in the left hind limb with 10^5 PFU of rsT3D, rsT3D-σ3Y354H, or rsT3D-σ3G198E,Y354H. Mice (n = 18, 21, and 21 for T3D, T3D-σ3Y354H and rsT3D-σ3G198E,Y354H, respectively) were monitored for survival for 21 days. *, $P < 0$ .001 as determined by log-rank test in comparison to T3D.

Mice infected with T3D-σ3Y354H have increased viral loads at early timepoints of infection. We hypothesized that rsT3D-σ3Y354H replicates more rapidly *in vivo* than rsT3D, resulting in earlier dissemination and more widespread systemic disease. To test this hypothesis, I inoculated newborn mice in the hindlimb with 10^5 PFU of either rsT3D or rsT3D-σ3Y354H. Mice were euthanized at days 2, 4, 8, and 12 post-inoculation, and titers of reovirus in the hindlimb muscle, brain, spleen, liver, heart, and intestine were determined by plaque assay (Figure III-2). Animals inoculated with rsT3D-σ3Y354H had significantly higher titers in the hindlimb muscle at post-inoculation days 2 and 4 than those infected with rsT3D. Additionally, titers of rsT3D-σ3Y354H were higher at post-

inoculation days 2 and 4 at several sites of secondary replication, including the heart, liver, and spleen. However, at day 8 post-inoculation, differences in the titers rsT3D and rsT3D-σ3Y354H had largely dissipated, and by day 12 post-inoculation, there were no significant differences between the two viruses. I conclude that σ3-Y354H facilitates more rapid initial replication in infected hosts, in turn resulting in earlier systemic spread.

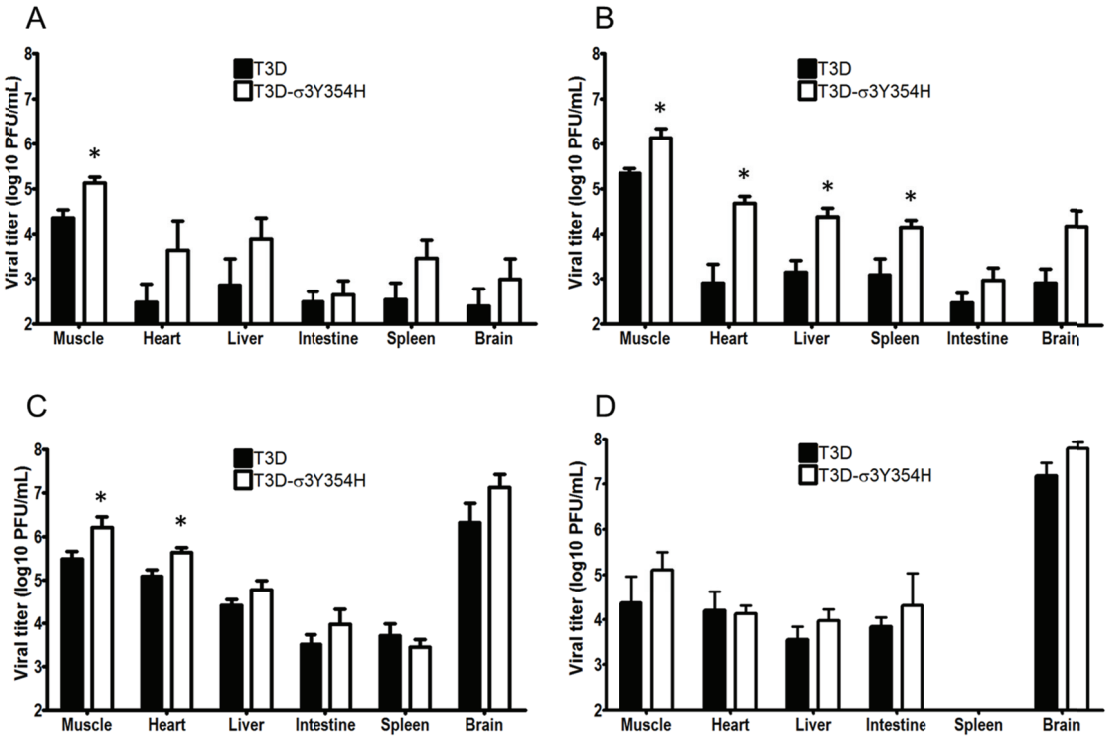

Figure III-2. Viral loads are higher in mice infected with rsT3D-σ3Y354H. Newborn C57/BL6 mice were inoculated in the left hind limb with 10^5 PFU of either T3D or T3D-σ3Y354H. At days 2 (A), 4 (B), 8 (C), and 12 (D) post-inoculation, animals were euthanized, hindlimb muscle, heart, brain, spleen, and intestine were resected, and viral titers in organ homogenates were determined by plaque assay. Results are expressed as mean viral titers for 6 to 9 animals for each time point. Error bars indicate standard errors of the means. * , $P < 0.05$ as determined by Mann-Whitney test in comparison to T3D.

Construction of reassortant T1L/T3D viruses. The Y354H mutation is selected using a variety of conditions in cell culture, and clearly enhances reovirus virulence *in vivo* in the experiments described thus far. However, it is absent from circulating reovirus strains except in the presence of suppressive second-site mutations (73) Accordingly, I hypothesized that enhanced susceptibility to proteolytic disassembly might reduce host-to-host transmission of reovirus, limiting the prevalence of σ3-Y354H. Natural reovirus infection is thought to be primarily fecal-oral (12, 75). However, strain T3D does not efficiently transit the digestive tract, as its σ1 attachment protein is cleaved by intestinal proteases (25, 103). Therefore, to test the effect of the σ3-Y354H mutation on transmission between littermates, I constructed a reassortant virus with eight gene segments from strain type 1 Lang (T1L) and the T3D M2 and S4 gene segments, which encode outer-capsid proteins μ1 and σ3, respectively (Figure III-3A). The T3D M2 and S4 alleles were included together in the reassortant viruses to preserve optimum interactions between σ3 and μ1 and their synergistic role in facilitating reovirus endosomal escape (85). Two versions of this reassortant virus were constructed, rsT1L-T3DM2,S4 and rsT1L-T3DM2,S4Y354H, respectively with and without the σ3-Y354H mutation. Genotypes of the reassortant viruses were verified using electrophoresis of viral genomic dsRNA (Figure III-3B).

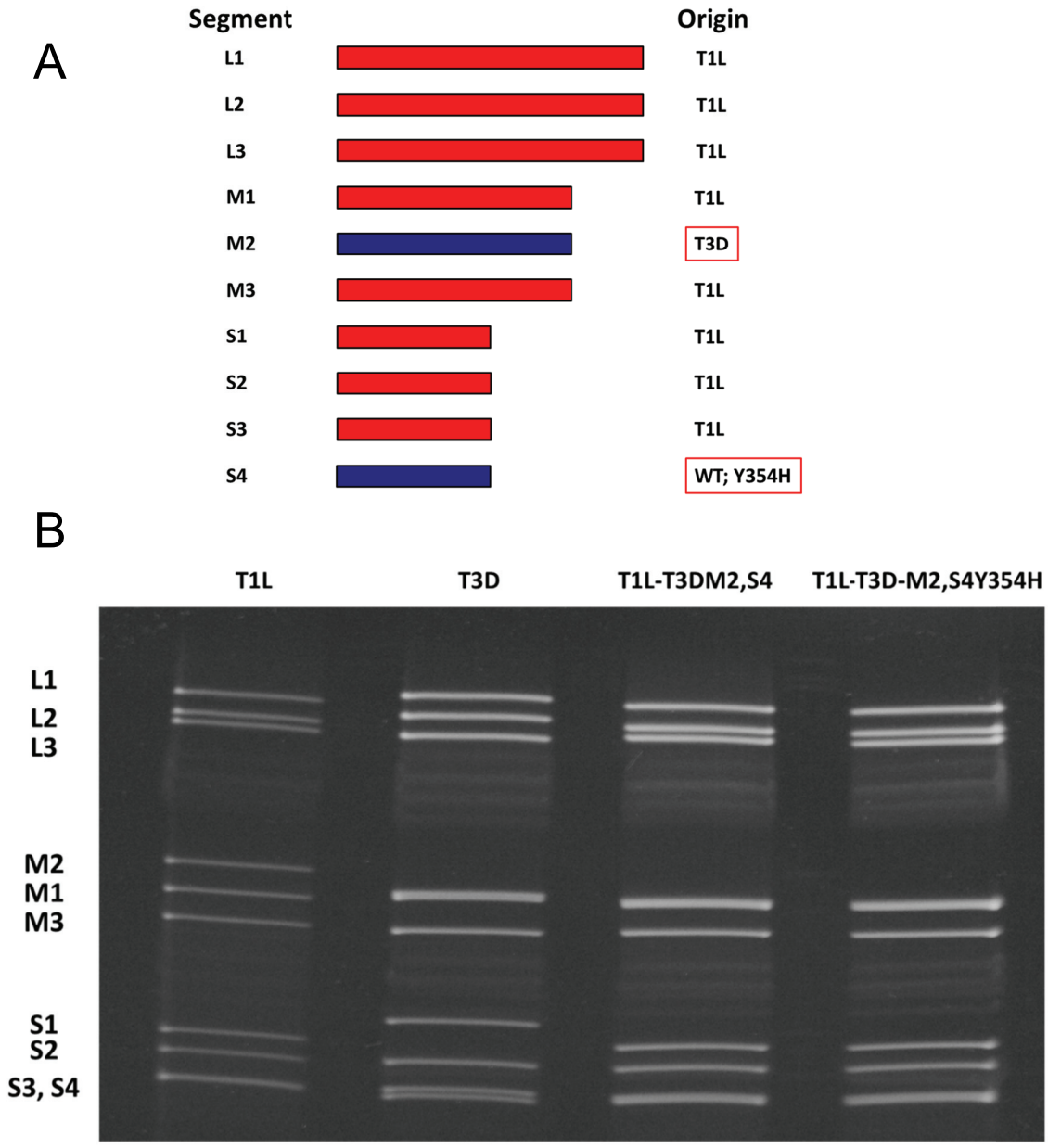

Figure III-3. Construction of T1L-T3D reassortant reovirus strains. (A) Schematic of the genomes of reassortant reovirus strains. Gene segments derived from T1L and T3D are shown in red and blue, respectively. Two reassortant strains were generated, incorporating either the wildtype S4 gene segment or S4-Y354H. (B) Electropheretic analysis of the dsRNA genomes of recombinant reassortant viruses. Purified virions of T1L, T3D, T1L-T3D-M2-S4, and T1L-T3D-M2-S4Y354H were electrophoresed in an SDS-polyacrylamide gel and stained with ethidium bromide to visualize viral gene segments. Size classes of gene segments (L, M, S) are shown.

The Y354H mutation enhances lethality of reovirus following peroral challenge. To determine whether capsid stability affects reovirus virulence following oral challenge, I inoculated newborn mice perorally with 10^4 PFU of the reassortant reovirus strains rsT1L-T3DM2,S4 and rsT1L-T3DM2,S4Y354H and monitored for survival (Figure III-4). Similar to the results gathered using rsT3D and rsT3Dσ3-Y354H, a significantly higher percentage of mice inoculated with rsT1L-T3DM2,S4Y354H succumbed to infection in comparison to those inoculated with rsT1L-T3DM2,S4. The reassortant strains express a serotype 1 σ1 attachment protein, which promotes efficient systemic spread but does not facilitate neural transmission (3, 14, 137). Accordingly, infected animals displayed lethargy beginning 8 days post-inoculation, but neurological findings were absent in mice infected with either reassortant strain. Therefore, introduction of the σ3-Y354H mutation enhances reovirus-mediated virulence independent of viral genetic background, route of inoculation, and mode of death.

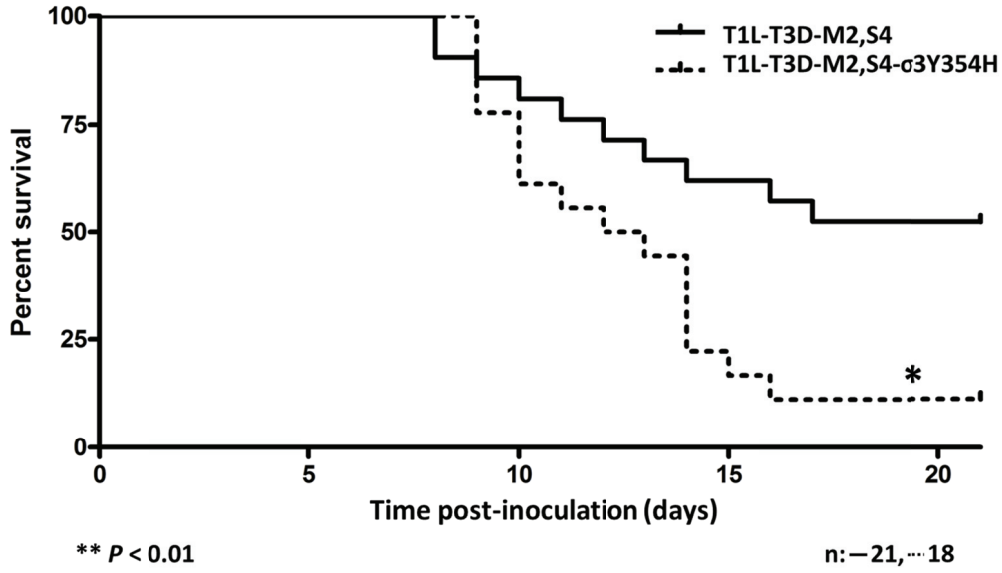

Figure III-4. Reassortant reovirus strains containing **σ3-Y354H** display enhanced virulence following peroral inoculation. Newborn C57/BL6 mice were inoculated perorally with 10^4 PFU of either T1L-T3D-M2-S4 or T1L-T3D-M2-S4Y354H. Mice (n = 21 and 18 for T1L-T3D-M2-S4 and T1L-T3D-M2-S4Y354H, respectively) were monitored for survival for 21 days. *, $P < 0.001$ as determined by log-rank test in comparison to T3D.

Viral loads of reassortant viruses. I hypothesized that the significantly enhanced lethality of rsT1L-T3DM2,S4Y354H compared with rsT1L-T3DM2,S4 might be due to differences in initial replication or dissemination of the two viruses. To test this hypothesis, I inoculated newborn mice perorally with 10^4 PFU of rsT1L-T3DM2,S4 and rsT1L-T3DM2,S4Y354H, and harvested brain, heart, liver, spleen, and intestine at days 2, 4, and 8 post-inoculation. Viral loads in these organs were determined by plaque assay (Fig III-5). Interestingly, there were no significant differences in titer between the two viruses in the selected organs at any timepoint tested. This finding raises the possibility that in the context of the reassortant viruses, σ3-Y354H enhances lethality via a different mechanism than the kinetic replication advantage observed following intramuscular inoculation (Figure III-2).

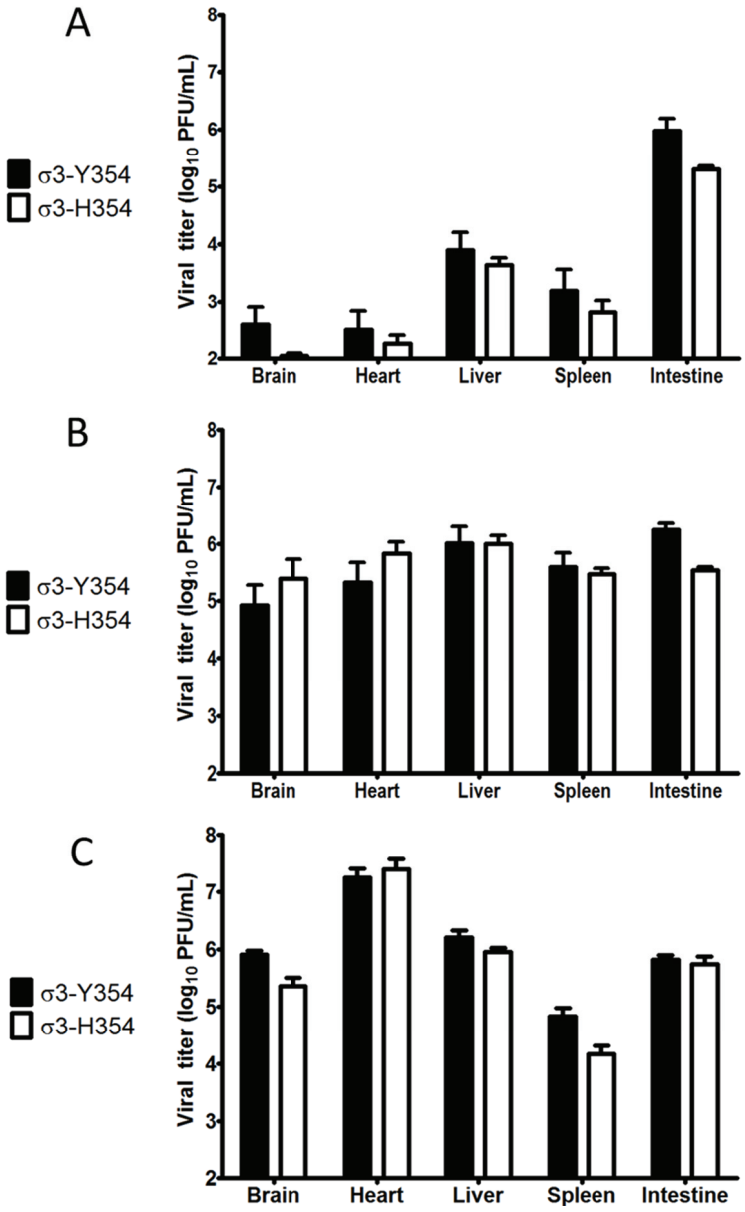

Figure III-5. Viral loads are comparable in mice infected with reassortant viruses. Newborn C57/BL6 mice were inoculated perorally with 10^4 PFU of either T1L-T3D-M2-S4 or T1L-T3D-M2-S4Y354H. At days 2 (A), 4 (B), and 8 (C) post-inoculation, animals were euthanized, brain, heart, liver, spleen, and intestine were resected, and viral titers in organ homogenates were determined by plaque assay. Results are expressed as mean viral titers for 6 to 9 animals for each time point. Error bars indicate standard errors of the means. * , $P < 0.05$ as determined by Mann-Whitney test in comparison to T1L-T3D-M2-S4.

The σ3-Y354H mutation exacerbates reovirus-induced myocarditis. Type 1 reovirus strains induce myocarditis in newborn mice following peroral inoculation (124, 126, 127). To investigate whether the σ3-Y354H mutation is associated with enhanced lethality in the T1L/T3D-M2,S4 genetic background by exacerbating reovirus-induced myocarditis, I inoculated newborn mice with 10^4 PFU of the reassortant reovirus strains rsT1L-T3DM2,S4 and rsT1L-T3DM2,S4Y354H. Hearts of infected mice were resected 8 days post-inoculation and examined histologically. Hearts of mice inoculated with rsT1L-T3DM2,S4Y354H displayed markedly greater gross pathology than hearts from rsT1L-T3DM2,S4-infected animals (Figure III-6A). Hearts were fixed in 10% formalin, embedded in paraffin, and sectioned. Sectioned cardiac tissue was stained with hematoxalin and eosin (Figure III-6B) and anti-reovirus antiserum (Figure III-6C). Cardiac tissue from rsT1L-T3DM2,S4Y354H infected mice displayed strikingly greater levels of tissue injury than those infected with rsT1L-T3DM2,S4, although reovirus antigen distribution was approximately equivalent. These results indicate that introduction of σ3-Y354H into the genetic background of T1L/T3DM2,S4 results in fulminant myocarditis, likely resulting in the differences in lethality following peroral challenge with the reassortant viruses.

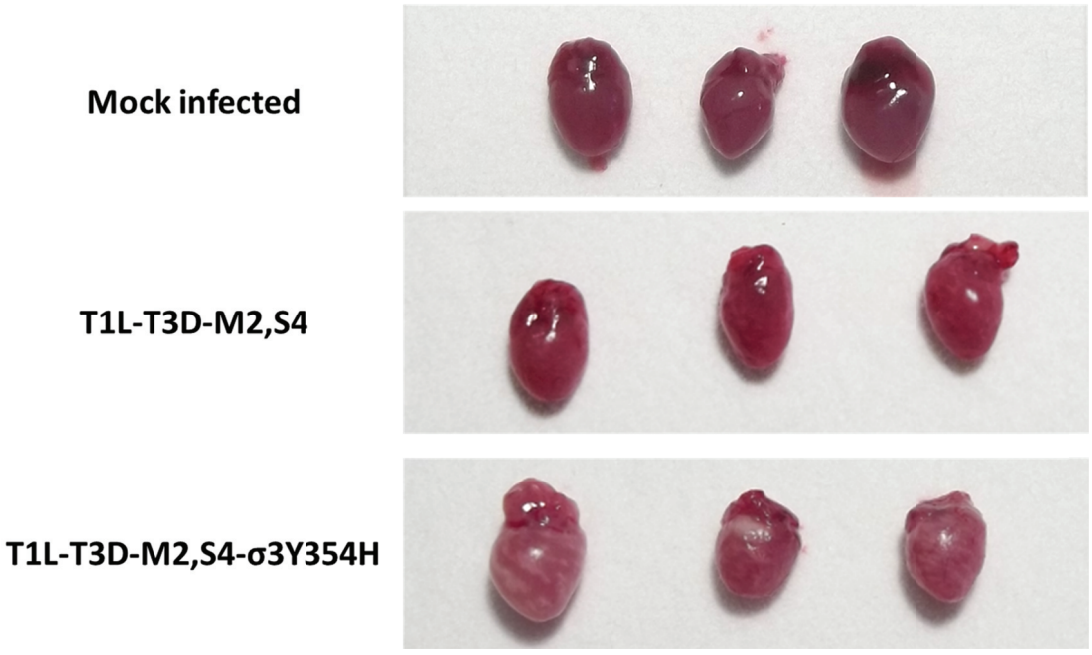

Figure III-6. The σ3-Y354H mutation promotes reovirus-induced myocarditis. Newborn C57/BL6 mice were inoculated perorally with 10^4 PFU of either T1L-T3D-M2-S4 or T1L-T3D-M2-S4Y354H. On day 8 post-inoculation, mice were euthanized, and hearts were resected and photographed for gross pathology (A). Hearts were sectioned and stained with H&E (B) and reovirus-specific polyclonal antiserum (C). Images were captured at 10X (top) and 40X (bottom).

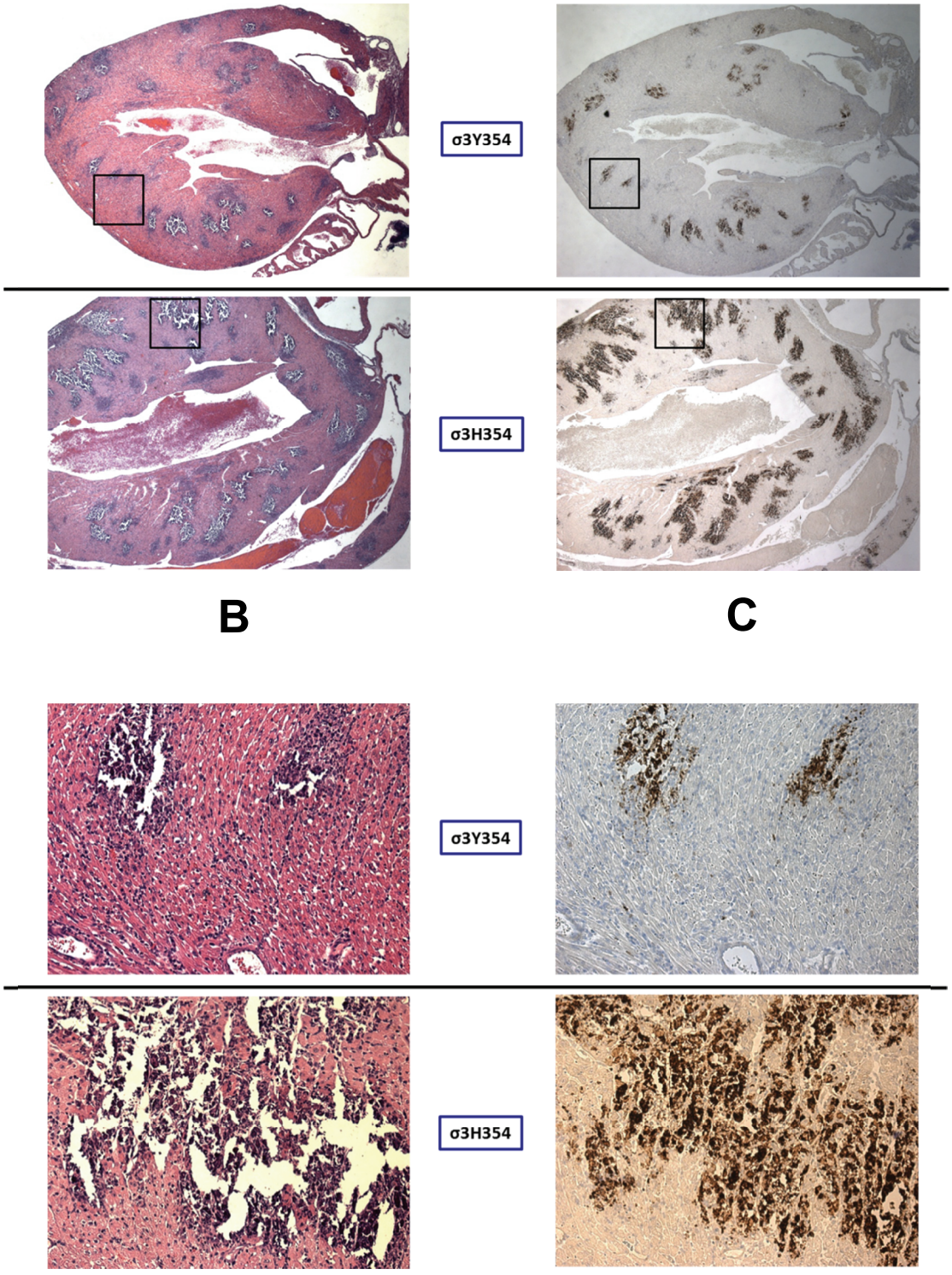

Figure III-6 (continued).

The Y354H mutation in σ3 increases the frequency of host-to-host transmission and severity of disease in uninfected littermates. Given the diminished biochemical stability imposed by σ3-Y354H (45), I hypothesized that σ3-Y354H-containing viruses might spread less efficiently between hosts due to diminished viability or decreased persistence on fomite surfaces. To test this hypothesis, I divided newborn mice into litters of eight animals each, inoculated two animals from each litter with 10^4 PFU of either rsT1L-T3DM2,S4 or rsT1L-T3DM2,S4Y354H, and replaced the infected pups with their uninfected littermates. Eight days post-inoculation, both inoculated and uninoculated littermates were euthanized, organs were resected, and viral titers were determined by plaque assay. Consistent with our previous findings, titers in animals inoculated with rsT1L-T3DM2,S4 and rsT1L-T3DM2,S4Y354H were comparable. However, titers in the intestine (Figure III-8A), heart (Figure III-8B), and brain (Figure III- 8C) of naïve littermates housed with animals inoculated with rsT1L-T3DM2,S4Y354H were significantly higher than in animals housed with animals inoculated with rsT1L-T3DM2,S4. This finding indicates that Y354H is associated with increased littermate transmission and increased replication yields in newly infected pups.

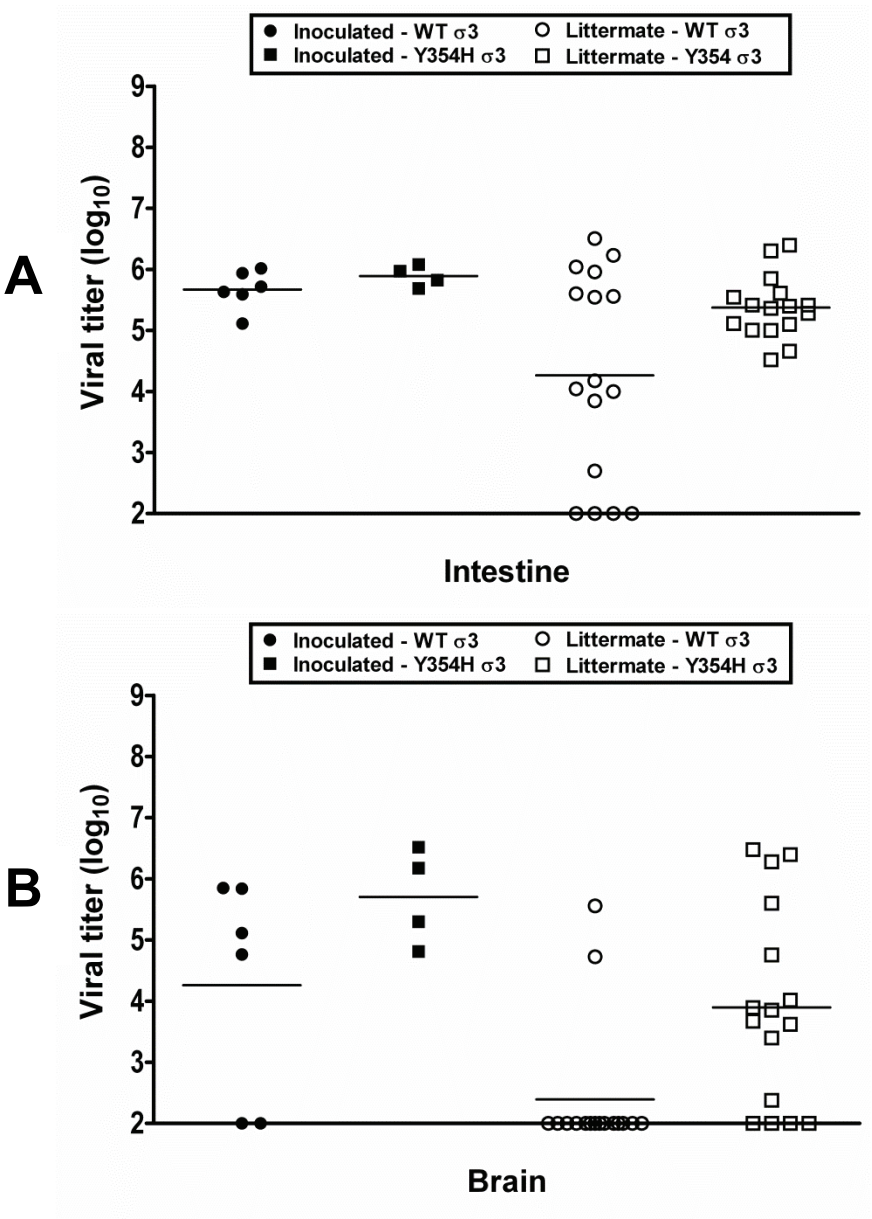

Figure III-7. The Y354H mutation enhances transmission of reovirus between littermates. Two newborn C57/BL6 mice from a litter of eight animals were inoculated perorally with 10^4 PFU of either T1L-T3D-M2-S4 or T1L-T3D-M2-S4Y354H. Eight days post inoculation, inoculated mice and uninoculated littermates were euthanized, intestine (A), brain (B), and heart (C) were resected, and viral titers were determined by plaque assay. Results are expressed as viral titers for each animal assayed. Filled shapes and open shapes indicate inoculated and uninoculated animals, respectively. * , $P < 0.05$ as determined by Mann-Whitney test in comparison to T1L-T3D-M2-S4.

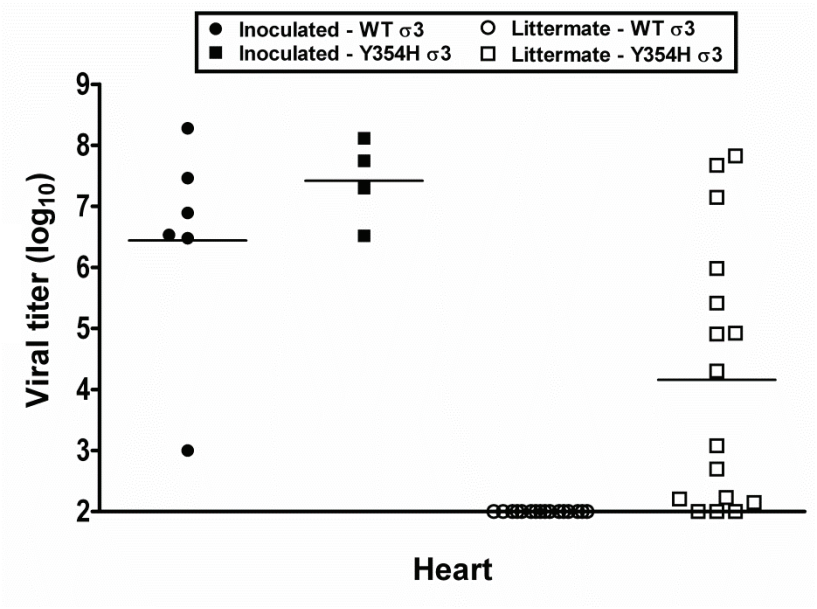

Figure III-7 (continued).

Discussion

To productively infect target cells, reovirus must undergo a stepwise disassembly cascade mediated by host proteases (17, 47, 133). The initial step in this uncoating process is the proteolytic cleavage of the outer-capsid protein, σ3. Proteolysis of σ3 allows subsequent cleavage of μ1 to generate μ1N, μ1-δ, and μ1-φ (19, 105), species that disrupt host cell membranes and allow the transcriptionally active viral core to access the cytoplasm. A single mutation in the σ3 C-terminus, Y354H, increases the rate of σ3 proteolysis and drives reovirus resistance to protease inhibitors such as E64 and ammonium chloride (147). The σ3-Y354H phenotype is not protease-specific; rather, σ3-Y354H induces a structural rearrangement that accelerates attack by a variety of proteases. I have previously shown that viruses with the σ3-Y354H mutation lose titer more rapidly when exposed to elevated temperature than do those with native σ3, indicating that σ3-Y354H reduces biophysical capsid stability. In addition, σ3-Y354H is largely absent from primary reovirus isolates, supporting the hypothesis that σ3-Y354H imposes fitness disadvantages at some stage of the reovirus replication cycle. Achieving the optimal balance between stability and instability is a challenge common to all nonenveloped viruses, but very little is known about the influence of capsid stability in disease pathogenesis. In this study, I used viruses containing σ3-Y354H to investigate the role of capsid stability in reovirus-mediated disease.

I inoculated mice in the left hindlimb with 10^5 PFU of either rsT3D or rsT3D-σ3Y354H and monitored infected animals for survival. Surprisingly, I found that rsT3D-σ3Y354H displayed significantly enhanced virulence compared with rsT3D. Strain T3D is neurotropic, and mice infected with either rsT3D or rsT3D-σ3Y354H developed

neurological findings, including paralysis and seizures. I observed that rsT3D-σ3Y354H replicated to higher titers at days 2 and 4 following inoculation in the hindlimb muscle, as well as sites of secondary replication, including the heart and liver. However, the two viruses reached equivalent peak titers in all tissues later in infection. These findings suggest that the σ3-Y354H mutation confers a replication advantage early in infection, allowing more rapid dissemination and seeding of secondary sites. The cumulative burden of viral replication over time may account for the enhanced lethality of T3D-σ3Y354H.

The natural route of reovirus infection is likely fecal-oral. However, T3D does not infect efficiently per orum because the T3D σ1 attachment protein is hypersensitive to proteolysis by digestive enzymes (25, 103). Accordingly, I engineered reassortant reovirus strains containing the T3D μ1 and σ3 proteins, both with and without Y354H, in an otherwise T1L genetic background. I infected newborn mice perorally with these viruses and again observed enhanced lethality in mice inoculated with the σ3-Y354H-containing virus. This observation indicates that σ3-Y354H enhances disease pathogenesis in multiple genetic backgrounds and via multiple routes of inoculation, strengthening the conclusion that σ3 is a reovirus virulence determinant. Interestingly, viral loads in infected organs were essentially equivalent between the two reassortant strains even at very early timepoints post-inoculation. The reassortant viruses feature a T1L σ1 attachment protein and are thus not neurotropic. However, there was frank cardiac pathology in the hearts of mice inoculated with both reassortant strains, although the effect was much more pronounced in mice infected with the σ3-Y354H reassortant. The σ3-Y354H reassortant induced profound cardiac tissue injury and dystrophic changes

in the hearts of infected animals. Interestingly for non-neurotropic strains of reovirus, both reassortants are quite virulent. The apparent LD_{50} value of the wildtype reassortant is approximately 10^4 PFU, while the σ3-Y354H reassortant is significantly less than that. Thus, the combination of a T3D outer capsid and a T1L core results in particularly virulent strains of reovirus, an effect exacerbated by σ3-Y354H.

Since σ3-Y354H imposes no obvious fitness penalty *in vivo,* I hypothesized that the mutation might impair host-to-host spread. Infecting naïve hosts requires some degree of environmental persistence, and previous studies have shown that σ3-Y354H diminishes the thermostability of the viral particle (45). To test this hypothesis, I separated newborn mice into litters of eight and inoculated two pups per litter with 10^4 PFU per orum with one of the reassortant reovirus strains. I then replaced them with their uninoculated littermates. After eight days, all of the mice were euthanized, and I assessed viral titers in the heart, brain, and intestine by plaque assay. Surprisingly, σ3-Y354H facilitates host-to-host spread, as uninoculated littermates of animals receiving the σ3-Y354H reassortant had a far greater burden of viral replication in all three tested organs than those receiving the wildtype reassortant.

The experiments described in this study demonstrate that σ3-Y354H enhances reovirus virulence and host-to-host spread. However, the precise mechanism by which the mutant virus mediates these effects is less clear. Mice inoculated with rsT3D and rsT3D-σ3Y354H intramuscularly had higher levels of viral replication early in infection, perhaps explaining the increased lethality observed in that infection protocol. However, the mechanism of σ3-Y354H-mediated enhanced virulence is less straightforward in animals inoculated perorally with the reassortant viruses. The σ3-Y354H reassortant

induces greater cardiac injury, likely leading to its increased mortality, but does not produce elevated titers in the heart that are significantly higher than those produced by wild-type virus. This finding suggests that σ3-Y354H alters the host response to reovirus infection, accounting for the enhanced tissue damage. Interferon induction and apoptosis are both important mediators of reovirus-mediated cardiac injury (39, 123, 128). Thus, σ3-Y354H might induce higher levels of apoptosis or suppress interferon signaling in some way. An alternative hypothesis is that cardiac myocytes and hindlimb muscle have lower constitutive levels of protease expression than other tissues, providing replication advantages to σ3-Y354H.

I found it remarkable that σ3-Y354H enhances littermate transmission, but the mechanism by which it does so is unclear. One possibility is that the σ3-Y354H reassortant is shed from the intestine of infected hosts in greater quantity than wildtype virus. Additionally, it remains unclear what fitness disadvantages limit the prevalence of σ3-Y354H. One intriguing possibility is that reovirus has evolved to be a mild, often asymptomatic pathogen. Inducing more severe disease in infected animals may be maladaptive in some way, perhaps by limiting the opportunity to shed viral progeny or provoking immune responses that limit viral replication. However, it is difficult to test this hypothesis without knowing more about the natural ecology of reovirus infection and transmission.

In summary, I have shown here that viruses with reduced outer-capsid stability display induce profoundly enhanced disease, an effect that is penetrant in different strains of reovirus and via multiple routes of inoculation. These studies establish σ3 as a new

reovirus virulence determinant. More broadly, this work may provide insights into the role of capsid structural stability in the pathogenesis of nonenveloped viruses.

CHAPTER IV

SUMMARY AND FUTURE DIRECTIONS

Like many nonenveloped viruses, reovirus must disassemble to productively infect host cells. The disassembly process can occur either inside a target cell or extracellularly in the airway or intestine and, in either case, it is dependent on host proteases. The rate-limiting step in reovirus disassembly is proteolysis of outer-capsid protein σ3. Thus, the suitability of σ3 as a protease substrate determines the efficiency of reovirus cell entry. My work focused on defining the mechanisms that maintain reovirus capsid stability at an optimal level for viral uncoating, replication, and pathogenesis.

The involvement of cathepsin proteases in viral cell entry was first documented in reovirus disassembly (47). A role for cathepsins has since been demonstrated in the replication programs of several other viruses, including Hendra virus, (111), Nipah virus (110), and Ebola virus (22), suggesting that dependence on host proteases to activate viral proteins is a conserved mechanism of entry across unrelated virus families. However, the manner in which enzyme-substrate interactions between the virus and host proteases influences disease pathogenesis remains murky. There is some suggestion that reovirus has the capacity to use a wide variety of proteases for disassembly, with cathepsins readily accessible in most tissues (70).

Previous work in the Dermody lab sought to define specialized roles played by cathepsins B, L, and S in reovirus pathogenesis using animals deficient for each enzyme (71). However, these studies were complicated by the fact that several cathepsin family

members have specialized roles in immunity. Thus, cathepsin-deficient animals have impaired viral clearance and increased mortality following reovirus challenge. Mice pretreated with the cathepsin L-specific inhibitor CLIK-148 are protected from reovirus-induced disease, a proof-of-concept for the idea of antiviral therapeutics targeted against host protease co-factors (71).

A tyrosine-to-histidine mutation in the C-terminus of σ3 had been selected in several independent studies using various inhibitors of protease activity (5, 49, 145). The σ3-Y354H mutation mediates enhanced susceptibility to a variety of proteases (27, 77) by inducing a structural alteration in the σ3 C-terminal domain (147). Viruses containing the mutation also undergo much more rapid disassembly when treated with purified proteases *in vitro* (77).

I began my work by analyzing the disassembly of T3A, a primary reovirus isolate that contains σ3-Y354H. I discovered that T3A undergoes disassembly with kinetics equivalent to prototype strain T3D, which lacks σ3-Y354H. The suppression of the σ3-Y354H phenotype is attributable to a second mutation in T3A σ3, a glycine-to-glutamate change at position 198. I found that viruses containing both the G198E and Y354H σ3 mutations phenocopied wild-type T3D in E64 sensitivity and *in vitro* disassembly kinetics. I also observed that viruses containing unsuppressed σ3-Y354H escaped from endosomes an average of 60 min before wildtype viruses, an effect suppressed by G198E. My experiments also revealed that σ3-Y354H is associated with more rapid titer loss at elevated temperature compared with virions of wildtype viruses, providing evidence that protease sensitivity and biophysical stability are linked. Finally, I observed multiple *de novo* mutations at position 198, including tryptophan and valine, indicating that the

destabilizing effects of σ3-Y354H places selection pressure on compensatory changes in G198.

Structural evidence indicates that residue 198 and residue 354 are directly opposed in the virion-distal domain of σ3. The G198E mutation introduces a negatively charged glutamate side chain that may serve to stabilize the positively charged His354 by electrostatic interactions and thus prevent His354 from dislocating the σ3 C-terminus. This conclusion requires a high-resolution structure of T3D-σ3G198E,Y354H which is currently in progress. Ultimately, my work identified a second residue in σ3 that acts in concert with the disruptive Y354H polymorphism to maintain consistent σ3 protease sensitivity. This finding strongly suggests that despite its advantages under certain types of selection, σ3-Y354H imposes a fitness penalty on circulating reovirus strains.

I next sought to define the effects of σ3-Y354H in reovirus-mediated disease pathogenesis. Given the findings made in analysis of T3A σ3, I anticipated that σ3-Y354H would impose some fitness cost to reovirus in infected hosts. However, when I inoculated animals with T3D and T3D-σ3Y354H, I found that the latter virus had greatly enhanced lethality, replicating to higher titers at early timepoints at both the site of inoculation and disseminated replication sites. As the natural route of reovirus transmission is thought to be fecal-oral, I engineered reassortant viruses containing either wildtype σ3 or σ3-Y354H and inoculated them perorally into newborn mice. I observed a very similar pattern of lethality between these viruses, namely, that a significantly higher percentage of mice succumbed to inoculation with the σ3-Y354H mutant. However, titers in various organs were equivalent between the wildtype and σ3-Y354H viruses at all timepoints tested. However, there was striking cardiac pathology in T3D-σ3Y354H-

infected animals accompanied by numerous histological lesions. Finally, I hypothesized that because σ3-Y354H diminishes the biochemical stability of reovirus virions, the mutation might diminish host-to-host transmission. Most surprisingly, naïve littermates of animals inoculated with σ3-Y354H-containing strains had far higher titers of virus in their brains, hearts, and intestines than littermates of animals inoculated with viruses containing wildtype σ3. To my knowledge, this is the first characterization of the patterns of disease induced by a nonenveloped virus with diminished capsid stability. This is also the first description of a reovirus strain with enhanced lethality, *in vivo* replication, and host-to-host transmissibility. Finally, this study identifies σ3 as a new determinant of reovirus disease virulence.

Future Directions

The enhanced pathogenesis induced by σ3-Y354H raises several interesting questions. First, what factors contribute to the enhanced cardiac injury induced by that virus? Reovirus-induced cardiac injury is associated with antagonism of IFN (4, 63, 106) and apoptosis induction (106). An important next step is to determine the effects of σ3-Y354H on viral replication in cultured cardiac myocytes. A careful study of replication and infectivity using primary cardiac cells is required to establish a baseline understanding of σ3-Y354H in cardiac tissue. To extend these studies, I propose a careful study of differences in IFN induction, apoptotic capacity, and cytokine profiling in cultured myocytes with viruses containing σ3-Y354H. It also is plausible that myocytes have diminished cathepsin expression, giving a comparative growth advantage to σ3-Y354-containing viruses. This concept can be easily tested in cell culture using

radiolabeled virus for *in vivo* scoring of σ3 and μ1 cleavage. Another virtue of using reovirus for these experiments is that there are excellent positive and negative controls for such experiments, namely ISVPs and E64. A thorough cell-culture study should reveal how Y354H induces cardiac damage. Finally, the survival and viral titer experiments should be repeated with a lower inoculum of virus. From Figure III-4, it is clear that 10^4 PFU of the Y354H reassortant is far higher than an LD_{50} value. Lower doses may magnify differences between the two viruses and allow for more nuanced understanding of how they differ *in vivo*.

Another major unanswered question from my work concerns the apparent enhancement of host-to-host transmission conferred by σ3-Y354H. The finding that littermates of mice inoculated with σ3-Y354H-containing virus have higher viral titers than controls suggests a number of possibilities. First, σ3-Y354H may cause enhanced viral shedding and release from the intestinal epithelia of infected animals. I would anticipate these differences being greatest at early timepoints post-inoculation, given the data presented in Figure II-2. Second, σ3-Y354H-containing viruses may be more infectious from fomite surfaces, perhaps related to their lower requirement for disassembly mediated by intestinal proteases. The littermate transmission experiment described in Chapter III is unlikely to replicate the preponderance of natural reovirus infection. A more stringent series of littermate transmission studies should be conducted, using exchanges of soiled bedding and longer incubation periods between hosts to more accurately replicate natural viral transmission. Another method for addressing this possibility is to carefully quantify shed virus or viral titers in intestinal tissue following peroral inoculation.

It is still unclear why σ3-Y354H is not present in circulating reovirus strains. Although reovirus sequence data are limited, the stark absence of σ3-Y354H except in the setting of suppressive mutations, along with the ease with which suppressor mutations arise *in vivo,* strongly suggests that diminishing the stability of the reovirus outer capsid is deleterious for the virus. One possibility is that σ3-Y354H reduces the duration of viral environmental persistence, limiting the opportunities for σ3-Y354H-containing viruses to infect new hosts. In Chapter II, I presented data showing that purified virions containing σ3-Y354H lose titer more rapidly when exposed to elevated temperatures than wildtype virions, indicating that σ3-Y354H does indeed reduce the biophysical stability of the viral capsid. However, I have been unable to identify another measure of stability by which σ3-Y354H imposes a fitness penalty. More detailed knowledge of the natural ecology of reovirus may be required to define the steps likely to limit transmission of σ3-Y354H. High-resolution structures of both T3D-σ3Y354H and T3D-σ3G198E,Y354H also may provide insights into the biophysical effects of those mutations on capsid stability. Such studies are currently in progress, in collaboration with Dr. B.V. Prasad at Baylor College of Medicine. Finally, the possibility exists that enhanced pathogenesis is maladaptive for reovirus at a population level. As most reovirus cases are asymptomatic, it is plausible that reovirus is optimally fit when infections remain subclinical.

Finally, the findings that diminished capsid stability enhances reovirus pathogenesis and host-to-host spread may have important clinical implications given the use of reovirus as an adjunct therapy for cancer. Although reovirus is generally well-tolerated by human patients, identification of factors that might enhance viral pathogenicity in infected hosts is vital for use of reovirus as an oncolytic agent.

Moreover, there is evidence that proteolytic disassembly plays an important role in reovirus-mediated oncolysis. The oncolytic potential of viruses containing σ3-Y354H should be evaluated using transformed cells in tissue culture. If σ3-Y354H enhances reovirus-mediated oncolysis, the next step would be to evaluate its efficacy in a small-animal tumor model. The importance of these experiments is twofold: first, enhanced oncolytic activity in cell culture merits evaluation in a more clinically relevant setting. More importantly, the enhanced pathogenicity σ3-Y354H should be carefully evaluated in a small animal model to ensure viruses containing that mutation are safe for use in a clinical setting. These experiments, if successful, may provide a rationale for evaluation of a new generation of reovirus oncolytic vectors that leverage σ3-Y354H for enhanced efficacy.

CHAPTER V

MATERIALS AND METHODS

Cells and viruses- Spinner-adapted murine L929 cells were grown in either suspension or monolayer cultures in Joklik's modified Eagle's minimal essential medium (SMEM; Lonza, Walkersville, MD) supplemented to contain 5% fetal bovine serum (Invitrogen; Carlsbad, CA), 2 mM L-glutamine (Invitrogen), 100 U of penicillin per mL, 100 U streptomycin per ml (Invitrogen), and 0.25 µg of amphotericin per ml (Sigma-Aldrich; St. Louis, MO). BHK-T7 cells were grown in Dulbecco's modified Eagle's minimal essential medium (Invitrogen) supplemented to contain 5% fetal calf serum, 2 mM L-glutamine, 2% MEM amino acid solution (Invitrogen), and 1 mg geneticin per ml (Invitrogen). Reovirus strain T3A is maintained as a laboratory stock. Recombinant strain (rs) T3D is a stock generated by plasmid-based reverse genetics from cloned T3D cDNAs (78). The engineered reovirus mutants rsT3D-σ3Y354H, rsT3D-σ3G198E,Y354H and the reassortant viruses rsT1L-T3D-M2-S4 and rsT1L-T3D-M2-S4Y354H were generated as described (77).

Generation of reovirus variants- Viruses containing engineered changes in σ3 protein were generated using reverse genetics (78). The S4 gene was excised from the pT7-M2-S2-S3-S4T3D plasmid (78) using HindIII and NheI to generate the tri-cistronic plasmid pT7-M2-S2-S3T3D. The pT7-S4T3D plasmid was used as template to generate pT7-S4T3DA28T+Y354H, pT7-S4T3DE108A+Y354H, pT7-S4T3DI180V+ Y354H,

pT7-S4T3DG198E+Y354H, pT7-S4T3DS215D+Y354H, pT7-S4T3DS233L+ Y354H, and pT7-S4T3DI347T+Y354H using Quickchange mutagenesis (Stratagene; La Jolla, CA). Monolayers of BHK-T7 cells (78) at 90% confluency (approximately 3×10^6 cells) seeded in 60-mm dishes (Costar; Corning Incorporated, Corning, NY) were co-transfected with 3.5 μg each of five plasmids representing the cloned reovirus T3D genome using 3 μl of TransIT-LT1 transfection reagent (Mirus Bio LLC; Madison, WI) per μg of plasmid DNA. Following 72 h of incubation, recombinant virus was isolated from transfected cells by plaque purification using monolayers of L929 cells (141). Virus stocks were passaged and titers were determined as described (51).

Growth of virus in cells treated with E64- Confluent monolayers of L929 cells (approximately 2×10^5 cells/well) in 24-well plates (Costar) were preincubated in SMEM supplemented to contain 0 to 200 μM E64 (Sigma-Aldrich) at 37°C for 4 h. The medium was removed, and cells were adsorbed with second- or third-passage virus stocks at an MOI of 2 PFU per cell. After incubation at 4°C for 1 h, the inoculum was removed, cells were washed with PBS, and 1 ml of fresh SMEM supplemented to contain 0 to 200 μM E64 was added. Cells were incubated at 37°C for 24 h and frozen and thawed twice. Viral titer in cell lysates was determined by plaque assay (141).

Treatment of reovirus virions with cathepsin L- Purified reovirus virions at a concentration of 2×10^{12} particles per ml in reaction buffer L (100 mM NaCl, 15 mM $MgCl_2$, 50 mM sodium acetate [pH 5.0]) were treated with 50 μg of purified, recombinant human cathepsin L (7) per mL in the presence of 5 mM dithiothreitol at 37°C for 0 to 4 h.

Aliquots were removed at various intervals, mixed with SDS sample buffer supplemented to contain 500 μM E64, and incubated on ice for 5 min to terminate protease activity. Reaction mixtures were analyzed by SDS-PAGE.

SDS-PAGE of reovirus structural proteins- Discontinuous SDS-PAGE was performed as described (79). Samples were incubated at 98°C for 5 min, loaded into wells of pre-cast 4 to 20% gradient Tris-tricine polyacrylamide gels (Bio-Rad Laboratories; Hercules, CA), and electrophoresed at a constant voltage of 180V for 1 h. Following electrophoresis, gels were stained using a Novex Colloidal Blue Staining Kit (Invitrogen) according to the manufacturer's instructions.

Densitometric analysis of reovirus structural proteins- Stained gels were visualized using an infrared imaging system (Li-Cor Biosciences; Lincoln, NE). Band intensities in the scanned images were quantified using Odyssey Application Software version 3.0.16 (Li-Cor). The relative amount of σ3 protein was determined by comparing the intensity of bands corresponding to σ3, which has an apparent molecular weight of ~ 41 kDa, to bands corresponding to viral core protein σ2, which has an apparent molecular weight of ~ 47 kDa and is not affected by protease treatment under these conditions (5).

Heat resistance of reovirus virions- Purified reovirus virions at a concentration of 2×10^8 particles per ml in virion storage buffer (150mM NaCl, 15mM $MgCl_2$, 10mM Tris [pH 7.4]) were treated at 55°C for 60 min. At 15-min intervals, samples were removed and placed on ice. Viral titers were determined by plaque assay (28).

Specific infectivity of reovirus virions- Fresh preparations of reovirus virions were generated in triplicate from second-passage lysate stocks as described (27). Particle density of each viral preparation was determined by quantifying absorbance at 260 nm and calculated using the equivalence 1 $O.D._{260}$ = 2.1 x 10^{12} particles/mL (130). Titer of each preparation was determined by plaque assay (28).

Kinetic ammonium chloride protection assay- Confluent monolayers of L929 cells (approximately 2×10^5 cells/well) in 24-well plates were adsorbed with second- or third-passage virus stocks at an MOI of 25 PFU per cell. After incubation at 4°C for 1 h, the inoculum was removed, cells were washed with PBS at 4°C, and 1 ml of pre-warmed SMEM was added. At various times post-adsorption, 25 μL of 1 M NH_4Cl was added to the medium to give a final concentration of 25 mM. At 20 h post-adsorption, the medium was removed, and cell monolayers were fixed with 1 mL of methanol at -20°C for a minimum of 30 min. Fixed monolayers were washed twice with PBS, blocked with 5% immunoglobin-free BSA (Sigma-Aldrich) in PBS, and incubated at 37°C for 30 min with rabbit polyclonal anti-reovirus serum at a 1:1000 dilution in PBS plus 0.5% Triton X-100. Monolayers were washed twice with PBS and incubated at 37°C for 30 min with a 1:1000 dilution of anti-rabbit goat immunoglobulin conjugated with Alexa 488 (Molecular Probes, Inc., Eugene, OR). Monolayers were washed twice and visualized by indirect immunofluorescence. Reovirus antigen-positive cells were quantitated by enumerating fluorescent cells in three random fields of view per well at 100–400 ×

magnification. Total cell number was quantified by enumerating 4',6-diamidino-2-phenylindole (DAPI)-stained nuclei.

Infection of mice- C57BL/6J mice were obtained from Jackson Laboratory. Two- or three-day-old mice were inoculated intramuscularly or perorally with purified reovirus diluted in PBS. Intramuscular inoculations (10 μl) were delivered into the left hind limb (hamstring muscle) using a Hamilton syringe and 30-gauge needle. Peroral inoculations (50 μl) were administered using a Hamilton syringe, 30-gauge needle, and Intramedic PE-10 polyethylene tubing (BD Biosciences) (3, 61, 136). For analysis of viral virulence, mice were monitored for symptoms of disease for 21 days postinoculation. Mice were euthanized when found to be moribund (defined by rapid or shallow breathing, lethargy, or paralysis). Data from these experiments are reported as "percent survival", although death was not used as an endpoint. For analysis of virus replication, mice were euthanized at various intervals post inoculation, and organs were collected into 1 ml of PBS and homogenized by freezing, thawing, and sonication. Viral titers in organ homogenates were determined by plaque assay using L929 cells. For immunohistochemical analysis, mice were euthanized at various intervals post inoculation, and organs were resected and fixed overnight in 10% formalin. Fixed organs were embedded in paraffin, and 6-μm histological sections were prepared. Sections were processed for hematoxalin and eosin staining, detection of reovirus protein using polyclonal antisera, detection of intracellular calcium using alizarin red, and detection of apoptotic cells using the NeuroTACS II system (Trevingen, Gaithersburg, MD). For littermate transmission studies, newborn mice were separated into litters of eight animals. Two animals per litter were inoculated perorally and replaced into original cages with

dams and uninoculated littermates. Both inoculated and uninoculated animals were euthanized eight days post inoculation, and viral titers were determined by plaque assay. Animal husbandry and experimental procedures were performed in accordance with Public Health Service policy and approved by the Vanderbilt University School of Medicine Institutional Animal Care and Use Committee.

APPENDIX

A. GENETIC AND PHARMACOLOGIC ALTERATION OF CATHEPSIN EXPRESSION INFLUENCES REOVIRUS PATHOGENESIS

This study used animals deficient for cathepsins B, L, and S to investigate the role played by different cathepsins family members in reovirus disease pathogenesis. Though genetic cathepsin ablation reduced peak reovirus titers, cathepsins L and S play important roles in adaptive immunity, and their absence impaired reovirus clearance, leading to delayed mortality. This study also provided evidence that transient pharmacologic cathepsin blockade, using the cathepsin L inhibitor CLIK-148, protected mice from reovirus challenge. My involvement in this study was in validating the inhibitory activity of CLIK-148 against recombinant cathepsin L *in vitro* as well as helping with mouse survival experiments.

Journal of Virology

Genetic and Pharmacologic Alteration of Cathepsin Expression Influences Reovirus Pathogenesis

Elizabeth M. Johnson, Joshua D. Doyle, J. Denise Wetzel, R. Paul McClung, Nobuhiko Katunuma, James D. Chappell, M. Kay Washington and Terence S. Dermody

J. Virol. **2009, 83(19):9630. DOI: 10.1128/JVI.01095-09.**
Published Ahead of Print 29 July 2009.

JOURNAL OF VIROLOGY, Oct. 2009, p. 9630–9640 Vol. 83, No. 19
0022-538X/09/$08.00+0 doi:10.1128/JVI.01095-09

Genetic and Pharmacologic Alteration of Cathepsin Expression Influences Reovirus Pathogenesis▽

Elizabeth M. Johnson,[1,2] Joshua D. Doyle,[1,2] J. Denise Wetzel,[2,3] R. Paul McClung,[2,3] Nobuhiko Katunuma,[4] James D. Chappell,[2,3,5] M. Kay Washington,[5,6] and Terence S. Dermody[1,2,3,6]*

Departments of Microbiology and Immunology,[1] Pediatrics,[3] and Pathology,[5] Vanderbilt Ingram Cancer Center,[6] and Elizabeth B. Lamb Center for Pediatric Research,[2] Vanderbilt University School of Medicine, Nashville, Tennessee, and Institute for Health Sciences, Tokushima Bunri University, Tokushima, Japan[4]

Received 28 May 2009/Accepted 21 July 2009

The cathepsin family of endosomal proteases is required for proteolytic processing of several viruses during entry into host cells. Mammalian reoviruses utilize cathepsins B (Ctsb), L (Ctsl), and S (Ctss) for disassembly of the virus outer capsid and activation of the membrane penetration machinery. To determine whether cathepsins contribute to reovirus tropism, spread, and disease outcome, we infected 3-day-old wild-type (wt), *Ctsb*$^{-/-}$, *Ctsl*$^{-/-}$, and *Ctss*$^{-/-}$ mice with the virulent reovirus strain T3SA+. The survival rate of *Ctsb*$^{-/-}$ mice was enhanced in comparison to that of wt mice, whereas the survival rates of *Ctsl*$^{-/-}$ and *Ctss*$^{-/-}$ mice were diminished. Peak titers at sites of secondary replication in all strains of cathepsin-deficient mice were lower than those in wt mice. Clearance of the virus was delayed in *Ctsl*$^{-/-}$ and *Ctss*$^{-/-}$ mice in comparison to the levels for wt and *Ctsb*$^{-/-}$ mice, consistent with a defect in cell-mediated immunity in mice lacking cathepsin L or S. Cathepsin expression was dispensable for establishment of viremia, but cathepsin L was required for maximal reovirus growth in the brain. Treatment of wt mice with an inhibitor of cathepsin L led to amelioration of reovirus infection. Collectively, these data indicate that cathepsins B, L, and S influence reovirus pathogenesis and suggest that pharmacologic modulation of cathepsin activity diminishes reovirus disease severity.

As obligate intracellular parasites, viruses must coopt basic cellular processes to enter host cells and deliver their genomes to the appropriate intracellular site for replication (45). Viral entry steps include attachment of the virus to the cell surface, penetration of the virus into the cell interior, disassembly of the viral capsid, and activation of the viral genetic program. These events are essential for the virus to transition from the extracellular environment to the cellular compartment in which viral transcription and replication occur. Entry steps also play key roles in viral pathogenesis, as these events often determine cell tropism within the infected host.

Mammalian orthoreoviruses (reoviruses) are important models for studies of virus cell entry and the pathogenesis of viral disease. Reoviruses form nonenveloped, double-shelled particles that contain a segmented, double-stranded RNA genome (70). Virtually all mammals, including humans, serve as hosts for reovirus infection (84). However, reovirus causes disease primarily in the very young (44, 77, 79). Newborn mice infected with reovirus sustain injury to a variety of organs, including the brain, heart, and liver (5, 56, 84). Mechanisms of reovirus-induced disease, including cellular determinants of viral spread and tropism, are only partially understood.

Reovirus entry into cells is initiated by the attachment of virions to cell surface receptors via the σ1 protein (41, 85) and internalization into cells by receptor-mediated endocytosis (6, 7, 24, 76). In cellular endosomes, virions undergo stepwise disassembly, forming discrete intermediates, the first of which is the infectious subvirion particle (ISVP) (7, 14, 74, 76). ISVPs are generated by proteolytic removal of the σ3 protein and cleavage of the μ1 protein to form particle-associated fragments δ and φ. Following formation of ISVPs, σ1 is shed and the μ1 cleavage fragments undergo conformational rearrangement, yielding the ISVP* (11, 12). ISVP*s penetrate endosomes to deliver transcriptionally active viral cores into the cytoplasm (54, 55).

Endocytic proteases cathepsins B and L catalyze reovirus virion-to-ISVP disassembly in murine fibroblasts, although cathepsin L is the major mediator of this process (23). These proteases are expressed in most organs, including the intestine, brain, heart, and liver (78). In P388D cells, a macrophage-like cell line, cathepsin S, mediates the uncoating of some reovirus strains (28). Cathepsin S expression is largely restricted to cells and tissues of the immune system (16), which may be important during enteric infection, as reovirus replication in the intestine occurs in mononuclear cells of Peyer's patches (25, 51). Cathepsin S is known to be expressed in mononuclear cells, including alveolar macrophages in the lung (72, 73) and microglial cells in the brain (61).

Cathepsins B, L, and S are responsible for unique, tissue-specific activities (65). Cathepsin B modulates pathological trypsinogen activation (30) and apoptosis induced by tumor necrosis factor alpha (29). Cathepsin L is required for hair follicle cycling and epidermal homeostasis (68). By virtue of its activity at neutral pH (9, 39), cathepsin S is thought to partic-

* Corresponding author. Mailing address: Lamb Center for Pediatric Research, D7235 MCN, Vanderbilt University School of Medicine, Nashville, TN 37232. Phone: (615) 343-9943. Fax: (615) 343-9723. E-mail: terry.dermody@vanderbilt.edu.

▽ Published ahead of print on 29 July 2009.

ipate in remodeling of the extracellular matrix (72, 89). Functions of cathepsins B, L, and S intersect in the regulation of adaptive immunity. Cathepsin L cleaves the invariant chain in cortical thymic epithelial cells (52) and is hypothesized to mediate efficient endosomal protein fragmentation to ensure diverse peptide generation in the thymus (33, 43). Through these functions, cathepsin L serves to facilitate positive selection of $CD4^+$ T cells (15, 35). Cathepsin S cleaves the invariant chain in peripheral antigen-presenting cells, leading to $CD4^+$ T-cell activation (53). Both cathepsin L (32) and cathepsin S (67) participate in $NK1.1^+$ T-cell selection in the thymus through proteolytic processing in thymocytes and antigen-presenting cells, respectively. As a result, cathepsin L-deficient (*Ctsl*$^{-/-}$) and cathepsin S-deficient (*Ctss*$^{-/-}$) mice have impairments in both $CD4^+$ and $NK1.1^+$ T-cell activities. Cathepsin S also processes antigen in endosomes for cross-presentation via the major histocompatibility complex class I pathway (71). Like cathepsins L (34) and S (63), cathepsin B processes endocytosed antigen for display by major histocompatibility complex class II molecules (46, 48). However, cathepsin B-deficient mice (*Ctsb*$^{-/-}$) do not display overt immunodeficiency (65).

Underscoring the importance of endosomal cathepsin proteases in host functions, viruses have usurped these enzymes to allow entry into the cytoplasm. In addition to reovirus, cathepsins catalyze proteolytic events required for membrane fusion of several important pathogens. Ebola virus requires both cathepsin B and cathepsin L for efficient cell entry (13), while severe acute respiratory syndrome coronavirus requires cathepsin L but also can utilize cathepsins B and S (36, 75). Hendra (58) and Nipah (57) viruses utilize cathepsin L for fusion protein processing, most likely at the stage of virion assembly (47). Despite the importance of cathepsins in viral growth, nothing is known about the function of these proteases in the pathogenesis of viral disease.

To determine the role of cathepsin proteases in viral virulence, we studied reovirus disease by using mice lacking a single cathepsin. Mice deficient for cathepsin B, L, or S were monitored for survival, disease symptoms, and viral replication following reovirus infection. We found that following peroral inoculation of reovirus, cathepsin deficiency leads to decreased viral replication in sites of secondary replication. However, *Ctsl*$^{-/-}$ and *Ctss*$^{-/-}$ mice succumb to doses of virus nonlethal to wild-type (wt) and *Ctsb*$^{-/-}$ animals. Although viremia is not affected by cathepsin deficiency, we observed alterations in disease pathogenesis in the hearts, livers, and brains of cathepsin-deficient animals. Furthermore, treatment of wt mice with an inhibitor of cathepsin L reduces disease severity. These studies demonstrate that cathepsin activity plays a key role in viral pathogenesis and identify a new target for antiviral drug development.

MATERIALS AND METHODS

Cells and viruses. L929 cells were maintained in Joklik's minimal essential medium (Lonza) supplemented to contain 10% fetal bovine serum, 2 mM L-glutamine, 100 U/ml penicillin, 100 μg/ml streptomycin (Invitrogen), and 25 ng/ml amphotericin B (Sigma-Aldrich). T3SA+ is a reassortant virus containing the S1 gene segment of strain T3C44MA and the remaining nine gene segments of strain T1L (4). Virus was purified after growth in L929 cells by CsCl gradient centrifugation (27). Viral titers were determined by a plaque assay (83). ISVPs were generated by treatment of 5×10^6 virions per ml with 20 μg of *N*-α-tosyl-L-lysine chloromethylketone-treated α-chymotrypsin type VII from bovine pancrease (Sigma-Aldrich) per ml at 37°C for 1 h.

Treatment of virions with purified cathepsins. Purified reovirus virions at a concentration of 10^{12} particles per ml, as determined by optical density at 260 nm, in reaction buffer B-L (50 mM sodium acetate [pH 5.0], 15 mM $MgCl_2$, 100 mM NaCl, 5 mM dithiothreitol) were treated with 400 μg/ml bovine spleen cathepsin B (Calbiochem-Novabiochem) or 100 μg/ml purified recombinant human cathepsin L (10) at 37°C for various intervals. Alternatively, purified virions at a concentration of 10^{12} particles per ml in reaction buffer S (50 mM sodium acetate [pH 6.0], 15 mM $MgCl_2$, 100 mM NaCl) were treated with 300 μg/ml purified recombinant human cathepsin S (Calbiochem) at 37°C for various intervals. Proteolysis was terminated by incubation of reaction mixtures on ice and addition of 1 mM (final concentration) E64 (Sigma-Aldrich), a pan-cysteine-containing protease inhibitor (3). A 30-μl aliquot of each reaction mixture was incubated with 7 μl of 6× sample buffer (350 mM Tris [pH 6.8], 9.3% dithiothreitol, 10% sodium dodecyl sulfate, 0.012% bromophenol blue) at 100°C for 5 min. Samples were loaded into wells of 10% polyacrylamide gels and electrophoresed. After electrophoresis, gels were fixed and stained using colloidal Coomassie blue (Invitrogen).

Mice. C57BL/6J mice (wt) were obtained from Jackson Laboratory. *Ctsb*$^{-/-}$ (21, 30) and *Ctsl*$^{-/-}$ (68) mice, each backcrossed to a C57BL/6 background at least eight times to ensure that all strains studied were of similar genetic backgrounds, were provided by D. Hanahan (San Francisco, CA). *Ctss*$^{-/-}$ mice, backcrossed at least 10 times to a C57BL/6 background (67), were provided by H. Chapman (San Francisco, CA).

Infection of mice. Newborn mice, 2 to 4 days old, weighing approximately 2 g were inoculated perorally or intracranially with purified reovirus virions diluted in phosphate-buffered saline (PBS). Peroral inoculations (50 μl) were delivered intragastrically (69). Intracranial inoculations (5 μl) were delivered to the left cerebral hemisphere by using a Hamilton syringe and 30-gauge needle (80). For analysis of virulence, mice were monitored for weight loss and symptoms of disease for 21 days after inoculation and euthanized when found to be moribund (defined by rapid or shallow breathing, severe lethargy, or paralysis). For analysis of viral replication, mice were euthanized at various intervals following inoculation, and organs were harvested into 1 ml of PBS before freezing, thawing, and homogenization by sonication (1, 5, 18), using a midrange setting on a VirSonic 100 sonicator (VirTis). Organ sizes did not noticeably differ between genotypes of mice. For analysis of viremia, mice were euthanized and decapitated at various intervals following inoculation. Whole blood was collected from the neck into a 1 ml syringe containing 100 μl Alsever's solution (Sigma) and frozen, thawed, and sonicated. Viral titers in organ and blood homogenates were determined by a plaque assay (83). Animal husbandry and experimental procedures were performed in accordance with Public Health Service policy and approved by the Vanderbilt University School of Medicine Institutional Animal Care and Use Committee.

Treatment of mice with an inhibitor of cathepsin L. Mice were inoculated intraperitoneally with approximately 100 μg/g average litter weight of CLIK-148 in dimethyl sulfoxide (DMSO) or DMSO alone in a volume of 10 μl. One hour following treatment, mice were inoculated perorally with PBS or reovirus T3SA+. Mice were subsequently treated with CLIK-148 daily for 7 days. Analysis of virulence was conducted for 21 days or mice were euthanized at 8 days postinoculation and organs resected for determination of viral titers by a plaque assay. Pups that had obvious injury from intraperitoneal injections or that died within 6 days postinoculation were eliminated from the study. CLIK-148 specificity in vitro and in vivo has previously been established (26, 37, 50, 88).

Statistical analysis. For survival experiments, curves were obtained using the Kaplan-Meier method and compared using the log rank test. For experiments in which viral titers in an organ or blood sample were determined, the Mann-Whitney test was used to calculate two-tailed *P* values. This test is appropriate for experimental data that display a non-Gaussian distribution (66). Mann-Whitney analysis lacks the power of the *t* test, and therefore, statistical significance is achieved less frequently with this method. All statistical analyses were performed using GraphPad Prism software.

Histology. Newborn mice, 2 to 4 days old, weighing approximately 2 g were inoculated perorally with purified reovirus virions diluted in PBS. At various intervals following inoculation, mice were euthanized, organs were resected, and a wedge of liver was removed for titer determination by a plaque assay. Remaining organs were incubated in 10% formalin at room temperature for 24 h, followed by incubation in 70% ethanol at room temperature. Fixed organs were embedded in paraffin, and 5-μm sections were prepared. Consecutively obtained sections were stained with hematoxylin and eosin for evaluation of histopathologic changes or processed for immunohistochemical detection of reovirus pro-

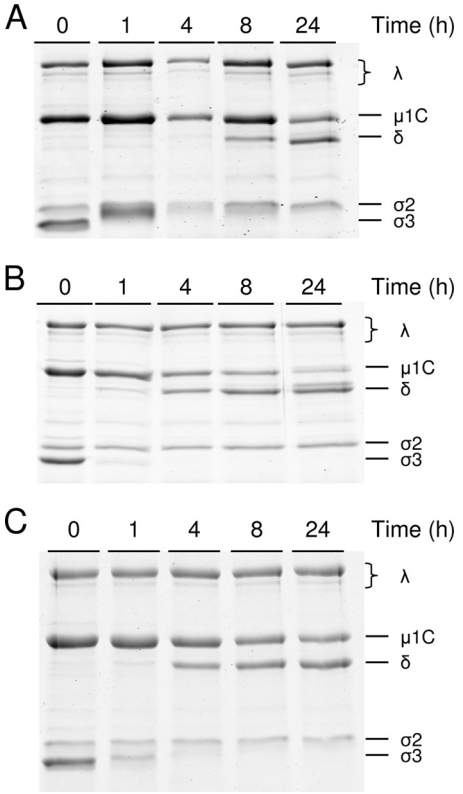

FIG. 1. Treatment of reovirus virions with cathepsins B, L, and S. Purified virions of T3SA+ were treated with 400 μg/ml cathepsin B (A), 100 μg/ml cathepsin L (B), or 300 μg/ml cathepsin S (C) at 37°C for the times shown. Equal numbers of viral particles were loaded into wells of 10% polyacrylamide gels and electrophoresed. Viral proteins are labeled on the right.

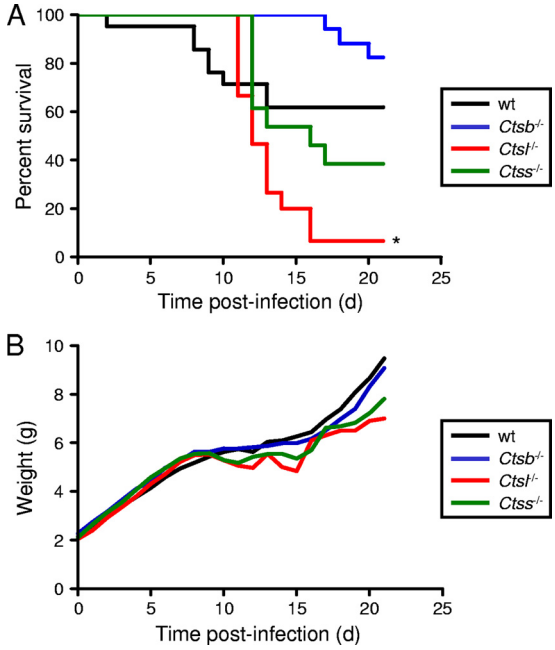

FIG. 2. Survival of wt and cathepsin-deficient mice following peroral inoculation. C57BL/6 wt and cathepsin-deficient mice, 2 to 4 days (d) old, were inoculated perorally with 10^7 PFU T3SA+. Mice (n = 14 to 21) were monitored for survival (A) and weight gain (B). (A) *, P values of <0.01, as determined by a log rank test, in comparison to the wt level. (B) Results are expressed as mean weight of all living infected animals. Statistical significance (P values of <0.05 as determined by Student's t test) in comparison to the level for wt mice was achieved for *Ctsb*$^{-/-}$ mice between days 2 and 8; for *Ctsl*$^{-/-}$ mice at days 1, 13, and 14; and for *Ctss*$^{-/-}$ mice at days 4 to 8, 11, and 14.

tein (56). The histology was reviewed by a pathologist blinded to the conditions of the experiment.

Quantitation of serum hepatic enzymes. Newborn mice, 2 to 4 days old, weighing approximately 2 g were inoculated perorally with purified reovirus virions diluted in PBS. At various intervals following inoculation, mice were euthanized and decapitated. Blood samples were collected and allowed to coagulate, and sera were separated by centrifugation. Sera were stored at −20°C, protected from light, and submitted in batches to Charles River Research Animal Diagnostic Services (Wilmington, MA). A small wedge of liver was resected concurrently with blood collection for correlative titer determination by a plaque assay.

Growth of reovirus in vitro in the presence of cathepsin inhibitors. Monolayers of L cells (2×10^5 cells) in 24-well plates were preincubated in medium supplemented to contain 10 to 100 μM CLIK-148 or 200 μM E64 for 4 h. The medium was removed, and cells were adsorbed with T3SA+ virions or ISVPs at a multiplicity of infection of 2 PFU per cell. After incubation at 4°C for 1 h, the inoculum was removed, cells were washed with PBS, and 1 ml fresh medium supplemented with CLIK-148 or E64 was added. After incubation at 37°C for 0 or 24 h, cells were frozen and thawed twice, and viral titers in cell lysates were determined by a plaque assay.

RESULTS

Processing of reovirus virions by purified cathepsin proteases. Cathepsins B (23), L (23), and S (28) can catalyze reovirus disassembly in vitro and in certain types of cells. Reovirus strain T3SA+ is a reassortant virus that contains the S1 gene segment from strain T3C44-MA on the genetic background of T1L (4). Following peroral inoculation of newborn mice, T3SA+ replicates in the intestine and disseminates systemically from that site to the brain, heart, and liver (5). To determine whether T3SA+ is susceptible to cathepsins B, L, and S, we incubated purified virions with each enzyme over a time course and resolved the resultant digestion mixtures by sodium dodecyl sulfate-polyacrylamide gel electrophoresis. Following incubation for 24 h with each protease, we observed complete degradation of σ3 and cleavage of μ1 to δ (Fig. 1). Therefore, treatment of T3SA+ virions with cathepsin B, L, or S results in formation of ISVPs.

Cathepsin deficiency differentially affects survival following reovirus infection. To determine the function of cathepsin proteases in reovirus disease, we inoculated wt, *Ctsb*$^{-/-}$, *Ctsl*$^{-/-}$, and *Ctss*$^{-/-}$ mice perorally with 10^7 PFU of reovirus T3SA+. Mice were monitored for 21 days after infection for morbidity and mortality. The cathepsin-null mice displayed differential survival patterns in comparison to wt animals. Following a 21-day observation interval, the survival rate of *Ctsb*$^{-/-}$ animals was greater than that of wt mice; 82% of *Ctsb*$^{-/-}$ mice survived, in comparison to 61% for wt mice (Fig. 2A). In contrast, the survival rates of *Ctsl*$^{-/-}$ and *Ctss*$^{-/-}$ mice were decreased in comparison to that of wt animals; only 7% and 39% of *Ctsl*$^{-/-}$ and *Ctss*$^{-/-}$ mice, respectively, survived T3SA+ infection. However, the mean survival time for each strain of cathepsin-deficient mice was increased in comparison to that for wt animals (Table 1). The disease phenotypes in all strains did not notably differ, with all strains of mice displaying

TABLE 1. Mean survival time following reovirus infection[a]

Genotype	No. of mice	Mortality (%)[b]	Mean survival time (days)[c]	P^d
wt	21	38.1	9.0 ± 1.2	
Ctsb$^{-/-}$	17	17.6	18.3 ± 0.9	0.0017
Ctsl$^{-/-}$	15	93.3	12.6 ± 0.5	0.0041
Ctss$^{-/-}$	13	61.5	13.3 ± 0.7	0.0098

[a] C57/Bl6 wt and cathepsin-deficient mice, 2 to 4 days old, were inoculated perorally with 10^7 PFU T3SA+. Mice were monitored for survival for 21 days.
[b] Percent animals dead after 21 days.
[c] Mean survival time, as defined by the average day of death for animals that succumbed to infection, in number of days ± standard error of the mean.
[d] *P* value, as determined by Student's *t* test, in comparison to the level for wt mice.

weakness and lethargy during the period of illness. All pups of wt and cathepsin-deficient strains inoculated with PBS and observed under identical conditions survived and did not display symptoms (data not shown). As a surrogate marker for disease severity, *Ctsb*$^{-/-}$ mice displayed approximately equivalent levels of weight gain in comparison to wt animals at the time of peak illness (Fig. 2B). However, *Ctsl*$^{-/-}$ and *Ctss*$^{-/-}$ mice had more weight loss than wt mice, and subsequent weight gain, indicative of recovery of these juvenile animals, was delayed. These findings suggest that despite the increased mortality of *Ctsl*$^{-/-}$ and *Ctss*$^{-/-}$ mice, these animals display slower kinetics of disease development. Thus, expression of cathepsins B, L, and S influences reovirus pathogenesis.

Peak reovirus titers are diminished in cathepsin-deficient mice. To understand differences in susceptibility to reovirus infection among the cathepsin-deficient mice, we inoculated 3-day-old mice perorally with a lower dose of T3SA+, 10^2 PFU, and quantified viral growth in selected organs. In comparison to wt mice, *Ctsb*$^{-/-}$ mice demonstrated equivalent growths of reovirus in the intestine, the site of primary replication, at all time points tested (Fig. 3A). Although titers were lower at day 4 in the livers of *Ctsb*$^{-/-}$ mice, peak titers at day 8 were equivalent to those in wt mice. In contrast, peak titers in the hearts and brains of *Ctsb*$^{-/-}$ mice were lower than those in wt mice, reaching statistical significance at day 12 in the brain. In concordance with these results, *Ctsb*$^{-/-}$ mice exhibited greater weight gain than wt mice at day 12 (Fig. 4), suggesting that lower titers in the heart and brain are associated with diminished disease and lead to enhanced survival. In these experiments, neither wt nor *Ctsb*$^{-/-}$ mice displayed signs of illness or succumbed to infection.

The trend displayed by *Ctsl*$^{-/-}$ mice differs from that of *Ctsb*$^{-/-}$ mice with respect to both peak titer and kinetics of disease progression. In contrast to what was found for *Ctsb*$^{-/-}$ mice, peak titers in all organs of *Ctsl*$^{-/-}$ mice were decreased in comparison to those for wt mice, reaching statistical significance in the heart at day 8 (Fig. 3B). However, viral clearance was delayed, as titers in *Ctsl*$^{-/-}$ mice were greater than those in wt mice at days 12, 16, and 20 postinoculation, reaching statistical significance in the intestine and liver at day 12. As expected from these results, the average weight of *Ctsl*$^{-/-}$ mice was significantly less than that of wt mice at day 20 (Fig. 4). Despite the lower dose of T3SA+ used in these experiments, several *Ctsl*$^{-/-}$ animals displayed overt signs of illness, including weakness and lethargy, and some died.

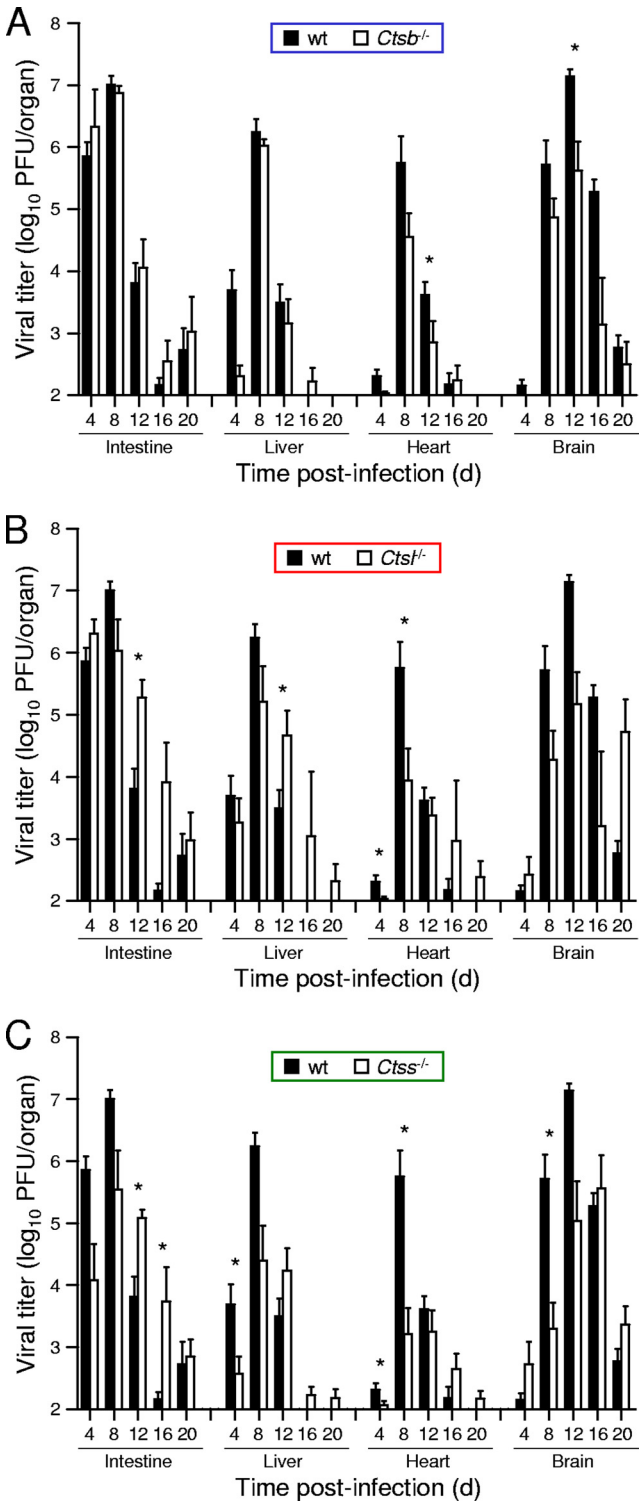

FIG. 3. Reovirus titers in organs of wt and cathepsin-deficient mice following peroral inoculation. C57BL/6 wt and *Ctsb*$^{-/-}$ (A), *Ctsl*$^{-/-}$ (B), and *Ctss*$^{-/-}$ (C) mice, 2 to 4 days (d) old, were inoculated perorally with 10^2 PFU T3SA+. Organs were resected at the times shown and homogenized by freeze-thawing and sonication. Viral titers in organ homogenates were determined by a plaque assay. Results are presented as mean viral titers in whole organs of 6 to 20 mice. Error bars represent standard errors of the means. *, *P* values of <0.05, as determined by a Mann-Whitney test, in comparison to the level for wt mice at the same time after inoculation. The limit of detection was 10^2 PFU/organ.

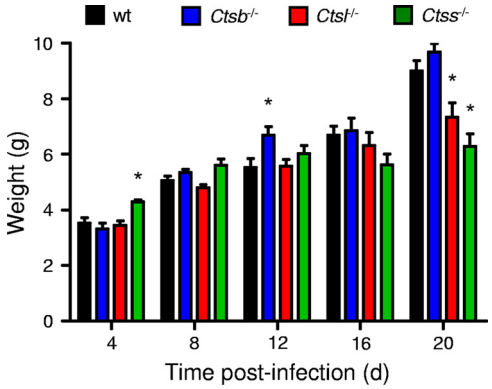

FIG. 4. Weights of mice following peroral inoculation with T3SA+. C57BL/6 wt and cathepsin-deficient mice, 2 to 4 (d) days old, were inoculated perorally with 10^2 PFU T3SA+. Mice were weighed only on the day of harvest, as indicated. Results are displayed as the mean weights of 6 to 20 animals. *, P values of <0.05, as determined by Student's t test, in comparison to the level for wt mice at the same time after inoculation.

The kinetics of viral growth in *Ctss*$^{-/-}$ mice were similar to those in *Ctsl*$^{-/-}$ mice. Peak titers in all organs of *Ctss*$^{-/-}$ animals were lower than those in wt mice, reaching statistical significance in the liver at day 4, in the heart at days 4 and 8, and in the brain at day 8 (Fig. 3C). As in *Ctsl*$^{-/-}$ mice, viral titers did not decrease in *Ctss*$^{-/-}$ mice between days 8 and 12, and titers in the intestines of *Ctss*$^{-/-}$ mice were actually greater than those in wt mice at days 12 and 16. These data suggest that viral clearance was delayed in *Ctss*$^{-/-}$ mice. Also, like *Ctsl*$^{-/-}$ mice, *Ctss*$^{-/-}$ mice infected with T3SA+ displayed signs of illness, including weakness and lethargy, diminished weight gain (Fig. 4), and mortality. Thus, peak reovirus titers were decreased in all strains of cathepsin-deficient mice, but mice deficient in cathepsin L or cathepsin S had higher viral titers at late times after inoculation and increased disease severity.

Inflammation in the liver is more severe in cathepsin L- and cathepsin S-deficient mice. To better understand why *Ctsl*$^{-/-}$ and *Ctss*$^{-/-}$ mice had greater susceptibility to reovirus infection than wt and *Ctsb*$^{-/-}$ mice, we compared histological sections of heart and liver from mice inoculated perorally with 10^6 PFU T3SA+. Animals chosen for histological analysis were matched for viral titer in the liver. Viral antigen staining in the hearts of all genotypes of mice localized primarily to the subepicardial myocardium, with little to moderate involvement of the deeper myocardium (data not shown). The extents of inflammatory cell infiltrates associated with infectious foci were consistent across all strains of mice.

In all mouse strains, infection in the liver centered on the bile duct epithelium (Fig. 5), as has been previously reported (5). Viral antigen and inflammation were more pronounced along large portal tracts; however, smaller portal tracts also were involved. Hepatic lobular involvement was present in all strains of mice in regions of increased reovirus antigen staining and inflammation. Although there was variability within each genotype of mice and some overlap between them, inflammation centered at the portal triads was more severe in *Ctsl*$^{-/-}$ and *Ctss*$^{-/-}$ than in wt and *Ctsb*$^{-/-}$ mice (Fig. 5, low-magnification panels showing increased numbers of leukocytes in panels C and D versus A and B).

Liver enzyme levels are increased in cathepsin L- and cathepsin S-deficient mice. To obtain biochemical evidence of biliary or hepatic injury in reovirus-infected mice, we assessed levels of total bilirubin (TBIL), alkaline phosphatase (ALK), alanine aminotransferase (ALT), and aspartate aminotransfer-

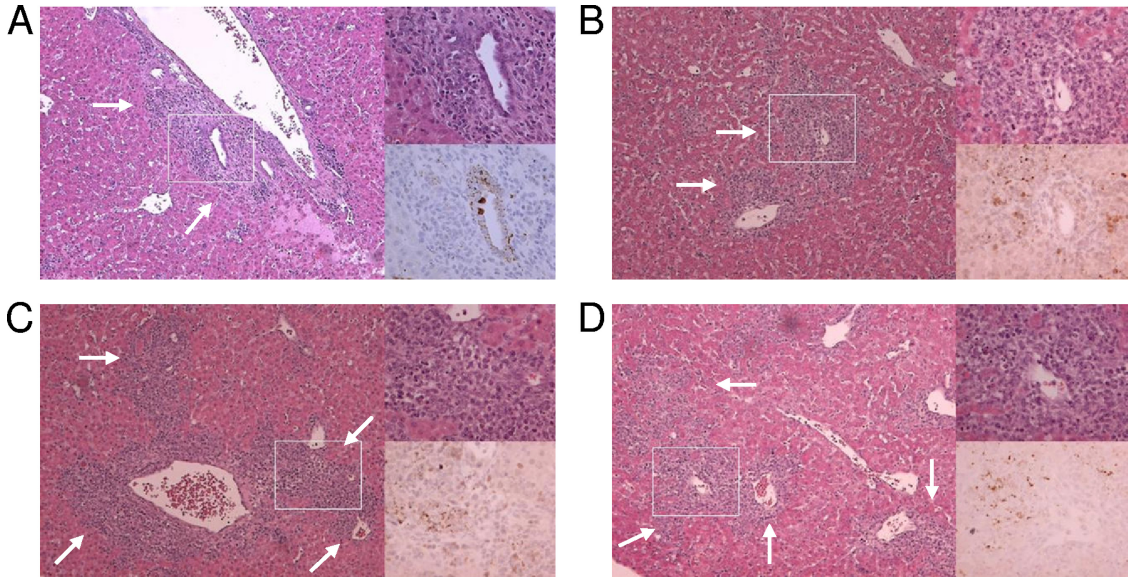

FIG. 5. Histological analysis of reovirus growth in the liver. C57BL/6 wt and cathepsin-deficient mice, 2 to 4 days old, were inoculated perorally with 10^6 PFU T3SA+. Livers were resected at day 8 postinfection, and a small wedge of liver was removed for titer determination by a plaque assay. The remaining liver was processed for histopathology, and consecutive sections were stained with hematoxylin and eosin or polyclonal reovirus antiserum. Representative samples from titer-matched livers are shown. Boxes indicate areas of enlargement shown in the panels on the right. Arrows indicate areas of inflammation. Original magnifications, ×10 and ×40. A, wt; B, *Ctsb*$^{-/-}$; C, *Ctsl*$^{-/-}$; D, *Ctss*$^{-/-}$.

TABLE 2. Bilirubin and liver enzyme levels in sera following reovirus infection[a]

Genotype	Concn in sera of indicated mouse group							
	Mock infected				Reovirus infected			
	TBIL (mg/dl)	ALK (U/liter)	ALT (U/liter)	AST (U/liter)	TBIL (mg/dl)	ALK (U/liter)	ALT (U/liter)	AST (U/liter)
wt	1.5	634	127	461	0.9 (0.3)	768 (140.8)	295 (224.8)	495 (231.2)
Ctsb$^{-/-}$	2.0	475	73	417	1.9 (0.2)	783 (109.0)	97.5 (31.1)	460.5 (105.1)
Ctsl$^{-/-}$	1.5	567	57	409	9.2* (1.1)	1282.4 (300.3)	60 (20.8)	439 (43.8)
Ctss$^{-/-}$	0.9	574	99	330	6.9* (2.0)	1709* (258.9)	858 (665.5)	2083.75 (856.8)

[a] C57/Bl6 wt and cathepsin-deficient mice, 2 to 4 days old, were inoculated perorally with PBS alone or 10^6 PFU T3SA+. At day 12 postinoculation, the liver was resected and blood was collected. A small wedge of liver was removed for titer determination by a plaque assay. Mean values from two mock-infected mice or three to five reovirus-infected mice with approximately equivalent viral titers in the liver are shown. *, P values of <0.05, as determined by Student's t test, in comparison to the level for wt mice. The standard errors of the means are shown in parentheses.

ase (AST) in mice that were either mock infected or infected with 10^6 PFU T3SA+. No biomarker of liver injury was elevated in mock-infected mice at any time point or in any strain of reovirus-infected mice at day 8 postinfection (data not shown). In contrast, levels of TBIL and ALK were increased in *Ctsl*$^{-/-}$ mice and levels of all four markers were increased in *Ctss*$^{-/-}$ mice at day 12 postinfection (Table 2). These results indicate more-severe hepatobiliary damage in reovirus-infected *Ctsl*$^{-/-}$ and *Ctss*$^{-/-}$ mice than in wt and *Ctsb*$^{-/-}$ animals.

Hematogenous dissemination of reovirus is unaffected by the absence of a single cathepsin protease following peroral inoculation. We thought it possible that the capacity of reovirus to either disseminate to sites of secondary infection in cathepsin-deficient mice or establish infection once reaching those sites might be reduced. To distinguish between these possibilities, we quantified viral titers in blood samples following peroral inoculation. Newborn mice were inoculated perorally with 10^6 PFU of T3SA+, and blood samples were collected at various times after inoculation. Reovirus established viremia in all strains of mice, reaching peak titers that did not differ significantly (Fig. 6). Therefore, the lack of a single cathepsin protease does not appear to alter the efficiency of reovirus hematogenous dissemination in mice.

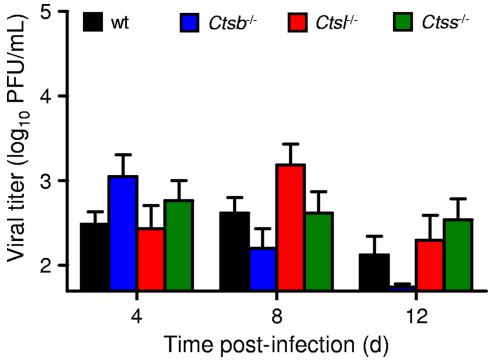

FIG. 6. Viremia in wt and cathepsin-deficient mice following peroral inoculation. C57BL/6 wt and cathepsin-deficient mice, 2 to 4 days (d) old, were inoculated perorally with 10^6 PFU T3SA+. Blood samples were collected at the times shown and homogenized by freeze-thawing and sonication. Viral titers in blood samples were determined by a plaque assay. Results are presented as mean viral titers of 9 to 14 mice. The limit of detection was 50 PFU/ml.

Growth of reovirus in the brain is diminished in cathepsin L-deficient mice following intracranial inoculation. To determine the effect of cathepsin deficiency on the capacity of reovirus to grow at a site of secondary replication, we quantified viral titers in the brain following intracranial inoculation of wt and cathepsin-deficient mice. This site was chosen for ease of direct inoculation. Titers of T3SA+ in the brains of wt, *Ctsb*$^{-/-}$, and *Ctss*$^{-/-}$ mice did not differ statistically (Fig. 7), suggesting that cathepsins B and S are not required for reovirus growth in the brain following direct inoculation into that site. However, titers of T3SA+ in the brains of *Ctsl*$^{-/-}$ mice were significantly lower on day 9 postinoculation, suggesting that cathepsin L is required for efficient growth of reovirus in the brain.

Treatment with an inhibitor of cathepsin L promotes survival following reovirus infection. Since titers of reovirus in organs of cathepsin-deficient mice are lower than those in wt mice, but mortality is increased in *Ctsl*$^{-/-}$ and *Ctss*$^{-/-}$ mice, we hypothesized that the immune defects accompanying genetic cathepsin L and cathepsin S deficiency might mask a cathepsin requirement for efficient viral growth. Therefore, we sought to

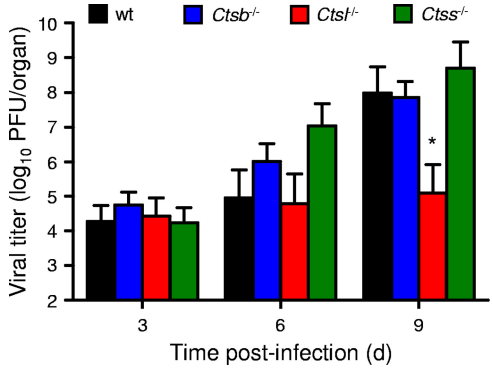

FIG. 7. Viral growth in the brains of wt and cathepsin-deficient mice following intracranial inoculation. C57BL/6 wt and cathepsin-deficient mice, 2 to 4 days (d) old, were inoculated intracranially with 10^2 PFU T3SA+. Brains were resected at the times shown and homogenized by freeze-thawing and sonication. Viral titers in brain homogenates were determined by a plaque assay. Results are expressed as mean viral titers in the brains of 9 to 13 mice. Error bars represent standard errors of the means. *, P values of <0.05, as determined by a Mann-Whitney test, in comparison to the level for wt mice at the same time after inoculation. The limit of detection was 10^2 PFU/brain.

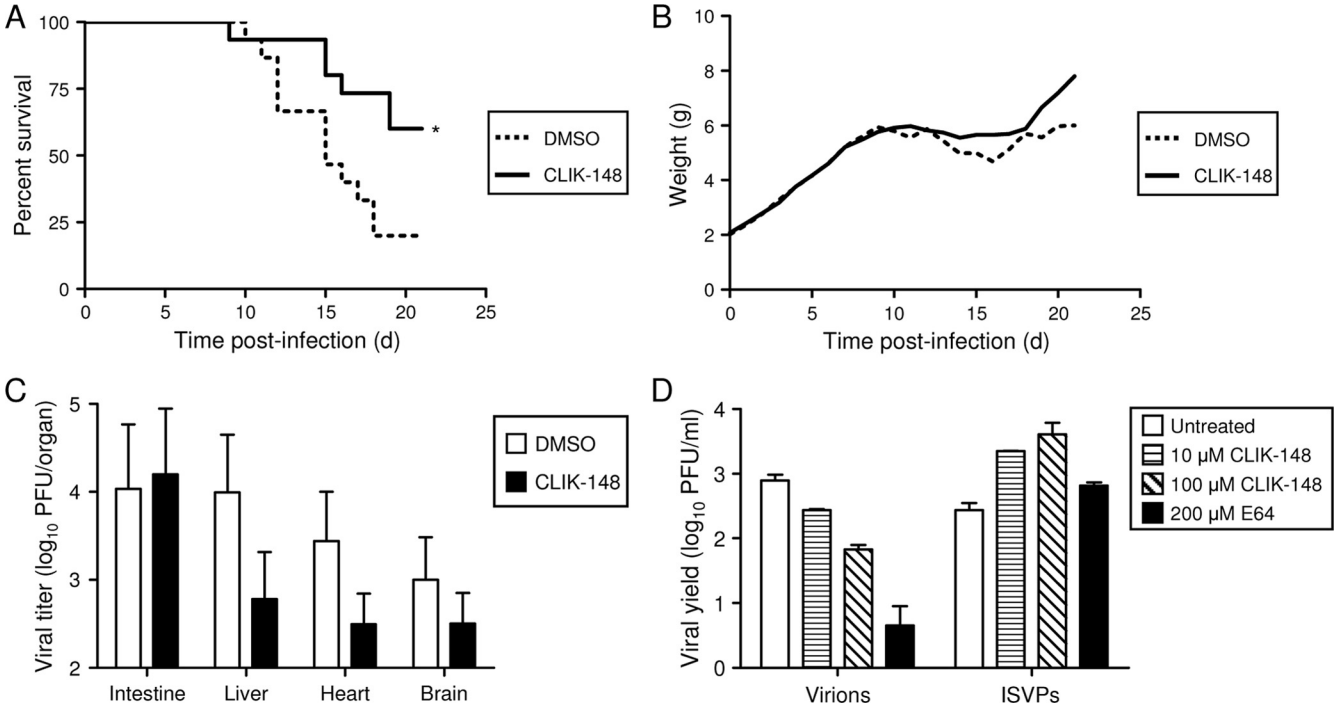

FIG. 8. (A to C) Treatment with an inhibitor of cathepsin L decreases disease severity. C57BL/6 wt mice, 2 to 4 days (d) old, were inoculated intraperitoneally with CLIK-148 at a dose of 100 μg/g average litter body weight or vehicle control 1 h prior to peroral inoculation with 10^7 PFU (A, B) or 10 PFU (C) T3SA+. Mice were treated intraperitoneally with CLIK-148 thereafter for 7 days. Mice ($n = 15$) were monitored for survival (A) and weight gain (B). (A) *, P values of <0.05, as determined by a log rank test, in comparison to the level for vehicle-treated mice. (B) All living mice were weighed each day. (C) Mice ($n = 9$ or 10) were euthanized at day 8 postinoculation, and viral titers in organs were determined by a plaque assay. Error bars represent standard errors of the means. (D) CLIK-148 inhibits infection by virions but not by ISVPs. Monolayers of L cells were preincubated for 4 h in medium with or without CLIK-148 or E64 at the concentrations shown. The medium was removed, and cells were adsorbed with T3SA+ virions or ISVPs at a multiplicity of infection of 2 PFU per cell. After 1 h, the inoculum was removed, fresh medium with or without CLIK-148 or E64 was added, and cells were incubated for 0 or 24 h. Viral titers in cell lysates were determined by a plaque assay. The results are presented as mean viral yields, calculated by dividing the titer at 24 h by the titer at 0 h for each concentration of CLIK-148 or E64 for duplicate wells.

determine whether reovirus disease could be ameliorated in wt mice by treatment with a cathepsin inhibitor. CLIK-148, a derivative of the pan-cysteine protease inhibitor E-64, inhibits cathepsin L in vivo (37, 38). Mice were treated with CLIK-148 at a dose of approximately 100 μg/g body weight via intraperitoneal injection 1 h prior to peroral inoculation with 10^7 PFU T3SA+ and then every 24 h for 7 days. In comparison to mice treated with vehicle alone, a significantly greater percentage of mice treated with CLIK-148 survived (Fig. 8A). At day 21, 40% of CLIK-148-treated mice succumbed, whereas 80% of vehicle-treated mice died. As a surrogate marker for disease, CLIK-148-treated mice exhibited only minimal weight loss, followed by substantial weight gain through the course of the experiment, whereas vehicle-treated mice exhibited more-severe weight loss and gained weight more slowly during the recovery phase (Fig. 8B). Mock-infected mice treated with CLIK-148 or vehicle alone showed no signs of drug toxicity and had survival rates of 100% (data not shown). These results suggest that treatment with a cathepsin L inhibitor dampens the severity of reovirus disease.

Treatment with an inhibitor of cathepsin L diminishes reovirus growth at sites of secondary replication. To determine whether the cause of diminished mortality following treatment with CLIK-148 is related to viral growth, we quantified viral titers in various organs of wt mice treated with CLIK-148. Mice were treated with CLIK-148 at a dose of approximately 100 μg/g body weight via intraperitoneal injection 1 h prior to peroral inoculation with 10 PFU T3SA+ and then every 24 h for 7 days. On day 8 postinfection, organs were harvested and titers determined by a plaque assay. Although titers in vehicle-treated and CLIK-148-treated mice were equivalent in the intestine, titers were reduced at sites of secondary replication in the CLIK-148-treated mice in comparison to those in vehicle-treated mice (Fig. 8C). More striking, perhaps, was that of the five CLIK-148-treated animals with detectable titers in the intestine, only two exhibited virus dissemination to other organs. However, of the seven vehicle-treated mice with detectable titers in the intestine, six had disseminated virus. Thus, pharmacologic blockade of cathepsin L activity diminishes reovirus dissemination to sites of secondary replication.

Treatment with CLIK-148 inhibits reovirus entry into cells. To define the block to infection imposed by CLIK-148, murine L cells were treated with various concentrations of CLIK-148 prior to infection with T3SA+ virions and in vitro-generated ISVPs. ISVPs are capable of penetrating cells at the plasma membrane and are resistant to inhibitors of proteolytic disassembly (2, 17, 19, 76, 86). In comparison to viral yields in untreated cells, yields in cells treated with 100 μM CLIK-148

TABLE 3. Reovirus pathogenesis in cathepsin-deficient mice

Genotype	Survival rate	AST level	Level in mice inoculated perorally					Level of replication in brain in mice inoculated intracranially
			Replication in intestine	Replication in liver	Replication in heart	Replication in brain	Viremia	
Ctsb$^{-/-b}$	↑	↑	⇆	⇆	↓	↓	⇆	⇆
Ctsl$^{-/-b}$	↓	↑	↓	↓	↓	↓	⇆	↓
Ctss$^{-/-b}$	↓	↑	↓	↓	↓	↓	⇆	⇆
wt plus CLIK-148[c]	↑	ND	⇆	↓	↓	↓	ND	ND

[a] ↑, increase; ↓, decrease; ⇆, no change; ND, not determined.
[b] Results shown are in comparison to the level for wt mice.
[c] Results shown are in comparison to the level for wt mice treated with DMSO.

were diminished 10-fold (Fig. 8D). Treatment with 200 μM E64, which blocks the activity of both cathepsin B and cathepsin L (3), diminished viral yields 100-fold. Yields produced following infection by ISVPs were not decreased in cells treated with either inhibitor, demonstrating that the block imposed by CLIK-148 occurs at a stage in viral replication prior to generation of ISVPs.

DISCUSSION

In this study, we found that cathepsins B, L, and S are individually required for development of peak viral titers at sites of secondary replication and thus influence reovirus disease (Table 3). Survival is enhanced in mice lacking cathepsin B but diminished in mice lacking cathepsin L or cathepsin S, likely reflecting the differential importance of these cathepsins in adaptive immunity. Importantly, treatment with an inhibitor of cathepsin L activity, which uncouples cathepsin functions in reovirus disassembly and immunity, enhances survival. These findings indicate a key role for cathepsin proteases in viral pathogenesis.

There are 11 cysteine proteases in the papain superfamily encoded by the human genome (8, 40, 82). Of these, several have been linked to disease in humans or animals. In addition to roles in Alzheimer's disease (31), atherosclerosis (42), cancer (49), and osteoporosis (81), cathepsins B, L, and S are important mediators of cell entry by several viruses (13, 23, 28, 36, 58). Although members of the cathepsin family show some redundancy of function, there exist specific roles for each protease. Therefore, we hypothesized that the proteases capable of mediating reovirus disassembly would serve nonredundant functions in reovirus pathogenesis by virtue of their specialized host functions.

Reovirus virions are uncoated in late endosomes or lysosomes by cathepsins B (23), L (23), or S (28). We reasoned that deficiency in the proteases that catalyze uncoating might lead to decreased viral growth and diminished disease severity. Only mice deficient in expression of cathepsin B fit this profile. *Ctsb*$^{-/-}$ mice had an increased survival rate in comparison to wt mice when infected with a high dose of reovirus, whereas *Ctsl*$^{-/-}$ and *Ctss*$^{-/-}$ mice displayed decreased survival rates. In concordance with this observation, reovirus produced lower titers at sites of secondary replication in *Ctsb*$^{-/-}$ mice than in wt mice, and *Ctsb*$^{-/-}$ mice displayed greater weight gain. These results suggest that cathepsin B is required for reovirus to establish high-titer infection and exert pathological effects.

The decreased survival rates of *Ctsl*$^{-/-}$ and *Ctss*$^{-/-}$ mice in comparison to that of wt mice raised the possibility that viral loads might be higher in these animals. However, reovirus produced lower peak titers at sites of secondary replication in both genotypes of mice in comparison to those in wt and *Ctsb*$^{-/-}$ mice. Diminished survival rates among *Ctsl*$^{-/-}$ and *Ctss*$^{-/-}$ mice are likely attributable to defects in immune function in these animals (15), with resultant failure to resolve viral infection. Indeed, viral titers in the intestine at day 12 were significantly higher in both *Ctsl*$^{-/-}$ and *Ctss*$^{-/-}$ mice than those in wt animals. As viral titers in wt mice decreased from day 8 to day 12, viral titers in *Ctsl*$^{-/-}$ and *Ctss*$^{-/-}$ mice did not. We think it most likely that the absence of functional CD4$^+$ T cells leads to inefficient viral clearance. Consequently, tissue injury is sustained for a longer period of time. This conclusion is supported by the kinetics of survival following infection. Although *Ctsl*$^{-/-}$ and *Ctss*$^{-/-}$ mice die at higher frequency than wt mice, survival times of the cathepsin-deficient mice are prolonged. Thus, the immune deficiency displayed by mice lacking cathepsin L or cathepsin S is associated with enhanced reovirus virulence.

The paradox that *Ctsl*$^{-/-}$ and *Ctss*$^{-/-}$ mice display increased disease severity and mortality despite lower peak titers suggests that *Ctsl*$^{-/-}$ and *Ctss*$^{-/-}$ mice are more susceptible to the pathological effects of reovirus infection than are wt mice. The disease phenotype of these mice included lethargy, gallbladder distention, intestinal obstruction, and oily hair (5, 20, 87), a syndrome associated with viral replication in intrahepatic bile duct epithelium, biliary obstruction, and fat malabsorption (5, 59, 60, 62, 87). However, the disease symptoms did not include spastic movements of the extremities, overt seizures, or paralysis, indicative of encephalitis. We think that death of reovirus-infected animals lacking cathepsin L or cathepsin S resulted from damage to the liver and heart. Histological analysis of the heart did not reveal striking differences in pathological injury in the different strains of mice, perhaps due to the high viral loads in the hearts of all mice. However, the increase in inflammatory infiltrate surrounding portal triads, coupled with the results of liver enzyme profiling, supports the conclusion that damage to the liver contributed to the poor outcome of reovirus-infected *Ctsl*$^{-/-}$ and *Ctss*$^{-/-}$ mice.

The observation that cathepsin-deficient mice inoculated with reovirus had lower titers at sites of secondary replication prompted us to investigate how individual cathepsins promote viral pathogenesis. We envision two possibilities. First, cathepsin expression might allow the virus to disseminate systemically in the host. Second, cathepsin expression might be required for

growth at sites of secondary replication once those sites are reached. All strains of mice had detectable virus in the blood, suggesting that cathepsin deficiency does not block reovirus spread from the intestine into the bloodstream. However, these proteases could be required for reovirus exit from the bloodstream into the surrounding tissues, for example, by promoting viral growth in endothelium or extravasation of infected lymphocytes from blood vessels into host tissues.

While cathepsins B and S are dispensable for reovirus growth in the brain, cathepsin L is not. Following intracranial inoculation, titers in *Ctsl*$^{-/-}$ mice were decreased in comparison to those in the other mouse strains tested. Cathepsin S is required for maximal growth of reovirus in the intestine, as titers of reovirus in the intestines of *Ctss*$^{-/-}$ mice are lower than those in all other strains. It is possible that decreased titers in the intestines of *Ctss*$^{-/-}$ mice are insufficient to allow efficient viral dissemination to sites of secondary replication. However, peak reovirus titers in the brains of *Ctss*$^{-/-}$ mice following peroral inoculation are greater than those in *Ctsb*$^{-/-}$ mice, suggesting that viral spread is independent of titer in the intestine. Since spread to the brain is less affected in *Ctss*$^{-/-}$ mice, and virus is present in the blood of *Ctss*$^{-/-}$ mice, cathepsin S may be important for reovirus growth at other sites of secondary replication, including the heart and liver, at which sites peak titers are less than those in wt mice. Cathepsin B also may be important for growth in the heart, as titers at that site in *Ctsb*$^{-/-}$ mice are decreased in comparison to those in wt mice, while titers in the intestine and liver are not. It is noteworthy that in mouse fibroblasts, although both cathepsin B and cathepsin L can mediate reovirus uncoating, cathepsin L is more efficient (23). Our data following both peroral and intracranial inoculation support this conclusion in that peak titers in all organs tested are lower in *Ctsl*$^{-/-}$ mice than in *Ctsb*$^{-/-}$ mice. These findings suggest that cathepsin L is required for efficient reovirus growth in tissues other than the intestine.

To eliminate the confounding variables present in the gene deletion experiments, we sought to determine the effect of a cathepsin inhibitor on reovirus pathogenesis. Mice treated with CLIK-148, which specifically inhibits cathepsin L (37, 38), had increased resistance to reovirus infection in comparison to vehicle-treated controls, as assessed by both survival and viral titers at sites of secondary replication. Because survival was increased in CLIK-148-treated mice but decreased in *Ctsl*$^{-/-}$ mice, we think that the inhibition of viral replication is specific and that immune functions are preserved. Furthermore, since the mice treated with CLIK-148 did not display defects in fur growth characteristic of *Ctsl*$^{-/-}$ mice (68), we conclude that pharmacologic inhibition of cathepsin L is not as complete as genetic ablation. Successful pharmacologic attenuation of reovirus disease with a cathepsin inhibitor raises the possibility that cathepsin inhibitor therapy could be effective for other viruses that require cathepsin proteolysis for cell entry. Ebola virus (13), Nipah virus (22, 57), Hendra virus (58), and severe acute respiratory syndrome coronavirus (36) utilize cathepsin proteases to enter cells. Treatment of cells with chloroquine inhibits Hendra and Nipah virus infection (64), most likely via interference with viral fusion glycoprotein processing by cathepsin L. The absence of inhibitor-associated toxicity in this study and others (37, 38), along with the efficacy of CLIK-148 treatment in the amelioration of disease (this study), suggests that cathepsin inhibitors should be evaluated for therapeutic efficacy against these viruses.

We have shown that cathepsin proteases are required for efficient reovirus infection in mice. Cathepsins promote optimal growth at specific sites of reovirus replication in the host and influence survival following reovirus infection. Organ-specific differences in infection of cathepsin-deficient mice highlight distinct roles for these proteases in vivo. A better understanding of the function of cathepsin proteases in the pathogenesis of viral infections should lead to novel therapeutics for a variety of important human pathogens.

ACKNOWLEDGMENTS

We thank Mark Boothby, Graham Carpenter, Anne Kenworthy, and Borden Lacy for helpful suggestions. We thank Hal Chapman, Doug Hanahan, and Johanna Joyce for providing the mice used in these experiments. We thank Jessica Summers and the Vanderbilt University Division of Animal Care for expert animal husbandry. We thank Pam Wirth, Melissa Downing, and Frances Shook from the Vanderbilt Immunohistochemistry Core for sample preparation. We thank Guo-Ping Shi for help with CLIK-148 administration, Charles Cobb for fluorometry assistance, John Mort for provision of cathepsin L, and Greg Wilson for assistance with cathepsin digestion of virions.

This work was supported by Public Health Service awards T32 AI07611 (E.M.J.), T32 GM08554 (J.D.D.), and R01 AI32539 and the Elizabeth B. Lamb Center for Pediatric Research. Additional support was provided by Public Health Service awards P30 CA68485 for the Vanderbilt-Ingram Cancer Center and P60 DK20593 for the Vanderbilt Diabetes Research and Training Center.

REFERENCES

1. **Antar, A. A. R., J. L. Konopka, J. A. Campbell, R. A. Henry, A. L. Perdigoto, B. D. Carter, A. Pozzi, T. W. Abel, and T. S. Dermody.** 2009. Junctional adhesion molecule-A is required for hematogenous dissemination of reovirus. Cell Host Microbe **5:**59–71.
2. **Baer, G. S., and T. S. Dermody.** 1997. Mutations in reovirus outer-capsid protein σ3 selected during persistent infections of L cells confer resistance to protease inhibitor E64. J. Virol. **71:**4921–4928.
3. **Barrett, A. J., A. A. Kembhavi, M. A. Brown, H. Kirschke, C. G. Knight, M. Tamai, and K. Hanada.** 1982. L-*trans*-Epoxysuccinyl-leucylamido(4-guanidino)butane (E-64) and its analogues as inhibitors of cysteine proteinases including cathepsins B, H and L. Biochem. J. **201:**189–198.
4. **Barton, E. S., J. L. Connolly, J. C. Forrest, J. D. Chappell, and T. S. Dermody.** 2001. Utilization of sialic acid as a coreceptor enhances reovirus attachment by multistep adhesion strengthening. J. Biol. Chem. **276:**2200–2211.
5. **Barton, E. S., B. E. Youree, D. H. Ebert, J. C. Forrest, J. L. Connolly, T. Valyi-Nagy, K. Washington, J. D. Wetzel, and T. S. Dermody.** 2003. Utilization of sialic acid as a coreceptor is required for reovirus-induced biliary disease. J. Clin. Investig. **111:**1823–1833.
6. **Borsa, J., B. D. Morash, M. D. Sargent, T. P. Copps, P. A. Lievaart, and J. G. Szekely.** 1979. Two modes of entry of reovirus particles into L cells. J. Gen. Virol. **45:**161–170.
7. **Borsa, J., M. D. Sargent, P. A. Lievaart, and T. P. Copps.** 1981. Reovirus: evidence for a second step in the intracellular uncoating and transcriptase activation process. Virology **111:**191–200.
8. **Bromme, D., and J. Kaleta.** 2002. Thiol-dependent cathepsins: pathophysiological implications and recent advances in inhibitor design. Curr. Pharm. Des. **8:**1639–1658.
9. **Bromme, D., A. Steinert, S. Friebe, S. Fittkau, B. Wiederanders, and H. Kirschke.** 1989. The specificity of bovine spleen cathepsin S. A comparison with rat liver cathepsins L and B. Biochem. J. **264:**475–481.
10. **Carmona, E., É. Dufour, C. Plouffe, S. Takebe, P. Mason, J. S. Mort, and R. Ménard.** 1996. Potency and selectivity of the cathepsin L propeptide as an inhibitor of cysteine proteases. Biochemistry **35:**8149–8157.
11. **Chandran, K., D. L. Farsetta, and M. L. Nibert.** 2002. Strategy for nonenveloped virus entry: a hydrophobic conformer of the reovirus membrane penetration protein μ1 mediates membrane disruption. J. Virol. **76:**9920–9933.
12. **Chandran, K., J. S. Parker, M. Ehrlich, T. Kirchhausen, and M. L. Nibert.** 2003. The δ region of outer-capsid protein μ1 undergoes conformational change and release from reovirus particles during cell entry. J. Virol. **77:**13361–13375.
13. **Chandran, K., N. J. Sullivan, U. Felbor, S. P. Whelan, and J. M. Cunning-**

ham. 2005. Endosomal proteolysis of the Ebola virus glycoprotein is necessary for infection. Science **308:**1643–1645.
14. **Chang, C. T., and H. J. Zweerink.** 1971. Fate of parental reovirus in infected cell. Virology **46:**544–555.
15. **Chapman, H. A.** 2006. Endosomal proteases in antigen presentation. Curr. Opin. Immunol. **18:**78–84.
16. **Chapman, H. A., R. J. Riese, and G. P. Shi.** 1997. Emerging roles for cysteine proteases in human biology. Annu. Rev. Physiol. **59:**63–88.
17. **Clark, K. M., J. D. Wetzel, J. Bayley, D. H. Ebert, S. A. McAbee, E. K. Stoneman, G. S. Baer, Y. Zhu, G. J. Wilson, B. V. V. Prasad, and T. S. Dermody.** 2006. Reovirus variants selected for resistance to ammonium chloride have mutations in viral outer-capsid protein σ3. J. Virol. **80:**671–681.
18. **Danthi, P., C. M. Coffey, J. S. Parker, T. W. Abel, and T. S. Dermody.** 2008. Independent regulation of reovirus membrane penetration and apoptosis by the μ1 φ domain. PLoS Pathog. **4:**e1000248.
19. **Dermody, T. S., M. L. Nibert, J. D. Wetzel, X. Tong, and B. N. Fields.** 1993. Cells and viruses with mutations affecting viral entry are selected during persistent infections of L cells with mammalian reoviruses. J. Virol. **67:**2055–2063.
20. **Derrien, M., J. W. Hooper, and B. N. Fields.** 2003. The M2 gene segment is involved in the capacity of reovirus type 3Abney to induce the oily fur syndrome in neonatal mice, a S1 gene segment-associated phenotype. Virology **305:**25–30.
21. **Deussing, J., W. Roth, P. Saftig, C. Peters, H. L. Ploegh, and J. A. Villadangos.** 1998. Cathepsins B and D are dispensable for major histocompatibility complex class II-mediated antigen presentation. Proc. Natl. Acad. Sci. USA **95:**4516–4521.
22. **Diederich, S., L. Thiel, and A. Maisner.** 2008. Role of endocytosis and cathepsin-mediated activation in Nipah virus entry. Virology **375:**391–400.
23. **Ebert, D. H., J. Deussing, C. Peters, and T. S. Dermody.** 2002. Cathepsin L and cathepsin B mediate reovirus disassembly in murine fibroblast cells. J. Biol. Chem. **277:**24609–24617.
24. **Ehrlich, M., W. Boll, A. Van Oijen, R. Hariharan, K. Chandran, M. L. Nibert, and T. Kirchhausen.** 2004. Endocytosis by random initiation and stabilization of clathrin-coated pits. Cell **118:**591–605.
25. **Fleeton, M., N. Contractor, F. Leon, J. D. Wetzel, T. S. Dermody, and B. Kelsall.** 2004. Peyer's patch dendritic cells process viral antigen from apoptotic epithelial cells in the intestine of reovirus-infected mice. J. Exp. Med. **200:**235–245.
26. **Funkelstein, L., T. Toneff, C. Mosier, S. R. Hwang, F. Beuschlein, U. D. Lichtenauer, T. Reinheckel, C. Peters, and V. Hook.** 2008. Major role of cathepsin L for producing the peptide hormones ACTH, beta-endorphin, and alpha-MSH, illustrated by protease gene knockout and expression. J. Biol. Chem. **283:**35652–35659.
27. **Furlong, D. B., M. L. Nibert, and B. N. Fields.** 1988. Sigma 1 protein of mammalian reoviruses extends from the surfaces of viral particles. J. Virol. **62:**246–256.
28. **Golden, J. W., J. A. Bahe, W. T. Lucas, M. L. Nibert, and L. A. Schiff.** 2004. Cathepsin S supports acid-independent infection by some reoviruses. J. Biol. Chem. **279:**8547–8557.
29. **Guicciardii, M. E., J. Deussing, H. Miyoshi, S. F. Bronk, P. A. Svingen, C. Peters, S. H. Kaufmann, and G. J. Gores.** 2000. Cathepsin B contributes to TNF-α-mediated hepatocyte apoptosis by promoting mitochondrial release of cytochrome c. J. Clin. Investig. **106:**1127–1137.
30. **Halangk, W., M. Lerch, B. Brandt-Nedelev, W. Roth, M. Ruthenbuerger, T. Reinheckel, W. Domschke, H. Lippert, C. Peters, and J. Deussing.** 2000. Role of cathepsin B in intracellular trypsinogen activation and the onset of acute pancreatitis. J. Clin. Investig. **106:**773–781.
31. **Haque, A., N. L. Banik, and S. K. Ray.** 2008. New insights into the roles of endolysosomal cathepsins in the pathogenesis of Alzheimer's disease: cathepsin inhibitors as potential therapeutics. CNS Neurol. Disord. Drug Targets **7:**270–277.
32. **Honey, K., K. Benlagha, C. Beers, K. Forbush, L. Teyton, M. J. Kleijmeer, A. Y. Rudensky, and A. Bendelac.** 2002. Thymocyte expression of cathepsin L is essential for NKT cell development. Nat. Immunol. **3:**1069–1074.
33. **Honey, K., T. Nakagawa, C. Peters, and A. Rudensky.** 2002. Cathepsin L regulates CD4+ T cell selection independently of its effect on invariant chain: a role in the generation of positively selecting peptide ligands. J. Exp. Med. **195:**1349–1358.
34. **Hsieh, C. S., P. deRoos, K. Honey, C. Beers, and A. Y. Rudensky.** 2002. A role for cathepsin L and cathepsin S in peptide generation for MHC class II presentation. J. Immunol. **168:**2618–2625.
35. **Hsing, L. C., and A. Y. Rudensky.** 2005. The lysosomal cysteine proteases in MHC class II antigen presentation. Immunol. Rev. **207:**229–241.
36. **Huang, I.-C., B. J. Bosch, F. Li, W. Li, K. H. Lee, S. Ghiran, N. Vasilieva, T. S. Dermody, S. C. Harrison, P. R. Dormitzer, M. Farzan, P. J. Rottier, and H. Choe.** 2006. SARS coronavirus, but not human coronavirus NL63, utilizes cathepsin L to infect ACE2-expressing cells. J. Biol. Chem. **281:**3198–3203.
37. **Katunuma, N., E. Murata, H. Kakegawa, A. Matsui, H. Tsuzuki, H. Tsuge, D. Turk, V. Turk, M. Fukushima, Y. Tada, and T. Asao.** 1999. Structure based development of novel specific inhibitors for cathepsin L and cathepsin S in vitro and in vivo. FEBS Lett. **458:**6–10.
38. **Katunuma, N., H. Tsuge, M. Nukatsuka, T. Asao, and M. Fukushima.** 2002. Structure-based design of specific cathepsin inhibitors and their application to protection of bone metastases of cancer cells. Arch. Biochem. Biophys. **397:**305–311.
39. **Kirschke, H., B. Wiederanders, D. Bromme, and A. Rinne.** 1989. Cathepsin S from bovine spleen. Purification, distribution, intracellular localization and action on proteins. Biochem. J. **264:**467–473.
40. **Lander, E. S., L. M. Linton, B. Birren, C. Nusbaum, M. C. Zody, J. Baldwin, K. Devon, K. Dewar, M. Doyle, W. FitzHugh, R. Funke, D. Gage, K. Harris, A. Heaford, J. Howland, L. Kann, J. Lehoczky, R. LeVine, P. McEwan, K. McKernan, J. Meldrim, J. P. Mesirov, C. Miranda, W. Morris, J. Naylor, C. Raymond, M. Rosetti, R. Santos, A. Sheridan, C. Sougnez, N. Stange-Thomann, N. Stojanovic, A. Subramanian, D. Wyman, J. Rogers, J. Sulston, R. Ainscough, S. Beck, D. Bentley, J. Burton, C. Clee, N. Carter, A. Coulson, R. Deadman, P. Deloukas, A. Dunham, I. Dunham, R. Durbin, L. French, D. Grafham, S. Gregory, T. Hubbard, S. Humphray, A. Hunt, M. Jones, C. Lloyd, A. McMurray, L. Matthews, S. Mercer, S. Milne, J. C. Mullikin, A. Mungall, R. Plumb, M. Ross, R. Shownkeen, S. Sims, R. H. Waterston, R. K. Wilson, L. W. Hillier, J. D. McPherson, M. A. Marra, E. R. Mardis, L. A. Fulton, A. T. Chinwalla, K. H. Pepin, W. R. Gish, S. L. Chissoe, M. C. Wendl, K. D. Delehaunty, T. L. Miner, A. Delehaunty, J. B. Kramer, L. L. Cook, R. S. Fulton, D. L. Johnson, P. J. Minx, S. W. Clifton, T. Hawkins, E. Branscomb, P. Predki, P. Richardson, S. Wenning, T. Slezak, N. Doggett, J. F. Cheng, A. Olsen, S. Lucas, C. Elkin, E. Uberbacher, M. Frazier, et al.** 2001. Initial sequencing and analysis of the human genome. Nature **409:**860–921.
41. **Lee, P. W. K., E. C. Hayes, and W. K. Joklik.** 1981. Protein σ1 is the reovirus cell attachment protein. Virology **108:**156–163.
42. **Lutgens, S. P., K. B. Cleutjens, M. J. Daemen, and S. Heeneman.** 2007. Cathepsin cysteine proteases in cardiovascular disease. FASEB J. **21:**3029–3041.
43. **Maehr, R., J. D. Mintern, A. E. Herman, A. M. Lennon-Dumenil, D. Mathis, C. Benoist, and H. L. Ploegh.** 2005. Cathepsin L is essential for onset of autoimmune diabetes in NOD mice. J. Clin. Investig. **115:**2934–2943.
44. **Mann, M. A., D. M. Knipe, G. D. Fischbach, and B. N. Fields.** 2002. Type 3 reovirus neuroinvasion after intramuscular inoculation: direct invasion of nerve terminals and age-dependent pathogenesis. Virology **303:**222–231.
45. **Marsh, M., and A. Helenius.** 2006. Virus entry: open sesame. Cell **124:**729–740.
46. **Matsunaga, Y., T. Saibara, H. Kido, and N. Katunuma.** 1993. Participation of cathepsin B in processing of antigen presentation to MHC class II. FEBS Lett. **324:**325–330.
47. **Meulendyke, K. A., M. A. Wurth, R. O. McCann, and R. E. Dutch.** 2005. Endocytosis plays a critical role in proteolytic processing of the Hendra virus fusion protein. J. Virol. **79:**12643–12649.
48. **Mizuochi, T., S. T. Yee, M. Kasai, T. Kakiuchi, D. Muno, and E. Kominami.** 1994. Both cathepsin B and cathepsin D are necessary for processing of ovalbumin as well as for degradation of class II MHC invariant chain. Immunol. Lett. **43:**189–193.
49. **Mohamed, M. M., and B. F. Sloane.** 2006. Cysteine cathepsins: multifunctional enzymes in cancer. Nat. Rev. Cancer **6:**764–775.
50. **Moriyama, T., M. Wada, R. Urade, M. Kito, N. Katunuma, T. Ogawa, and R. D. Simoni.** 2001. 3-hydroxy-3-methylglutaryl coenzyme A reductase is sterol-dependently cleaved by cathepsin L-type cysteine protease in the isolated endoplasmic reticulum. Arch. Biochem. Biophys. **386:**205–212.
51. **Morrison, L. A., R. L. Sidman, and B. N. Fields.** 1991. Direct spread of reovirus from the intestinal lumen to the central nervous system through vagal autonomic nerve fibers. Proc. Natl. Acad. Sci. USA **88:**3852–3856.
52. **Nakagawa, T., W. Roth, P. Wong, A. Nelson, A. Farr, J. Deussing, J. A. Villadangos, H. Ploegh, C. Peters, and A. Y. Rudensky.** 1998. Cathepsin L: critical role in Ii degradation and CD4 T cell selection in the thymus. Science **280:**450–453.
53. **Nakagawa, T. Y., W. H. Brissette, P. D. Lira, R. J. Griffiths, N. Petrushova, J. Stock, J. D. McNeish, S. E. Eastman, E. D. Howard, S. R. Clarke, E. F. Rosloniec, E. A. Elliott, and A. Y. Rudensky.** 1999. Impaired invariant chain degradation and antigen presentation and diminished collagen-induced arthritis in cathepsin S null mice. Immunity **10:**207–217.
54. **Nibert, M. L., A. L. Odegard, M. A. Agosto, K. Chandran, and L. A. Schiff.** 2005. Putative autocleavage of reovirus μ1 protein in concert with outer-capsid disassembly and activation for membrane permeabilization. J. Mol. Biol. **345:**461–474.
55. **Odegard, A. L., K. Chandran, X. Zhang, J. S. Parker, T. S. Baker, and M. L. Nibert.** 2004. Putative autocleavage of outer capsid protein μ1, allowing release of myristoylated peptide μ1N during particle uncoating, is critical for cell entry by reovirus. J. Virol. **78:**8732–8745.
56. **O'Donnell, S. M., M. W. Hansberger, J. L. Connolly, J. D. Chappell, M. J. Watson, J. M. Pierce, J. D. Wetzel, W. Han, E. S. Barton, J. C. Forrest, T. Valyi-Nagy, F. E. Yull, T. S. Blackwell, J. N. Rottman, B. Sherry, and T. S. Dermody.** 2005. Organ-specific roles for transcription factor NF-κB in reovirus-induced apoptosis and disease. J. Clin. Investig. **115:**2341–2350.

57. **Pager, C. T., W. W. Craft, Jr., J. Patch, and R. E. Dutch.** 2006. A mature and fusogenic form of the Nipah virus fusion protein requires proteolytic processing by cathepsin L. Virology **346:**251–257.
58. **Pager, C. T., and R. E. Dutch.** 2005. Cathepsin L is involved in proteolytic processing of the Hendra virus fusion protein. J. Virol. **79:**12714–12720.
59. **Papadimitriou, J. M.** 1968. The biliary tract in acute murine reovirus 3 infection. Am. J. Pathol. **52:**595–601.
60. **Parashar, K., M. J. Tarlow, and M. A. McCrae.** 1992. Experimental reovirus type 3-induced murine biliary tract disease. J. Pediatr. Surg. **27:**843–847.
61. **Petanceska, S., P. Canoll, and L. A. Devi.** 1996. Expression of rat cathepsin S in phagocytic cells. J. Biol. Chem. **271:**4403–4409.
62. **Phillips, P. A., D. Keast, J. M. Papadimitriou, M. N. Walters, and N. F. Stanley.** 1969. Chronic obstructive jaundice induced by reovirus type 3 in weanling mice. Pathology **1:**193–203.
63. **Pluger, E. B., M. Boes, C. Alfonso, C. J. Schroter, H. Kalbacher, H. L. Ploegh, and C. Driessen.** 2002. Specific role for cathepsin S in the generation of antigenic peptides in vivo. Eur. J. Immunol. **32:**467–476.
64. **Porotto, M., G. Orefice, C. Yokoyama, B. Mungall, R. Realubit, M. Sganga, M. Aljofan, M. Whitt, F. Glickman, and A. Moscona.** 2009. Simulating henipavirus multicycle replication in a screening assay leads to identification of a promising candidate for therapy. J. Virol. **83:**5148–5155.
65. **Reinheckel, T., J. Deussing, W. Roth, and C. Peters.** 2001. Towards specific functions of lysosomal cysteine peptidases: phenotypes of mice deficient for cathepsin B or cathepsin L. Biol. Chem. **382:**735–741.
66. **Richardson, B. A., and J. Overbaugh.** 2005. Basic statistical considerations in virological experiments. J. Virol. **79:**669–676.
67. **Riese, R. J., G. P. Shi, J. Villadangos, D. Stetson, C. Driessen, A. M. Lennon-Dumenil, C. L. Chu, Y. Naumov, S. M. Behar, H. Ploegh, R. Locksley, and H. A. Chapman.** 2001. Regulation of CD1 function and NK1.1(+) T cell selection and maturation by cathepsin S. Immunity **15:**909–919.
68. **Roth, W., J. Deussing, V. Botchkarev, M. Pauly-Evers, P. Saftig, A. Hafner, P.Schmidt, W. Schmahl, J. Scherer, I. Anton-Lamprechet, K. Von Figura, R. Paus, and C. Peters.** 2000. Cathepsin L deficiency as molecular defect of furless: hyperproliferation of keratinocytes and perturbation of hair follicle cycling. FASEB J. **14:**2075–2086.
69. **Rubin, D. H., and B. N. Fields.** 1980. Molecular basis of reovirus virulence: role of the M2 gene. J. Exp. Med. **152:**853–868.
70. **Schiff, L. A., M. L. Nibert, and K. L. Tyler.** 2007. Orthoreoviruses and their replication, p. 1853–1915. *In* D. M. Knipe and P. M. Howley (ed.), Fields virology, 5th ed., vol. 2. Lippincott Williams & Wilkins, Philadelphia, PA.
71. **Shen, L., L. J. Sigal, M. Boes, and K. L. Rock.** 2004. Important role of cathepsin S in generating peptides for TAP-independent MHC class I crosspresentation in vivo. Immunity **21:**155–165.
72. **Shi, G. P., J. S. Munger, J. P. Meara, D. H. Rich, and H. A. Chapman.** 1992. Molecular cloning and expression of human alveolar macrophage cathepsin S, an elastinolytic cysteine protease. J. Biol. Chem. **267:**7258–7262.
73. **Shi, G. P., A. C. Webb, K. E. Foster, J. H. Knoll, C. A. Lemere, J. S. Munger, and H. A. Chapman.** 1994. Human cathepsin S: chromosomal localization, gene structure, and tissue distribution. J. Biol. Chem. **269:**11530–11536.
74. **Silverstein, S. C., C. Astell, D. H. Levin, M. Schonberg, and G. Acs.** 1972. The mechanism of reovirus uncoating and gene activation *in vivo*. Virology **47:**797–806.
75. **Simmons, G., D. N. Gosalia, A. J. Rennekamp, J. D. Reeves, S. L. Diamond, and P. Bates.** 2005. Inhibitors of cathepsin L prevent severe acute respiratory syndrome coronavirus entry. Proc. Natl. Acad. Sci. USA **102:**11876–11881.
76. **Sturzenbecker, L. J., M. L. Nibert, D. B. Furlong, and B. N. Fields.** 1987. Intracellular digestion of reovirus particles requires a low pH and is an essential step in the viral infectious cycle. J. Virol. **61:**2351–2361.
77. **Tardieu, M., M. L. Powers, and H. L. Weiner.** 1983. Age-dependent susceptibility to reovirus type 3 encephalitis: role of viral and host factors. Ann. Neurol. **13:**602–607.
78. **Turk, V., B. Turk, and D. Turk.** 2001. Lysosomal cysteine proteases: facts and opportunities. EMBO J. **20:**4629–4633.
79. **Tyler, K. L., E. S. Barton, M. L. Ibach, C. Robinson, T. Valyi-Nagy, J. A. Campbell, P. Clarke, S. M. O'Donnell, J. D. Wetzel, and T. S. Dermody.** 2004. Isolation and molecular characterization of a novel type 3 reovirus from a child with meningitis. J. Infect. Dis. **189:**1664–1675.
80. **Tyler, K. L., R. T. Bronson, K. B. Byers, and B. N. Fields.** 1985. Molecular basis of viral neurotropism: experimental reovirus infection. Neurology **35:**88–92.
81. **Vasiljeva, O., T. Reinheckel, C. Peters, D. Turk, V. Turk, and B. Turk.** 2007. Emerging roles of cysteine cathepsins in disease and their potential as drug targets. Curr. Pharm. Des. **13:**387–403.
82. **Venter, J. C., M. D. Adams, E. W. Myers, P. W. Li, R. J. Mural, G. G. Sutton, H. O. Smith, M. Yandell, C. A. Evans, R. A. Holt, J. D. Gocayne, P. Amanatides, R. M. Ballew, D. H. Huson, J. R. Wortman, Q. Zhang, C. D. Kodira, X. H. Zheng, L. Chen, M. Skupski, G. Subramanian, P. D. Thomas, J. Zhang, G. L. Gabor Miklos, C. Nelson, S. Broder, A. G. Clark, J. Nadeau, V. A. McKusick, N. Zinder, A. J. Levine, R. J. Roberts, M. Simon, C. Slayman, M. Hunkapiller, R. Bolanos, A. Delcher, I. Dew, D. Fasulo, M. Flanigan, L. Florea, A. Halpern, S. Hannenhalli, S. Kravitz, S. Levy, C. Mobarry, K. Reinert, K. Remington, J. Abu-Threideh, E. Beasley, K. Biddick, V. Bonazzi, R. Brandon, M. Cargill, I. Chandramouliswaran, R. Charlab, K. Chaturvedi, Z. Deng, V. Di Francesco, P. Dunn, K. Eilbeck, C. Evangelista, A. E. Gabrielian, W. Gan, W. Ge, F. Gong, Z. Gu, P. Guan, T. J. Heiman, M. E. Higgins, R. R. Ji, Z. Ke, K. A. Ketchum, Z. Lai, Y. Lei, Z. Li, J. Li, Y. Liang, X. Lin, F. Lu, G. V. Merkulov, N. Milshina, H. M. Moore, A. K. Naik, V. A. Narayan, B. Neelam, D. Nusskern, D. B. Rusch, S. Salzberg, W. Shao, B. Shue, J. Sun, Z. Wang, A. Wang, X. Wang, J. Wang, M. Wei, R. Wides, C. Xiao, C. Yan, et al.** 2001. The sequence of the human genome. Science **291:**1304–1351.
83. **Virgin, H. W., IV, R. Bassel-Duby, B. N. Fields, and K. L. Tyler.** 1988. Antibody protects against lethal infection with the neurally spreading reovirus type 3 (Dearing). J. Virol. **62:**4594–4604.
84. **Virgin, H. W., K. L. Tyler, and T. S. Dermody.** 1997. Reovirus, p. 669–699. *In* N. Nathanson (ed.), Viral pathogenesis. Lippincott-Raven, New York, NY.
85. **Weiner, H. L., K. A. Ault, and B. N. Fields.** 1980. Interaction of reovirus with cell surface receptors. I. Murine and human lymphocytes have a receptor for the hemagglutinin of reovirus type 3. J. Immunol. **124:**2143–2148.
86. **Wetzel, J. D., G. J. Wilson, G. S. Baer, L. R. Dunnigan, J. P. Wright, D. S. H. Tang, and T. S. Dermody.** 1997. Reovirus variants selected during persistent infections of L cells contain mutations in the viral S1 and S4 genes and are altered in viral disassembly. J. Virol. **71:**1362–1369.
87. **Wilson, G. A., L. A. Morrison, and B. N. Fields.** 1994. Association of the reovirus S1 gene with serotype 3-induced biliary atresia in mice. J. Virol. **68:**6458–6465.
88. **Yang, M., Y. Zhang, J. Pan, J. Sun, J. Liu, P. Libby, G. K. Sukhova, A. Doria, N. Katunuma, O. D. Peroni, M. Guerre-Millo, B. B. Kahn, K. Clement, and G. P. Shi.** 2007. Cathepsin L activity controls adipogenesis and glucose tolerance. Nat. Cell Biol. **9:**970–977.
89. **Yasuda, Y., J. Kaleta, and D. Bromme.** 2005. The role of cathepsins in osteoporosis and arthritis: rationale for the design of new therapeutics. Adv. Drug Deliv. Rev. **57:**973–993.

REFERENCES

1. **Alain, T., T. S. Kim, X. Lun, A. Liacini, L. A. Schiff, D. L. Senger, and P. A. Forsyth.** 2007. Proteolytic disassembly is a critical determinant for reovirus oncolysis. Mol. Ther. **15:**1512-21.

2. **Amerongen, H. M., G. A. R. Wilson, B. N. Fields, and M. R. Neutra.** 1994. Proteolytic processing of reovirus is required for adherence to intestinal M cells. Journal of Virology **68:**8428-8432.

3. **Antar, A. A. R., J. L. Konopka, J. A. Campbell, R. A. Henry, A. L. Perdigoto, B. D. Carter, A. Pozzi, T. W. Abel, and T. S. Dermody.** 2009. Junctional adhesion molecule-A is required for hematogenous dissemination of reovirus. Cell Host Microbe **5:**59-71.

4. **Azzam-Smoak, K., D. L. Noah, M. J. Stewart, M. A. Blum, and B. Sherry.** 2002. Interferon regulatory factor-1, interferon-beta, and reovirus-induced myocarditis. Virology **298:**20-29.

5. **Baer, G. S., and T. S. Dermody.** 1997. Mutations in reovirus outer-capsid protein σ3 selected during persistent infections of L cells confer resistance to protease inhibitor E64. Journal of Virology **71:**4921-4928.

6. **Baer, G. S., D. H. Ebert, C. J. Chung, A. H. Erickson, and T. S. Dermody.** 1999. Mutant cells selected during persistent reovirus infection do not express mature cathepsin L and do not support reovirus disassembly. Journal of Virology **73:**9532-9543.

7. **Barton, E. S., J. L. Connolly, J. C. Forrest, J. D. Chappell, and T. S. Dermody.** 2001. Utilization of sialic acid as a coreceptor enhances reovirus attachment by multistep adhesion strengthening. Journal of Biological Chemistry **276:**2200-2211.

8. **Barton, E. S., J. C. Forrest, J. L. Connolly, J. D. Chappell, Y. Liu, F. Schnell, A. Nusrat, C. A. Parkos, and T. S. Dermody.** 2001. Junction adhesion molecule is a receptor for reovirus. Cell **104:**441-451.

9. **Barton, E. S., B. E. Youree, D. H. Ebert, J. C. Forrest, J. L. Connolly, T. Valyi-Nagy, K. Washington, J. D. Wetzel, and T. S. Dermody.** 2003. Utilization of sialic acid as a coreceptor is required for reovirus-induced biliary disease. Journal of Clinical Investigation **111:**1823-1833.

10. **Bass, D. M., D. Bodkin, R. Dambrauskas, J. S. Trier, B. N. Fields, and J. L. Wolf.** 1990. Intraluminal proteolytic activation plays an important role in replication of type 1 reovirus in the intestines of neonatal mice. Journal of Virology **64:**1830-1833.

11. **Baty, C. J., and B. Sherry.** 1993. Cytopathogenic effect in cardiac myocytes but not in cardiac fibroblasts is correlated with reovirus-induced acute myocarditis. Journal of Virology **67:**6295-6298.

12. **Bodkin, D. K., and B. N. Fields.** 1989. Growth and survival of reovirus in intestinal tissue: role of the L2 and S1 genes. Journal of Virology **63:**1188-1193.

13. **Boehme, K. W., J. M. Frierson, J. L. Konopka, T. Kobayashi, and T. S. Dermody.** 2011. The reovirus σ1s protein is a determinant of hematogenous but not neural virus dissemination in mice. Journal of Virology **85:**11781-90.

14. **Boehme, K. W., K. M. Guglielmi, and T. S. Dermody.** 2009. Reovirus nonstructural protein σ1s is required for establishment of viremia and systemic dissemination. Proceedings of the National Academy of Sciences USA **106:**19986-19991.

15. **Borsa, J., T. P. Copps, M. D. Sargent, D. G. Long, and J. D. Chapman.** 1973. New intermediate subviral particles in the in vitro uncoating of reovirus virions by chymotrypsin. Journal of Virology **11:**552-564.

16. **Borsa, J., B. D. Morash, M. D. Sargent, T. P. Copps, P. A. Lievaart, and J. G. Szekely.** 1979. Two modes of entry of reovirus particles into L cells. Journal of General Virology **45:**161-170.

17. **Borsa, J., M. D. Sargent, P. A. Lievaart, and T. P. Copps.** 1981. Reovirus: evidence for a second step in the intracellular uncoating and transcriptase activation process. Virology **111:**191-200.

18. **Carmona, E., É. Dufour, C. Plouffe, S. Takebe, P. Mason, J. S. Mort, and R. Ménard.** 1996. Potency and selectivity of the cathepsin L propeptide as an inhibitor of cysteine proteases. Biochemistry **35:**8149-8157.

19. **Chandran, K., and Max L. Nibert.** 2001. Presented at the American Society for Virology Conference, Madison, WI.

20. **Chandran, K., D. L. Farsetta, and M. L. Nibert.** 2002. Strategy for nonenveloped virus entry: a hydrophobic conformer of the reovirus membrane penetration protein μ1 mediates membrane disruption. Journal of Virology **76:**9920-9933.

21. **Chandran, K., J. S. Parker, M. Ehrlich, T. Kirchhausen, and M. L. Nibert.** 2003. The delta region of outer-capsid protein μ1 undergoes conformational change and release from reovirus particles during cell entry. Journal of Virology **77:**13361-13375.

22. **Chandran, K., N. J. Sullivan, U. Felbor, S. P. Whelan, and J. M. Cunningham.** 2005. Endosomal proteolysis of the Ebola virus glycoprotein is necessary for infection. Science **308:**1643-1645.

23. **Chandran, K., S. B. Walker, Y. Chen, C. M. Contreras, L. A. Schiff, T. S. Baker, and M. L. Nibert.** 1999. In vitro recoating of reovirus cores with baculovirus-expressed outer-capsid proteins μ1 and σ3. Journal of Virology **73:**3941-3950.

24. **Chang, C. T., and H. J. Zweerink.** 1971. Fate of parental reovirus in infected cell. Virology **46:**544-555.

25. **Chappell, J. D., E. S. Barton, T. H. Smith, G. S. Baer, D. T. Duong, M. L. Nibert, and T. S. Dermody.** 1998. Cleavage susceptibility of reovirus attachment protein σ1 during proteolytic disassembly of virions is determined by a sequence polymorphism in the σ1 neck. Journal of Virology **72:**8205-8213.

26. **Chappell, J. D., A. Prota, T. S. Dermody, and T. Stehle.** 2002. Crystal structure of reovirus attachment protein σ1 reveals evolutionary relationship to adenovirus fiber. EMBO Journal **21:**1-11.

27. **Clark, K. M., J. D. Wetzel, Y. Gu, D. H. Ebert, S. A. McAbee, E. K. Stoneman, G. S. Baer, Y. Zhu, G. J. Wilson, B. V. V. Prasad, and T. S. Dermody.** 2006. Reovirus variants selected for resistance to ammonium chloride have mutations in viral outer-capsid protein σ3. Journal of Virology **80:**671-681.

28. **Clarke, P., R. L. Debiasi, S. M. Meintzer, B. A. Robinson, and K. L. Tyler.** 2005. Inhibition of NF-kappa B activity and cFLIP expression contribute to viral-induced apoptosis. Apoptosis **10:**513-524.

29. **Cleveland, D. R., H. Zarbl, and S. Millward.** 1986. Reovirus guanyltransferase is L2 gene product lambda 2. Journal of Virology **60:**307-311.

30. **Coffey, C. M., A. Sheh, I. S. Kim, K. Chandran, M. L. Nibert, and J. S. Parker.** 2006. Reovirus outer capsid protein μ1 induces apoptosis and associates with lipid droplets, endoplasmic reticulum, and mitochondria. Journal of Virology **80:**8422-8438.

31. **Connolly, J. L., and T. S. Dermody.** 2002. Virion disassembly is required for apoptosis induced by reovirus. Journal of Virology **76:**1632-1641.

32. **Connolly, J. L., S. E. Rodgers, P. Clarke, D. W. Ballard, L. D. Kerr, K. L. Tyler, and T. S. Dermody.** 2000. Reovirus-induced apoptosis requires activation of transcription factor NF-κB. Journal of Virology **74:**2981-2989.

33. **Coombs, K. M.** 1998. Stoichiometry of reovirus structural proteins in virus, ISVP, and core particles. Virology **243:**218-228.

34. **Cox, P., M. Griffith, M. Angles, D. Deere, and C. Ferguson.** 2005. Concentrations of pathogens and indicators in animal feces in the Sydney watershed. Appl Environ Microbiol **71:**5929-34.

35. **Danthi, P., C. M. Coffey, J. S. Parker, T. W. Abel, and T. S. Dermody.** 2008. Independent regulation of reovirus membrane penetration and apoptosis by the μ1 ϕ domain. PLoS Pathogens **4:**e1000248.

36. **Danthi, P., T. Kobayashi, G. H. Holm, M. W. Hansberger, T. W. Abel, and T. S. Dermody.** 2008. Reovirus apoptosis and virulence are regulated by host cell membrane-penetration efficiency. J. Virol. **82:**161-172.

37. **Danthi, P., A. J. Pruijssers, A. K. Berger, G. H. Holm, S. S. Zinkel, and T. S. Dermody.** Accepted for publication with revisions. Bid regulates the pathogenesis of neurotropic reovirus. PLoS Pathogens.

38. **DeBiasi, R., C. Edelstein, B. Sherry, and K. Tyler.** 2001. Calpain inhibition protects against virus-induced apoptotic myocardial injury. Journal of Virology **75:**351-361.

39. **DeBiasi, R. L., B. A. Robinson, J. S. Leser, R. D. Brown, C. S. Long, and P. Clarke.** 2010. Critical role for death-receptor mediated apoptotic signaling in viral myocarditis. Journal of Cardiac Failure **16:**901-910.

40. **DeBiasi, R. L., B. A. Robinson, B. Sherry, R. Bouchard, R. D. Brown, M. Rizeq, C. Long, and K. L. Tyler.** 2004. Caspase inhibition protects against reovirus-induced myocardial injury in vitro and in vivo. Journal of Virology **78:**11040-11050.

41. **Decaro, N., M. Campolo, C. Desario, D. Ricci, M. Camero, E. Lorusso, G. Elia, A. Lavazza, V. Martella, and C. Buonavoglia.** 2005. Virological and molecular characterization of a mammalian orthoreovirus type 3 strain isolated from a dog in Italy. Vet Microbiol **109:**19-27.

42. **Dermody, T. S., M. L. Nibert, R. Bassel-Duby, and B. N. Fields.** 1990. A σ1 region important for hemagglutination by serotype 3 reovirus strains. Journal of Virology **64:**5173-5176.

43. **Dermody, T. S., M. L. Nibert, J. D. Wetzel, X. Tong, and B. N. Fields.** 1993. Cells and viruses with mutations affecting viral entry are selected during persistent infections of L cells with mammalian reoviruses. Journal of Virology **67:**2055-2063.

44. **Diederich, S., L. Thiel, and A. Maisner.** 2008. Role of endocytosis and cathepsin-mediated activation in Nipah virus entry. Virology **375:**391-400.

45. **Doyle, J. D., P. Danthi, E. A. Kendall, L. S. Ooms, J. D. Wetzel, and T. S. Dermody.** 2012. Molecular determinants of proteolytic disassembly of the reovirus outer capsid. Journal of Biological Chemistry **287:**8029-38.

46. **Dryden, K. A., G. Wang, M. Yeager, M. L. Nibert, K. M. Coombs, D. B. Furlong, B. N. Fields, and T. S. Baker.** 1993. Early steps in reovirus infection are associated with dramatic changes in supramolecular structure and protein conformation:

analysis of virions and subviral particles by cryoelectron microscopy and image reconstruction. Journal of Cell Biology **122:**1023-41.

47. **Ebert, D. H., J. Deussing, C. Peters, and T. S. Dermody.** 2002. Cathepsin L and cathepsin B mediate reovirus disassembly in murine fibroblast cells. Journal of Biological Chemistry **277:**24609-24617.

48. **Ebert, D. H., S. A. Kopecky-Bromberg, and T. S. Dermody.** 2004. Cathepsin B is inhibited in mutant cells selected during persistent reovirus infection. The Journal of Biological Chemistry **279:**3837-3851.

49. **Ebert, D. H., J. D. Wetzel, D. E. Brumbaugh, S. R. Chance, L. E. Stobie, G. S. Baer, and T. S. Dermody.** 2001. Adaptation of reovirus to growth in the presence of protease inhibitor E64 segregates with a mutation in the carboxy terminus of viral outer-capsid protein σ3. Journal of Virology **75:**3197-3206.

50. **Ehrlich, M., W. Boll, A. Van Oijen, R. Hariharan, K. Chandran, M. L. Nibert, and T. Kirchhausen.** 2004. Endocytosis by random initiation and stabilization of clathrin-coated pits. Cell **118:**591-605.

51. **Furlong, D. B., M. L. Nibert, and B. N. Fields.** 1988. Sigma 1 protein of mammalian reoviruses extends from the surfaces of viral particles. Journal of Virology **62:**246-56.

52. **Gentsch, J. R., and A. F. Pacitti.** 1987. Differential interaction of reovirus type 3 with sialylated receptor components on animal cells. Virology **161:**245-248.

53. **Gillies, S., S. Bullivant, and A. R. Bellamy.** 1971. Viral RNA polymerases: electron microscopy of reovirus reaction cores. Science **174:**694-696.

54. **Gollamudi, R., M. H. Ghalib, K. K. Desai, I. Chaudhary, B. Wong, M. Einstein, M. Coffey, G. M. Gill, K. Mettinger, J. M. Mariadason, S. Mani, and S. Goel.** 2009. Intravenous administration of Reolysin, a live replication competent RNA virus is safe in patients with advanced solid tumors. Invest New Drugs **28:**641-9.

55. **Gomatos, P. J., and I. Tamm.** 1963. The secondary structure of reovirus RNA. Proceedings of the National Academy of Sciences USA **49:**707-714.

56. **Goody, R. J., C. C. Hoyt, and K. L. Tyler.** 2005. Reovirus infection of the CNS enhances iNOS expression in areas of virus-induced injury. Exp Neurol **195:**379-390.

57. **Goody, R. J., S. A. Schittone, and K. L. Tyler.** 2008. Experimental reovirus-induced acute flaccid paralysis and spinal motor neuron cell death. Journal of Neuropathology and Experimental Neurology **67:**231-239.

58. **Guglielmi, K. M., E. Kirchner, G. H. Holm, T. Stehle, and T. S. Dermody.** 2007. Reovirus binding determinants in junctional adhesion molecule-A. Journal of Biological Chemistry **282:**17930-40.

59. **Halonen, P.** 1961. Growth, stability and hemagglutination of a reovirus. Ann Med Exp Biol Fenn **39:**132-42.

60. **Hand, R., and I. Tamm.** 1973. Reovirus-effect of noninfective viral components on cellular deoxyribonucleic acid synthesis. Journal of Virology **11:**223-231.

61. **Harlin, H., S. B. Reffey, C. S. Duckett, T. Lindsten, and C. B. Thompson.** 2001. Characterization of XIAP-deficient mice. Mol. Cell. Biol. **21:**3604-3608.

62. **Helander, A., K. J. Silvey, N. J. Mantis, A. B. Hutchings, K. Chandran, W. T. Lucas, M. L. Nibert, and M. R. Neutra.** 2003. The viral σ1 protein and glycoconjugates containing α2-3-linked sialic acid are involved in type 1 reovirus adherence to M cell apical surfaces. Journal of Virology **77:**7964-7977.

63. **Holm, G. H., A. J. Pruijssers, L. Li, P. Danthi, B. Sherry, and T. S. Dermody.** 2010. Interferon regulatory factor 3 attenuates reovirus myocarditis and contributes to viral clearance. J Virol **84:**6900-8.

64. **Honey, K., K. Benlagha, C. Beers, K. Forbush, L. Teyton, M. J. Kleijmeer, A. Y. Rudensky, and A. Bendelac.** 2002. Thymocyte expression of cathepsin L is essential for NKT cell development. Nature Immunology **3:**1069-1074.

65. **Hooper, J. W., and B. N. Fields.** 1996. Monoclonal antibodies to reovirus σ1 and μ1 proteins inhibit chromium release from mouse L cells. Journal of Virology **70:**672-677.

66. **Hoyt, C. C., S. M. Richardson-Burns, R. J. Goody, B. A. Robinson, R. L. Debiasi, and K. L. Tyler.** 2005. Nonstructural protein σ1s is a determinant of reovirus virulence and influences the kinetics and severity of apoptosis induction in the heart and central nervous system. J Virol **79:**2743-2753.

67. **Hrdy, D. B., D. H. Rubin, and B. N. Fields.** 1982. Molecular basis of reovirus neurovirulence: role of the M2 gene in avirulence. Proceedings of the National Academy of Sciences USA **79:**1298-1302.

68. **Ivanovic, T., M. A. Agosto, L. Zhang, K. Chandran, S. C. Harrison, and M. L. Nibert.** 2008. Peptides released from reovirus outer capsid form membrane pores that recruit virus particles. EMBO J **27:**1289-1298.

69. **Jackson, G. G., and R. L. Muldoon.** 1973. Viruses causing common respiratory infection in man. IV. Reoviruses and adenoviruses. Journal of Infectious Diseases **128:**811-833.

70. **Jané-Valbuena, J., L. A. Breun, L. A. Schiff, and M. L. Nibert.** 2002. Sites and determinants of early cleavages in the proteolytic processing pathway of reovirus surface protein σ3. Journal of Virology **76:**5184-5197.

71. **Johnson, E. M., J. D. Doyle, J. D. Wetzel, R. P. McClung, N. Katunuma, J. D. Chappell, M. K. Washington, and T. S. Dermody.** 2009. Genetic and pharmacologic alteration of cathepsin expression influences reovirus pathogenesis. J Virol **83:**9630-9640.

72. **Kasel, J. A., L. Rosen, and H. Evans.** 1963. Infection of human volunteers with a reovirus of bovine origin. Proceedings of the Society for Experimental Biology and Medicine **112:**979-981.

73. **Kedl, R., S. Schmechel, and L. Schiff.** 1995. Comparative sequence analysis of the reovirus S4 genes from 13 serotype 1 and serotype 3 field isolates. Journal of Virology **69:**552-559.

74. **Kelly, K., S. Nawrocki, A. Mita, M. Coffey, F. J. Giles, and M. Mita.** 2009. Reovirus-based therapy for cancer. Expert Opin Biol Ther **9:**817-830.

75. **Keroack, M., and B. N. Fields.** 1986. Viral shedding and transmission between hosts determined by reovirus L2 gene. Science **232:**1635-1638.

76. **Kirchner, E., K. M. Guglielmi, H. M. Strauss, T. S. Dermody, and T. Stehle.** 2008. Structure of reovirus σ1 in complex with its receptor junctional adhesion molecule-A. PLoS Pathogens **4:**e1000235.

77. **Kobayashi, T., A. A. R. Antar, K. W. Boehme, P. Danthi, E. A. Eby, K. M. Guglielmi, G. H. Holm, E. M. Johnson, M. S. Maginnis, S. Naik, W. B. Skelton, J. D. Wetzel, G. J. Wilson, J. D. Chappell, and T. S. Dermody.** 2007. A plasmid-based reverse genetics system for animal double-stranded RNA viruses. Cell Host Microbe **1:**147-157.

78. **Kobayashi, T., L. S. Ooms, M. Ikizler, J. D. Chappell, and T. S. Dermody.** 2010. An improved reverse genetics system for mammalian orthoreoviruses. Virology **2:**194-200.

79. **Laemmli, U. K.** 1970. Cleavage of structural proteins during the assembly of the head of bacteriophage T4. Nature **227:**680-685.

80. **Lal, R., D. Harris, S. Postel-Vinay, and J. de Bono.** 2009. Reovirus: Rationale and clinical trial update. Curr. Opin. Mol. Ther. **11:**532-9.

81. **Leone, G., R. Duncan, D. C. Mah, A. Price, L. W. Cashdollar, and P. W. K. Lee.** 1991. The N-terminal heptad repeat region of reovirus cell attachment protein sigma 1 is responsible for sigma 1 oligomer stability and possesses intrinsic oligomerization function. Virology **182:**336-345.

82. **Leone, G., D. C. W. Mah, and P. W. K. Lee.** 1991. The incorporation of reovirus cell attachment protein σ1 into virions requires the amino-terminal hydrophobic tail and the adjacent heptad repeat region. Virology **182:**346-350.

83. **Lerner, A. M., J. D. Cherry, and M. Finland.** 1963. Haemagglutination with reoviruses. Virology **19:**58-65.

84. **Lerner, A. M., J. D. Cherry, J. O. Klein, and M. Finland.** 1962. Infections with reoviruses. The New England Journal of Medicine **267:**947-952.

85. **Liemann, S., K. Chandran, T. S. Baker, M. L. Nibert, and S. C. Harrison.** 2002. Structure of the reovirus membrane-penetration protein, μ1, in a complex with its protector protein, σ3. Cell **108:**283-295.

86. **Liu, Y., A. Nusrat, F. J. Schnell, T. A. Reaves, S. Walsh, M. Ponchet, and C. A. Parkos.** 2000. Human junction adhesion molecule regulates tight junction resealing in epithelia. Journal of Cell Science **113:**2363-2374.

87. **Lucia-Jandris, P., J. W. Hooper, and B. N. Fields.** 1993. Reovirus M2 gene is associated with chromium release from mouse L cells. Journal of Virology **67:**5339-5345.

88. **Luongo, C. L., C. M. Contreras, D. L. Farsetta, and M. L. Nibert.** 1998. Binding site for S-adenosyl-L-methionine in a central region of mammalian orthoreovirus λ2 protein: evidence for activities in mRNA cap methylation. J Biol Chem **273:**23773-23780.

89. **Luongo, C. L., X. Zhang, S. B. Walker, Y. Chen, T. J. Broering, D. L. Farsetta, V. D. Bowman, T. S. Baker, and M. L. Nibert.** 2002. Loss of Activities for mRNA Synthesis Accompanies Loss of lambda2 Spikes from Reovirus Cores: An Effect of lambda2 on lambda1 Shell Structure. Virology **296:**24-38.

90. **Maginnis, M. S., J. C. Forrest, S. A. Kopecky-Bromberg, S. K. Dickeson, S. A. Santoro, M. M. Zutter, G. R. Nemerow, J. M. Bergelson, and T. S. Dermody.** 2006. β1 integrin mediates internalization of mammalian reovirus. Journal of Virology **80:**2760-2770.

91. **Maginnis, M. S., B. A. Mainou, A. M. Derdowski, E. M. Johnson, R. Zent, and T. S. Dermody.** 2008. NPXY motifs in the β1 integrin cytoplasmic tail are required for functional reovirus entry. Journal of Virology **82:**3181-3191.

92. **Mainou, B. A., and T. S. Dermody.** 2011. Src kinase mediates productive endocytic sorting of reovirus during cell entry. Journal of Virology **85:**3203-13.

93. **Mainou, B. A., and T. S. Dermody.** 2012. Transport to late endosomes is required for efficient reovirus infection. Journal of Virology **86:**8346-58.

94. **Martin-Padura, I., S. Lostaglio, M. Schneemann, L. Williams, M. Romano, P. Fruscella, C. Panzeri, A. Stoppacciaro, L. Ruco, A. Villa, D. Simmons, and E. Dejana.** 1998. Junctional adhesion molecule, a novel member of the immunoglobulin superfamily that distributes at intercellular junctions and modulates monocyte transmigration. Journal of Cell Biology **142:**117-127.

95. **Matoba, Y., B. Sherry, B. N. Fields, and T. W. Smith.** 1991. Identification of the viral genes responsible for growth of strains of reovirus in cultured mouse heart cells. Journal of Clinical Investigation **87:**1628-1633.

96. **Mendez, I. I., Y. M. She, W. Ens, and K. M. Coombs.** 2003. Digestion pattern of reovirus outer capsid protein σ3 determined by mass spectrometry. Virology **311:**289-304.

97. **Miyamoto, S. D., R. D. Brown, B. A. Robinson, K. L. Tyler, C. S. Long, and R. L. Debiasi.** 2009. Cardiac cell-specific apoptotic and cytokine responses to reovirus infection: determinants of myocarditic phenotype. J Card Fail **15:**529-39.

98. **Mohamed, M. M., and B. F. Sloane.** 2006. Cysteine cathepsins: multifunctional enzymes in cancer. Nature Reviews: Cancer **6:**764-775.

99. **Mori, Y., T. Yamashita, Y. Tanaka, Y. Tsuda, T. Abe, K. Moriishi, and Y. Matsuura.** 2007. Processing of capsid protein by cathepsin L plays a crucial role in replication of Japanese encephalitis virus in neural and macrophage cells. J Virol **81:**8477-8487.

100. **Morrison, L. A., R. L. Sidman, and B. N. Fields.** 1991. Direct spread of reovirus from the intestinal lumen to the central nervous system through vagal autonomic nerve fibers. Proceedings of the National Academy of Sciences USA **88:**3852-3856.

101. **Muthukrishnan, S., and A. J. Shatkin.** 1975. Reovirus genome RNA segments: resistance to S-1 nuclease. Virology **64:**96-105.

102. **Nakagawa, T., W. Roth, P. Wong, A. Nelson, A. Farr, J. Deussing, J. A. Villadangos, H. Ploegh, C. Peters, and A. Y. Rudensky.** 1998. Cathepsin L: critical role in Ii degradation and CD4 T cell selection in the thymus. Science **280:**450-453.

103. **Nibert, M. L., J. D. Chappell, and T. S. Dermody.** 1995. Infectious subvirion particles of reovirus type 3 Dearing exhibit a loss in infectivity and contain a cleaved σ1 protein. Journal of Virology **69:**5057-5067.

104. **Nibert, M. L., and B. N. Fields.** 1992. A carboxy-terminal fragment of protein μ1/μ1C is present in infectious subvirion particles of mammalian reoviruses and is proposed to have a role in penetration. Journal of Virology **66:**6408-6418.

105. **Nibert, M. L., A. L. Odegard, M. A. Agosto, K. Chandran, and L. A. Schiff.** 2005. Putative autocleavage of reovirus μ1 protein in concert with outer-capsid disassembly and activation for membrane permeabilization. Journal of Molecular Biology **345:**461-474.

106. **O'Donnell, S. M., M. W. Hansberger, J. L. Connolly, J. D. Chappell, M. J. Watson, J. M. Pierce, J. D. Wetzel, W. Han, E. S. Barton, J. C. Forrest, T. Valyi-Nagy, F. E. Yull, T. S. Blackwell, J. N. Rottman, B. Sherry, and T. S. Dermody.**

2005. Organ-specific roles for transcription factor NF-κB in reovirus-induced apoptosis and disease. Journal of Clinical Investigation **115:**2341-2350.

107. **Oberhaus, S. M., R. L. Smith, G. H. Clayton, T. S. Dermody, and K. L. Tyler.** 1997. Reovirus infection and tissue injury in the mouse central nervous system are associated with apoptosis. Journal of Virology **71:**2100-2106.

108. **Odegard, A. L., K. Chandran, X. Zhang, J. S. Parker, T. S. Baker, and M. L. Nibert.** 2004. Putative autocleavage of outer capsid protein μ1, allowing release of myristoylated peptide μ1N during particle uncoating, is critical for cell entry by reovirus. Journal of Virology **78:**8732-8745.

109. **Olland, A. M., J. Jané-Valbuena, L. A. Schiff, M. L. Nibert, and S. C. Harrison.** 2001. Structure of the reovirus outer capsid and dsRNA-binding protein σ3 at 1.8 Å resolution. EMBO Journal **20:**979-989.

110. **Pager, C. T., W. W. Craft, Jr., J. Patch, and R. E. Dutch.** 2006. A mature and fusogenic form of the Nipah virus fusion protein requires proteolytic processing by cathepsin L. Virology **346:**251-257.

111. **Pager, C. T., and R. E. Dutch.** 2005. Cathepsin L is involved in proteolytic processing of the Hendra virus fusion protein. Journal of Virology **79:**12714-12720.

112. **Rauschenfels, S., M. Krassmann, A. N. Al-Masri, W. Verhagen, J. Leonhardt, J. F. Kuebler, and C. Petersen.** 2009. Incidence of hepatotropic viruses in biliary atresia. Eur J Pediatr **168:**469-76.

113. **Reinisch, K. M., M. L. Nibert, and S. C. Harrison.** 2000. Structure of the reovirus core at 3.6 Å resolution. Nature **404:**960-967.

114. **Reiter, D. M., J. M. Frierson, E. E. Halvorson, T. Kobayashi, T. S. Dermody, and T. Stehle.** 2011. Crystal structure of reovirus attachment protein σ1 in complex with sialylated oligosaccharides. PLoS Pathogens **7:**e1002166.

115. **Richardson-Burns, S. M., D. J. Kominsky, and K. L. Tyler.** 2002. Reovirus-induced neuronal apoptosis is mediated by caspase 3 and is associated with the activation of death receptors. Journal of Neurovirology **8:**365-380.

116. **Rodgers, S. E., E. S. Barton, S. M. Oberhaus, B. Pike, C. A. Gibson, K. L. Tyler, and T. S. Dermody.** 1997. Reovirus-induced apoptosis of MDCK cells is not linked to viral yield and is blocked by Bcl-2. Journal of Virology **71:**2540-2546.

117. **Rosen, L.** 1962. Reoviruses in animals other than man. Annals of the New York Academy of Science **101:**461-465.

118. **Rubin, D. H., M. J. Kornstein, and A. O. Anderson.** 1985. Reovirus serotype 1 intestinal infection: a novel replicative cycle with ileal disease. Journal of Virology **53:**391-398.

119. **Rubin, D. H., D. B. Weiner, C. Dworkin, M. I. Greene, G. G. Maul, and W. V. Williams.** 1992. Receptor utilization by reovirus type 3: distinct binding sites on thymoma and fibroblast cell lines result in differential compartmentalization of virions. Microbial Pathogenesis **12:**351-365.

120. **Sabin, A. B.** 1959. Reoviruses: a new group of respiratory and enteric viruses formerly classified as ECHO type 10 is described. Science **130:**1387-1389.

121. **Scott, F. W., D. E. Kahn, and J. H. Gillespie.** 1970. Feline reovirus: isolation, characterization, and pathogenicity of a feline reovirus. American Journal of Veterinary Research **31:**11-20.

122. **Selb, B., and B. Weber.** 1994. A study of human reovirus IgG and IgA antibodies by ELISA and western blot. Journal of Virological Methods **47:**15-25.

123. **Sherry, B.** 2002. The role of interferon regulatory factors in the cardiac response to viral infection. Viral Immunology **15:**17-28.

124. **Sherry, B., C. J. Baty, and M. A. Blum.** 1996. Reovirus-induced acute myocarditis in mice correlates with viral RNA synthesis rather than generation of infectious virus in cardiac myocytes. J Virol **70:**6709-6715.

125. **Sherry, B., and M. A. Blum.** 1994. Multiple viral core proteins are determinants of reovirus-induced acute myocarditis. Journal of Virology **68:**8461-8465.

126. **Sherry, B., X. Y. Li, K. L. Tyler, J. M. Cullen, and H. W. Virgin.** 1993. Lymphocytes protect against and are not required for reovirus-induced myocarditis. Journal of Virology **67:**6119-6124.

127. **Sherry, B., F. J. Schoen, E. Wenske, and B. N. Fields.** 1989. Derivation and characterization of an efficiently myocarditic reovirus variant. Journal of Virology **63:**4840-4849.

128. **Sherry, B., J. Torres, and M. A. Blum.** 1998. Reovirus induction of and sensitivity to beta interferon in cardiac myocyte cultures correlate with induction of myocarditis and are determined by viral core proteins. Journal of Virology **72:**1314-1323.

129. **Silverstein, S. C., C. Astell, D. H. Levin, M. Schonberg, and G. Acs.** 1972. The mechanism of reovirus uncoating and gene activation in vivo. Virology **47:**797-806.

130. **Smith, R. E., H. J. Zweerink, and W. K. Joklik.** 1969. Polypeptide components of virions, top component and cores of reovirus type 3. Virology **39:**791-810.

131. **Stewart, M. J., M. A. Blum, and B. Sherry.** 2003. PKR's protective role in viral myocarditis. Virology **314:**92-100.

132. **Strong, J. E., M. C. Coffey, D. Tang, P. Sabinin, and P. W. Lee.** 1998. The molecular basis of viral oncolysis: usurpation of the Ras signaling pathway by reovirus. EMBO J **17:**3351-3362.

133. **Sturzenbecker, L. J., M. L. Nibert, D. B. Furlong, and B. N. Fields.** 1987. Intracellular digestion of reovirus particles requires a low pH and is an essential step in the viral infectious cycle. Journal of Virology **61:**2351-2361.

134. **Tai, J. H., J. V. Williams, K. M. Edwards, P. F. Wright, J. E. Crowe, and T. S. Dermody.** 2005. Prevalence of reovirus-specific antibodies in young children in Nashville, Tennessee. Journal of Infectious Diseases **191:**1221-1224.

135. **Tao, Y., D. L. Farsetta, M. L. Nibert, and S. C. Harrison.** 2002. RNA synthesis in a cage -- structural studies of reovirus polymerase λ3. Cell **111:**733-745.

136. **Tyler, K. L., R. T. Bronson, K. B. Byers, and B. N. Fields.** 1985. Molecular basis of viral neurotropism: experimental reovirus infection. Neurology **35:**88-92.

137. **Tyler, K. L., D. A. McPhee, and B. N. Fields.** 1986. Distinct pathways of viral spread in the host determined by reovirus S1 gene segment. Science **233:**770-774.

138. **Tyler, K. L., R. J. Sokol, S. M. Oberhaus, M. Le, F. M. Karrer, M. R. Narkewicz, R. W. Tyson, J. R. Murphy, R. Low, and W. R. Brown.** 1998. Detection of reovirus RNA in hepatobiliary tissues from patients with extrahepatic biliary atresia and choledochal cysts. Hepatology **27:**1475-1482.

139. **Tyler, K. L., M. K. Squier, S. E. Rodgers, S. E. Schneider, S. M. Oberhaus, T. A. Grdina, J. J. Cohen, and T. S. Dermody.** 1995. Differences in the capacity of reovirus strains to induce apoptosis are determined by the viral attachment protein σ1. Journal of Virology **69:**6972-6979.

140. **Tyler, K. L., M. K. T. Squier, A. L. Brown, B. Pike, D. Willis, S. M. Oberhaus, T. S. Dermody, and J. J. Cohen.** 1996. Linkage between reovirus-induced apoptosis and inhibition of cellular DNA synthesis: role of the S1 and M2 genes. Journal of Virology **70:**7984-7991.

141. **Virgin, H. W., IV, R. Bassel-Duby, B. N. Fields, and K. L. Tyler.** 1988. Antibody protects against lethal infection with the neurally spreading reovirus type 3 (Dearing). Journal of Virology **62:**4594-4604.

142. **Weiner, H. L., D. Drayna, D. R. Averill, Jr, and B. N. Fields.** 1977. Molecular basis of reovirus virulence: role of the S1 gene. Proceedings of the National Academy of Sciences USA **74:**5744-5748.

143. **Weiner, H. L., M. L. Powers, and B. N. Fields.** 1980. Absolute linkage of virulence and central nervous system tropism of reoviruses to viral hemagglutinin. Journal of Infectious Diseases **141:**609-616.

144. **Weiner, H. L., R. F. Ramig, T. A. Mustoe, and B. N. Fields.** 1978. Identification of the gene coding for the hemagglutinin of reovirus. Virology **86:**581-584.

145. **Wetzel, J. D., G. J. Wilson, G. S. Baer, L. R. Dunnigan, J. P. Wright, D. S. H. Tang, and T. S. Dermody.** 1997. Reovirus variants selected during persistent infections of L cells contain mutations in the viral S1 and S4 genes and are altered in viral disassembly. Journal of Virology **71:**1362-1369.

146. **Williams, L. A., I. Martin-Padura, E. Dejana, N. Hogg, and D. L. Simmons.** 1999. Identification and characterisation of human junctional adhesion molecule (JAM). Molecular Immunology **36:**1175-1188.

147. **Wilson, G. J., E. L. Nason, C. S. Hardy, D. H. Ebert, J. D. Wetzel, B. V. V. Prasad, and T. S. Dermody.** 2002. A single mutation in the carboxy terminus of reovirus outer-capsid protein σ3 confers enhanced kinetics of σ3 proteolysis, resistance to inhibitors of viral disassembly, and alterations in σ3 structure. Journal of Virology **76:**9832-9843.

148. **Wolf, J. L., D. H. Rubin, R. Finberg, R. S. Kaufman, A. H. Sharpe, J. S. Trier, and B. N. Fields.** 1981. Intestinal M cells: a pathway of entry of reovirus into the host. Science **212:**471-472.

149. **Yasuda, Y., J. Kaleta, and D. Bromme.** 2005. The role of cathepsins in osteoporosis and arthritis: rationale for the design of new therapeutics. Advanced Drug Delivery Reviews **57:**973-93.

150. **Zhang, X., S. B. Walker, P. R. Chipman, M. L. Nibert, and T. S. Baker.** 2003. Reovirus polymerase λ3 localized by cryo-electron microscopy of virions at a resolution of 7.6 A. Nat Struct Biol **10:**1011-1018.

151. **Zurney, J., T. Kobayashi, G. H. Holm, T. S. Dermody, and B. Sherry.** 2009. The reovirus μ2 protein inhibits interferon signaling through a novel mechanism involving nuclear accumulation of interferon regulatory factor 9. J Virol **83:**2178-2187.